

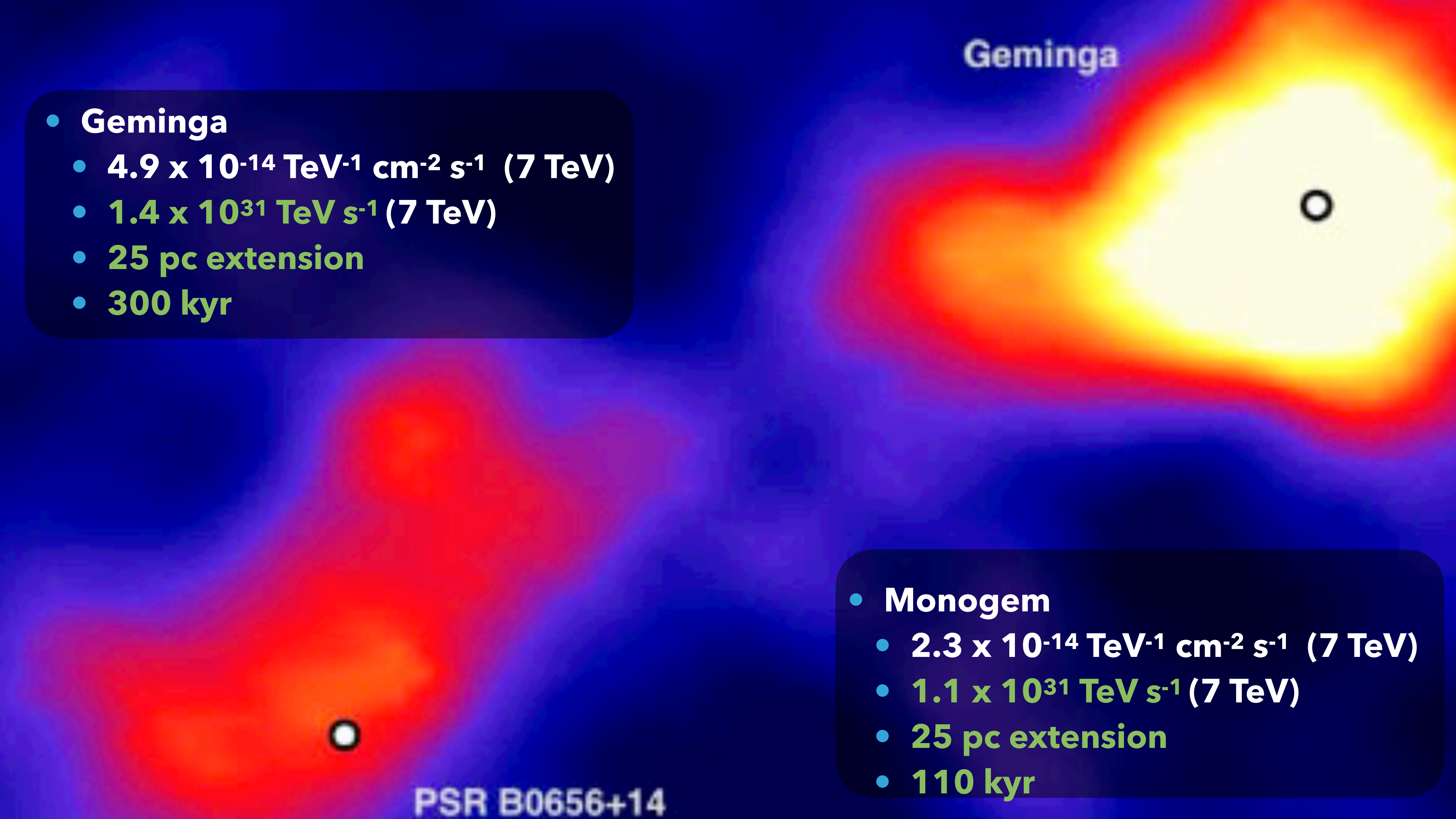
Geminga

# TeV Halos: Past, Present and Future

TIM LINDEN

PSR B0656+14





## Geminga

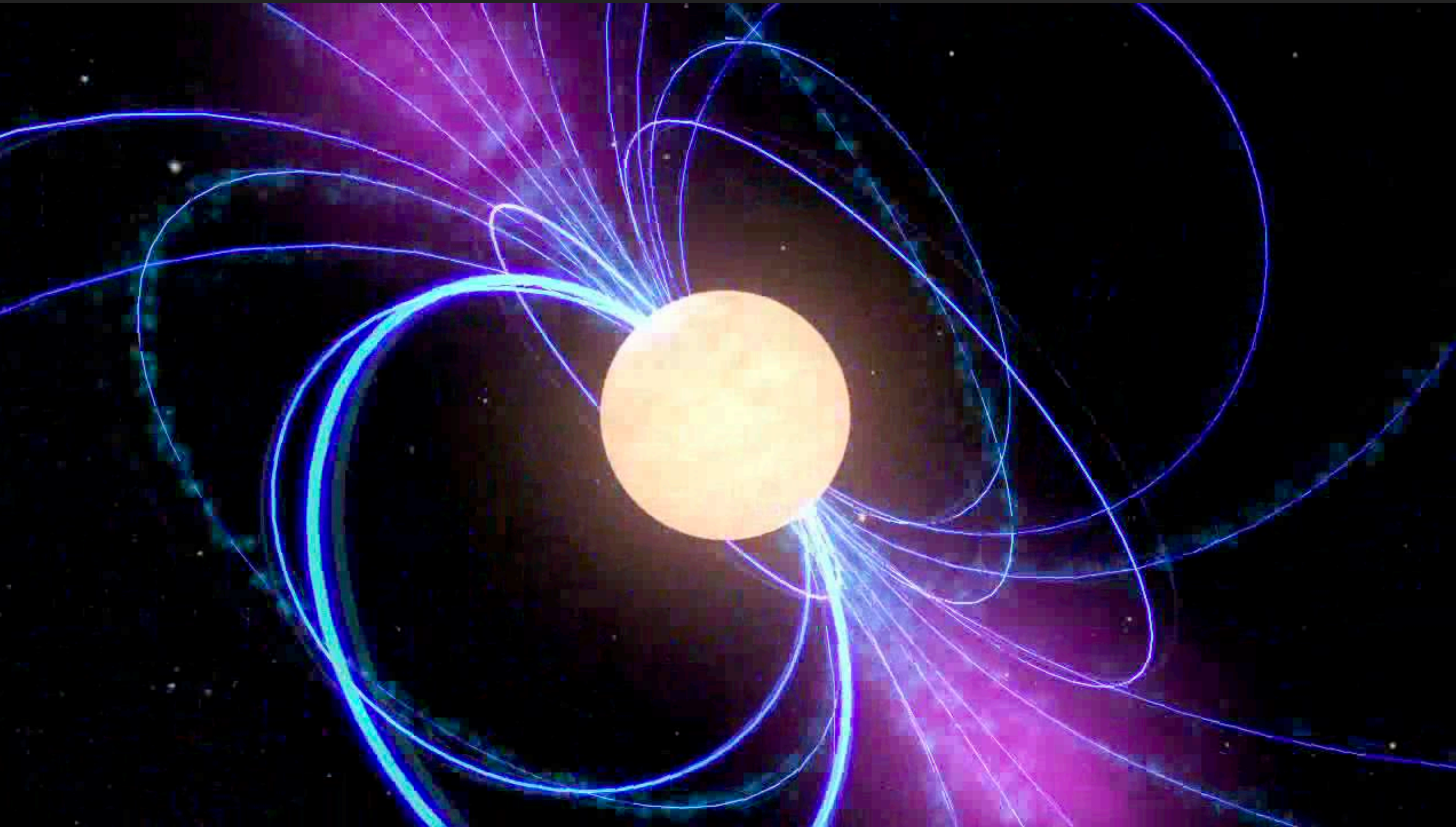
- **Geminga**
  - $4.9 \times 10^{-14} \text{ TeV}^{-1} \text{ cm}^{-2} \text{ s}^{-1}$  (7 TeV)
  - $1.4 \times 10^{31} \text{ TeV s}^{-1}$  (7 TeV)
  - 25 pc extension
  - 300 kyr

- **Monogem**
  - $2.3 \times 10^{-14} \text{ TeV}^{-1} \text{ cm}^{-2} \text{ s}^{-1}$  (7 TeV)
  - $1.1 \times 10^{31} \text{ TeV s}^{-1}$  (7 TeV)
  - 25 pc extension
  - 110 kyr

PSR B0656+14

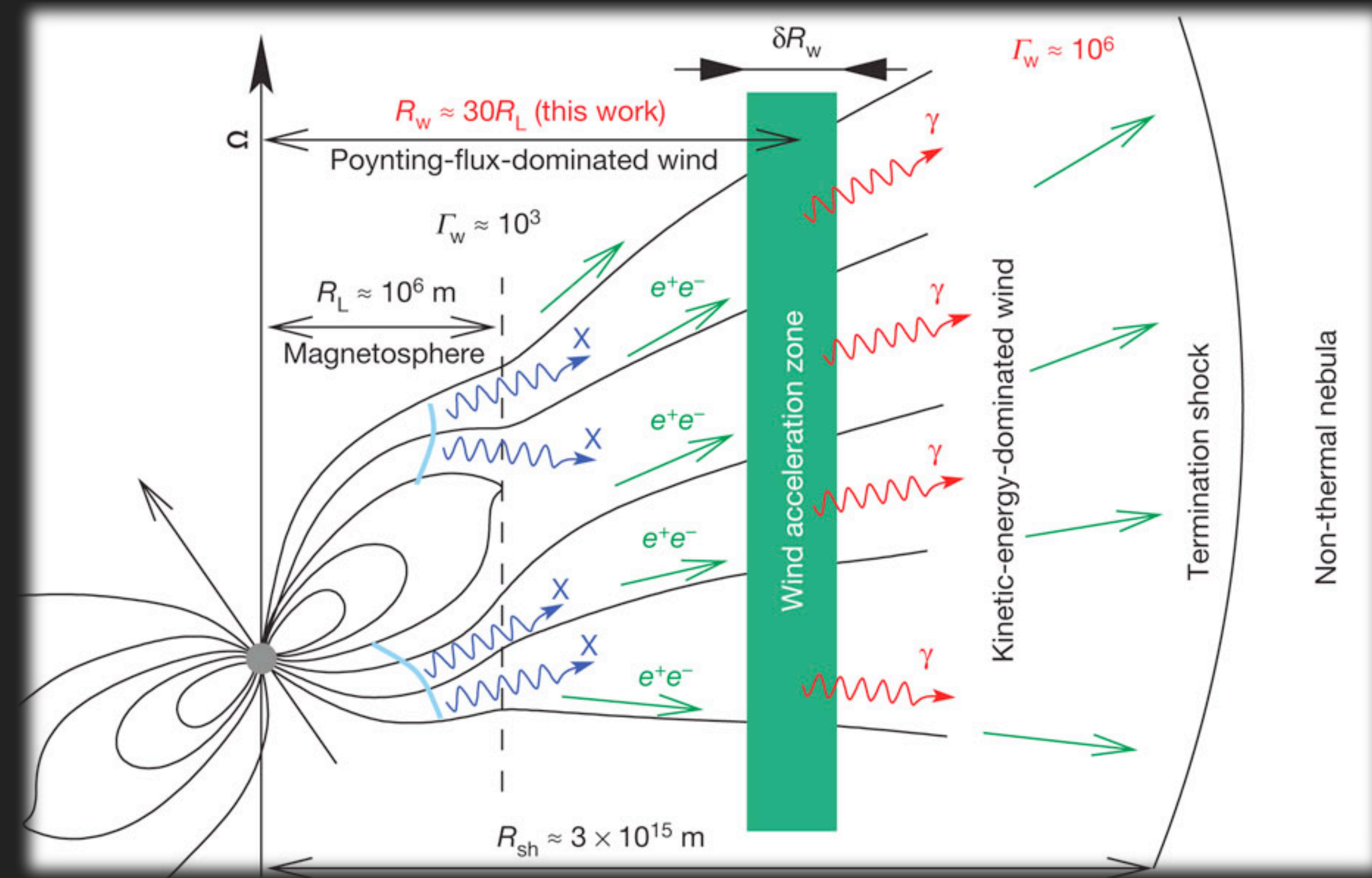
## TEV HALOS ARE NUMEROUS AND BRIGHT

---



► Rotational Kinetic Energy of the neutron star is the ultimate power source of all emission in this problem.

# PULSARS CONVERT POWER INTO ELECTRON AND POSITRON PAIRS



- Electrons boiled off the surface of the pulsar produce a cascade of  $e^+e^-$  pairs.

# EARLY LESSONS

Geminga

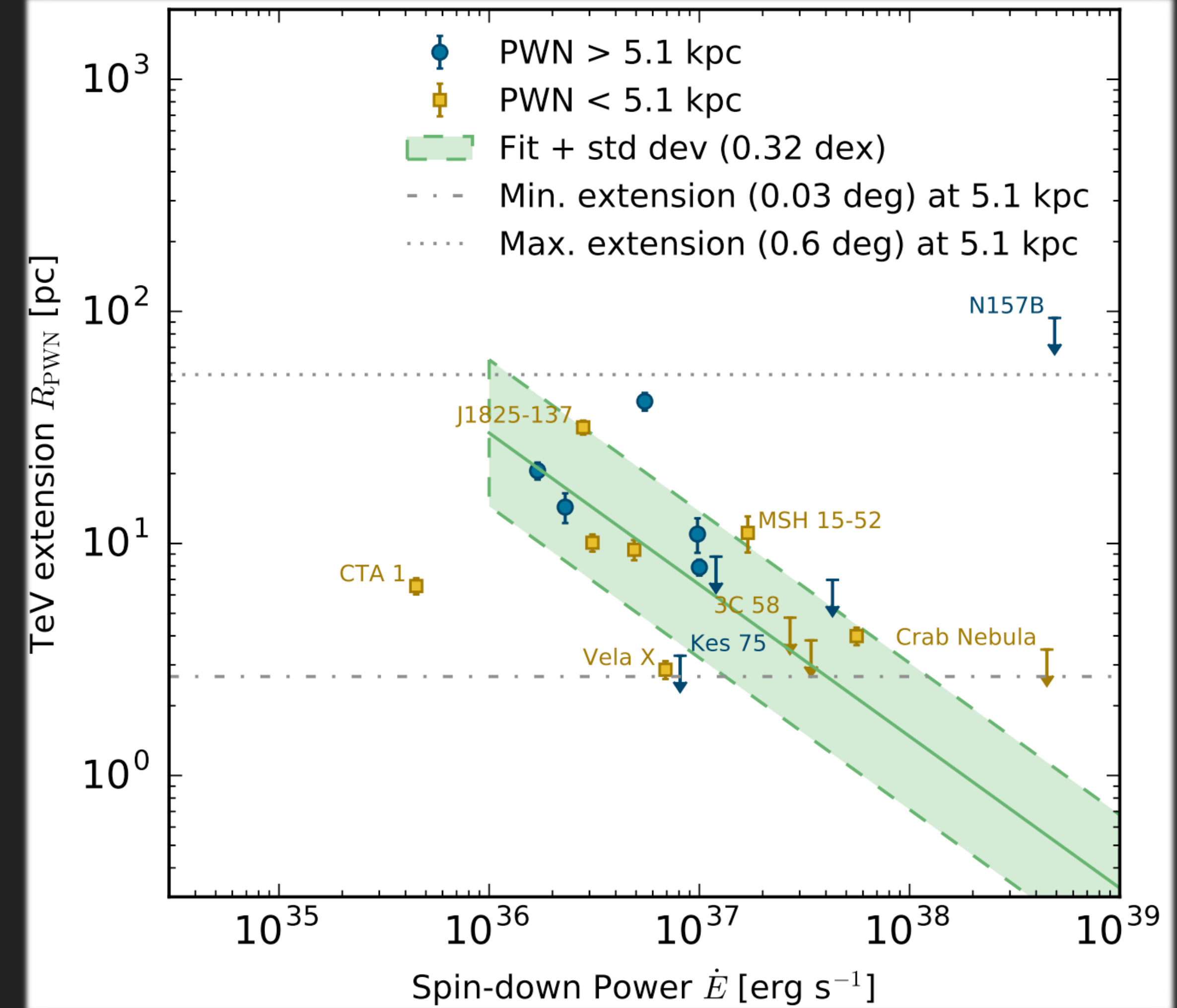
- 1.) Pulsars are **highly efficient  $e^+e^-$  accelerators.**
- 2.) Pulsar  $e^+e^-$  are **not confined in the source.**
- 3.) Regions near sources have **unusually low diffusion coefficients.**

# A NEW SOURCE CLASS

TeV Halos are much larger than PWN, especially at low spin down energies and large ages.

NOTE: The size of halos has the opposite time-dependence as the X-Ray PWN.

$$R_{\text{PWN}} \simeq 1.5 \left( \frac{\dot{E}}{10^{35} \text{ erg/s}} \right)^{1/2} \times \left( \frac{n_{\text{gas}}}{1 \text{ cm}^{-3}} \right)^{-1/2} \left( \frac{v}{100 \text{ km/s}} \right)^{-3/2} \text{ pc}$$



# EARLY LESSONS - THE GEMINGA-CENTRIC MODEL

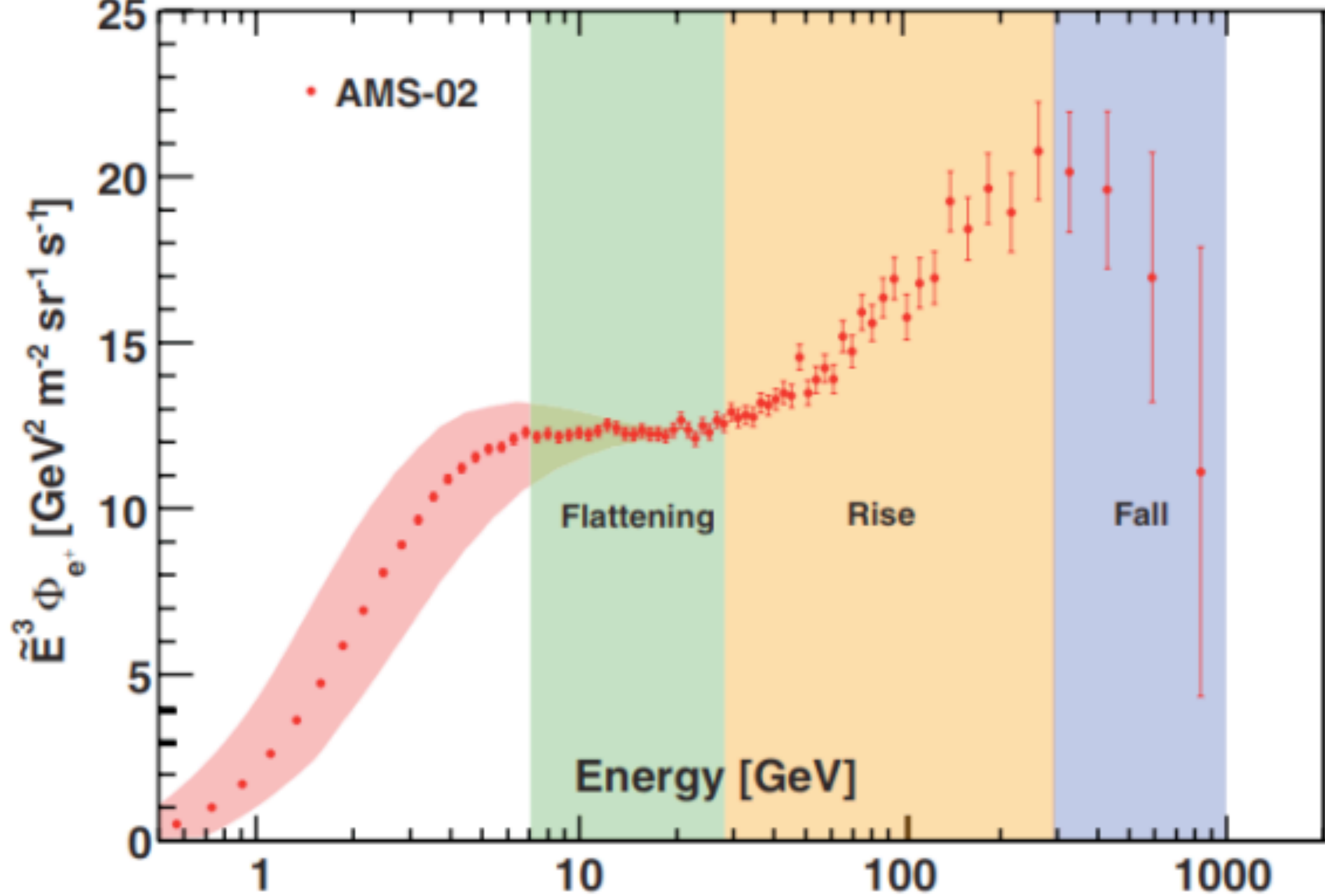
► **Make One Key Assumption:**

ATNF Name	Dec. (°)	Distance (kpc)	Age (kyr)	Spindown Lum. (erg s <sup>-1</sup> )	Spindown Flux (erg s <sup>-1</sup> kpc <sup>-2</sup> )	2HWC
J0633+1746	17.77	0.25	342	3.2e34	4.1e34	2HWC J0631+169
B0656+14	14.23	0.29	111	3.8e34	3.6e34	2HWC J0700+143
B1951+32	32.87	3.00	107	3.7e36	3.3e34	—
J1740+1000	10.00	1.23	114	2.3e35	1.2e34	—
J1913+1011	10.18	4.61	169	2.9e36	1.1e34	2HWC J1912+099
J1831-0952	-9.86	3.68	128	1.1e36	6.4e33	2HWC J1831-098
J2032+4127	41.45	1.70	181	1.7e35	4.7e33	2HWC J2031+415
B1822-09	-9.58	0.30	232	4.6e33	4.1e33	—
B1830-08	-8.45	4.50	147	5.8e35	2.3e33	—
J1913+0904	9.07	3.00	147	1.6e35	1.4e33	—
B0540+23	23.48	1.56	253	4.1e34	1.4e33	—

► **The following correlation is consistent with the data.**

$$\phi_{\text{TeV halo}} = \left( \frac{\dot{E}_{\text{psr}}}{\dot{E}_{\text{Geminga}}} \right) \left( \frac{d_{\text{Geminga}}^2}{d_{\text{psr}}^2} \right) \phi_{\text{Geminga}}$$

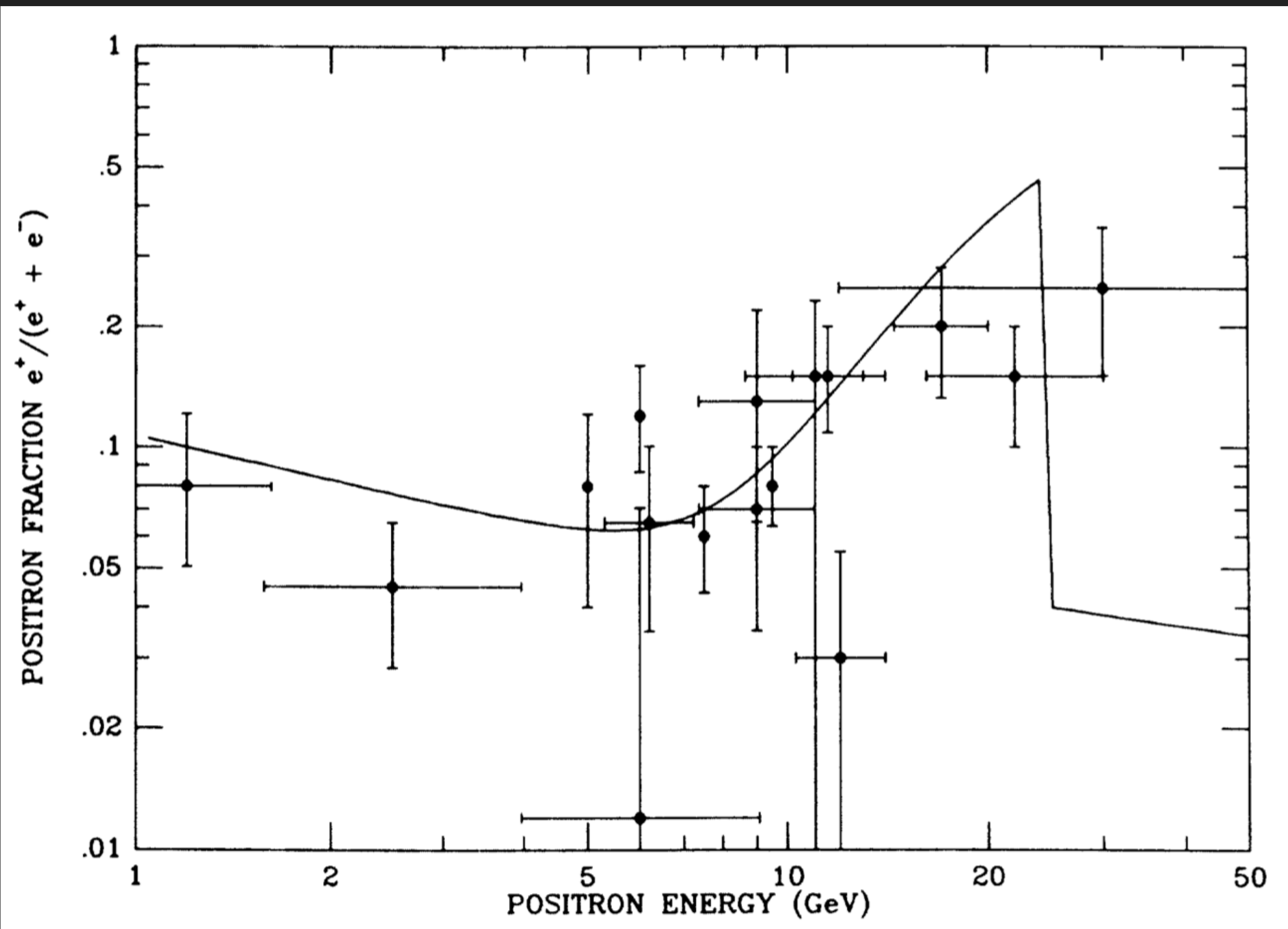
► **Note: Using Monogem would increases fluxes by nearly a factor of 2. The power law of this correlation doesn't greatly affect the results.**



# IMPLICATION 1: THE POSITRON EXCESS

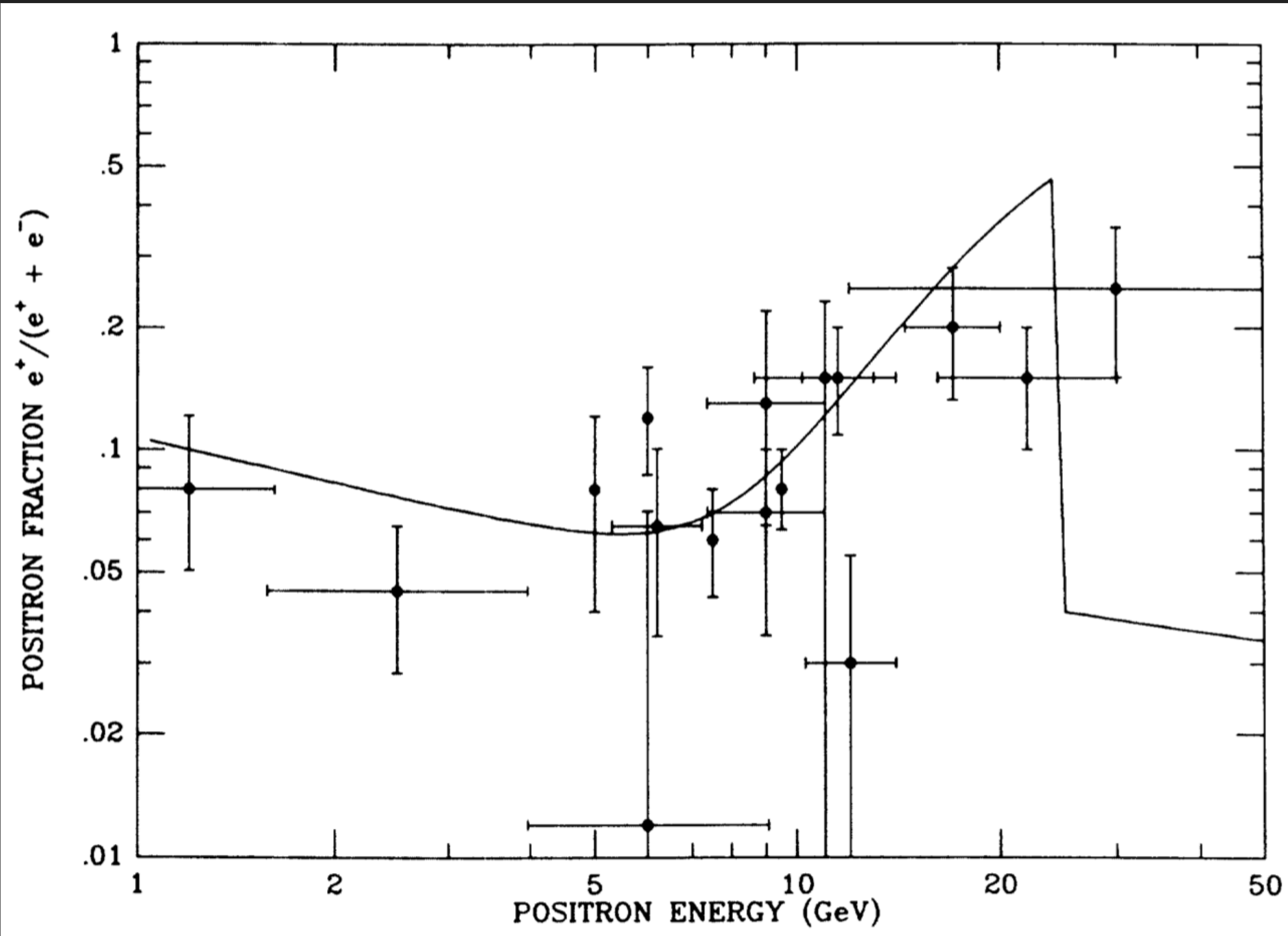
---

Turner & Wilczek (1989)

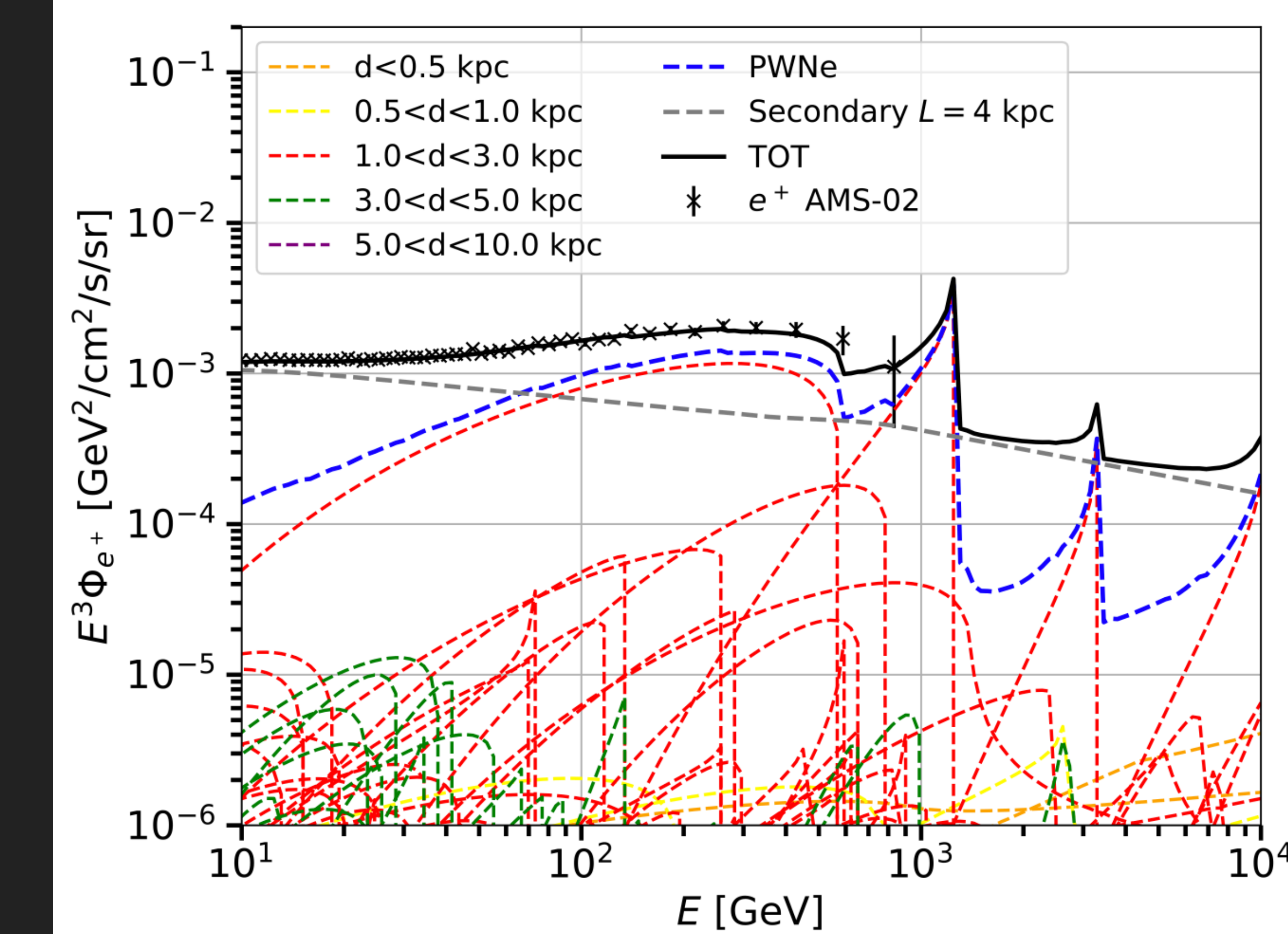


# IMPLICATION 1: THE POSITRON EXCESS

Turner & Wilczek (1989)



Orusa et al. (2021; 2107.06300)



- Previously believed that sharp spectral features in the positron spectrum could be produced by either dark matter or pulsars.

# IMPLICATION 1: THE POSITRON EXCESS

- What were the uncertainties in pulsar models?

- I: The  $e^+e^-$  production efficiency?

Profumo (0812.4457); Malyshev et al. (0903.1310)

%. A quantitative discussion of plausible values for  $f_{e^\pm}$  was recently given in Ref. [38]. We shall not review their discussion here, but Ref. [38] argues (see in particular their very informative App. B and C) that in the context of a standard model for the pulsar wind nebulae, a reasonable range for  $f_{e^\pm}$  falls between 1% and 30%.

- II: The  $e^+e^-$  spectrum.

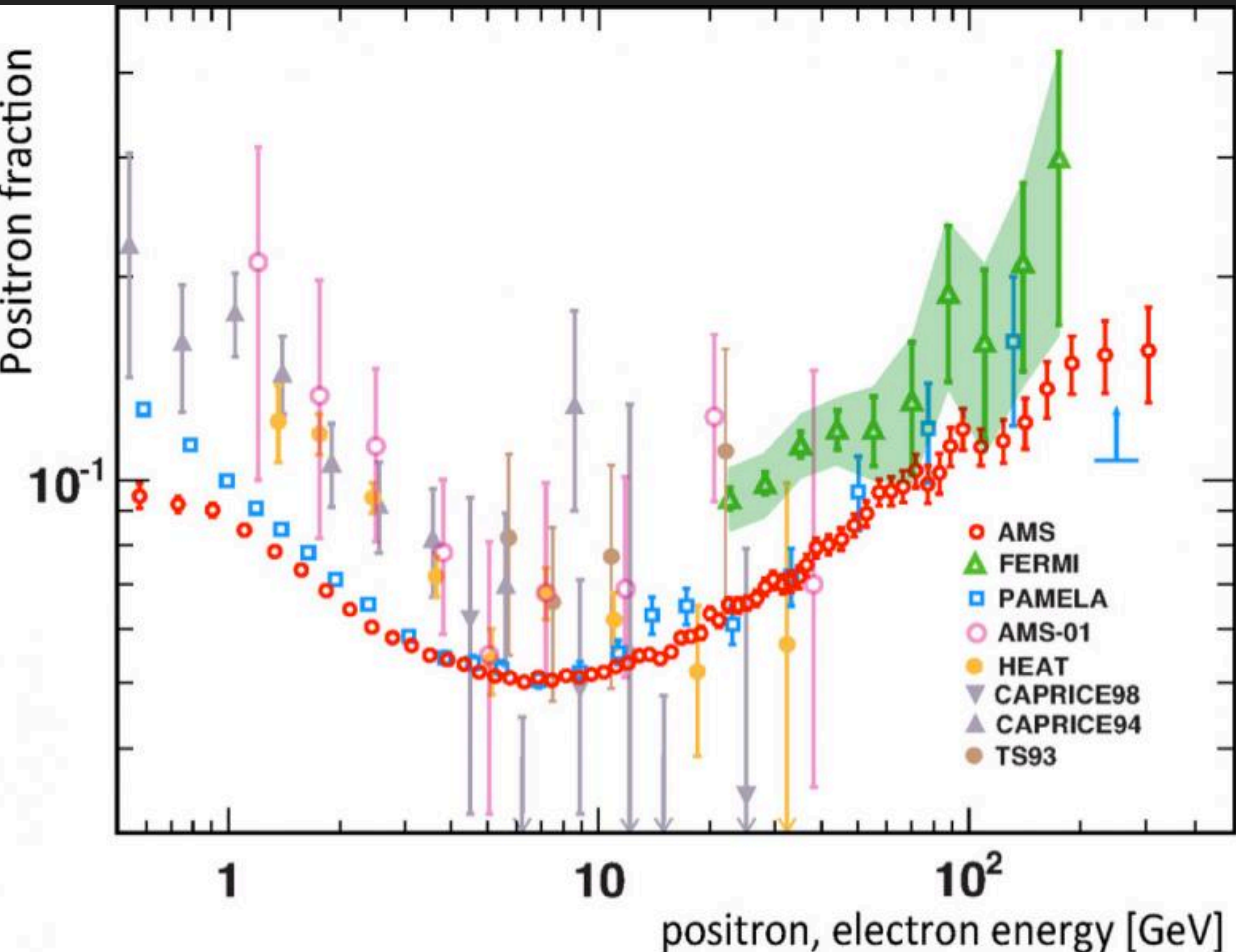
Hooper et al. (0810.1527)

part of their energy adiabatically because of the expansion of the wind. The energy spectrum injected by a single pulsar depends on the environmental parameters of the pulsar, but some attempts to calculate the average spectrum injected by a population of mature pulsars suggest that the spectrum may be relatively hard, having a slope of  $\sim 1.5\text{--}1.6$  [18]. This spectrum, however, results from a complex interplay of individual pulsar spectra, of the spatial and age distributions of pulsars in the Galaxy, and on the assumption that the chief channel for pulsar spin down is magnetic dipole radiation. Due to the related uncertainties, variations from this injection spectra cannot be ruled out. Typically, one concentrates the attention on pulsars of age  $\sim 10^5$  years because younger pulsars are likely to still

- III: The propagation of  $e^+e^-$  to Earth.

Malyshev et al. (0903.1310)

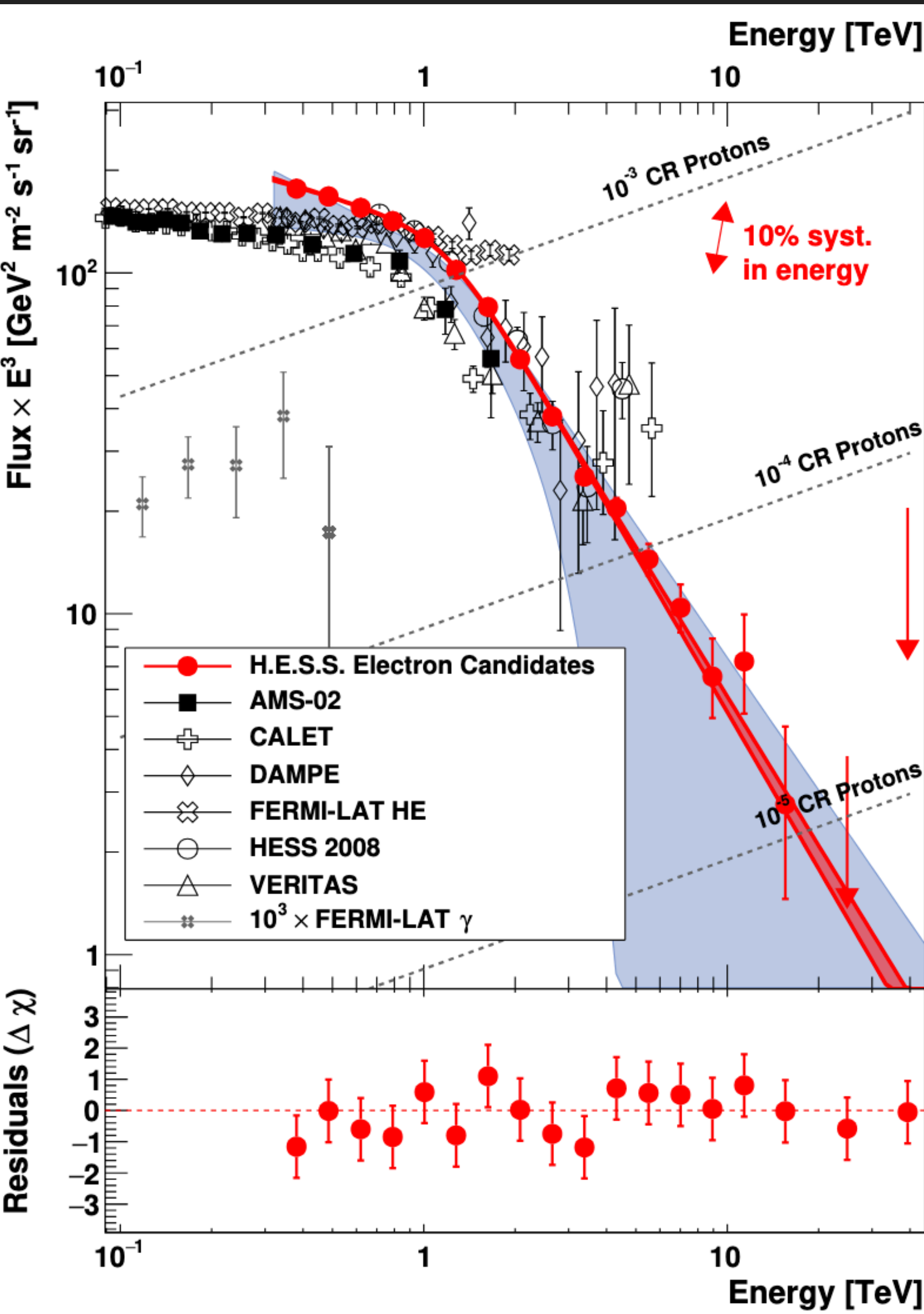
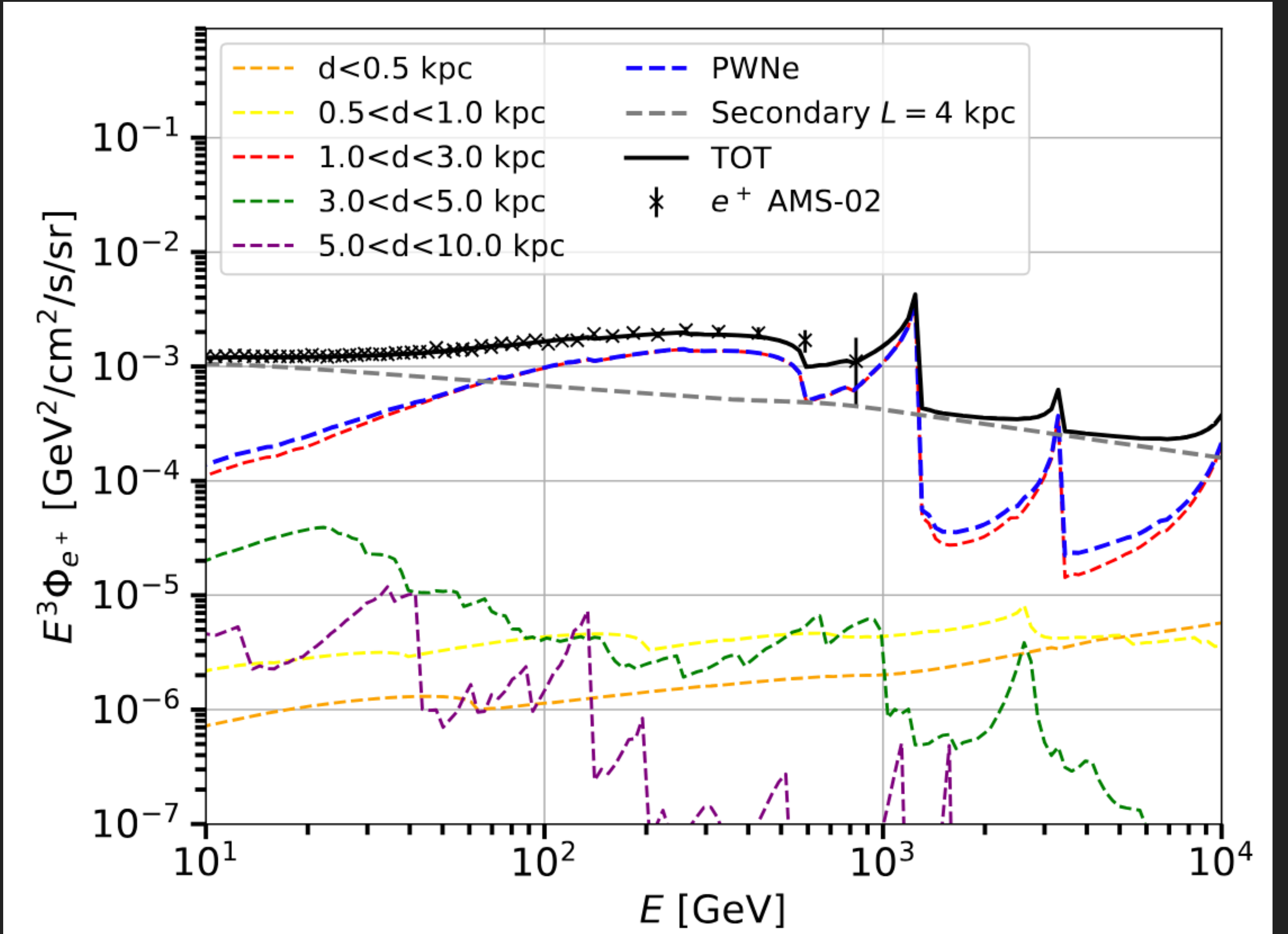
The observed spectrum on Earth of electrons and positrons injected by pulsars is also strongly dependent on propagation effects. In particular, the observed cutoff in the flux of electrons from a pulsar can be much smaller than the injection cutoff due to energy losses (“cooling”) during propagation. We define the cooling break,  $E_{br}(t)$ , as the maximal energy electrons can have after propagating for time  $t$ . Since – as stated above – the typical



# IMPLICATION 1: THE POSITRON EXCESS

H.E.S.S.. Collaboration (2024; 2411.08981)

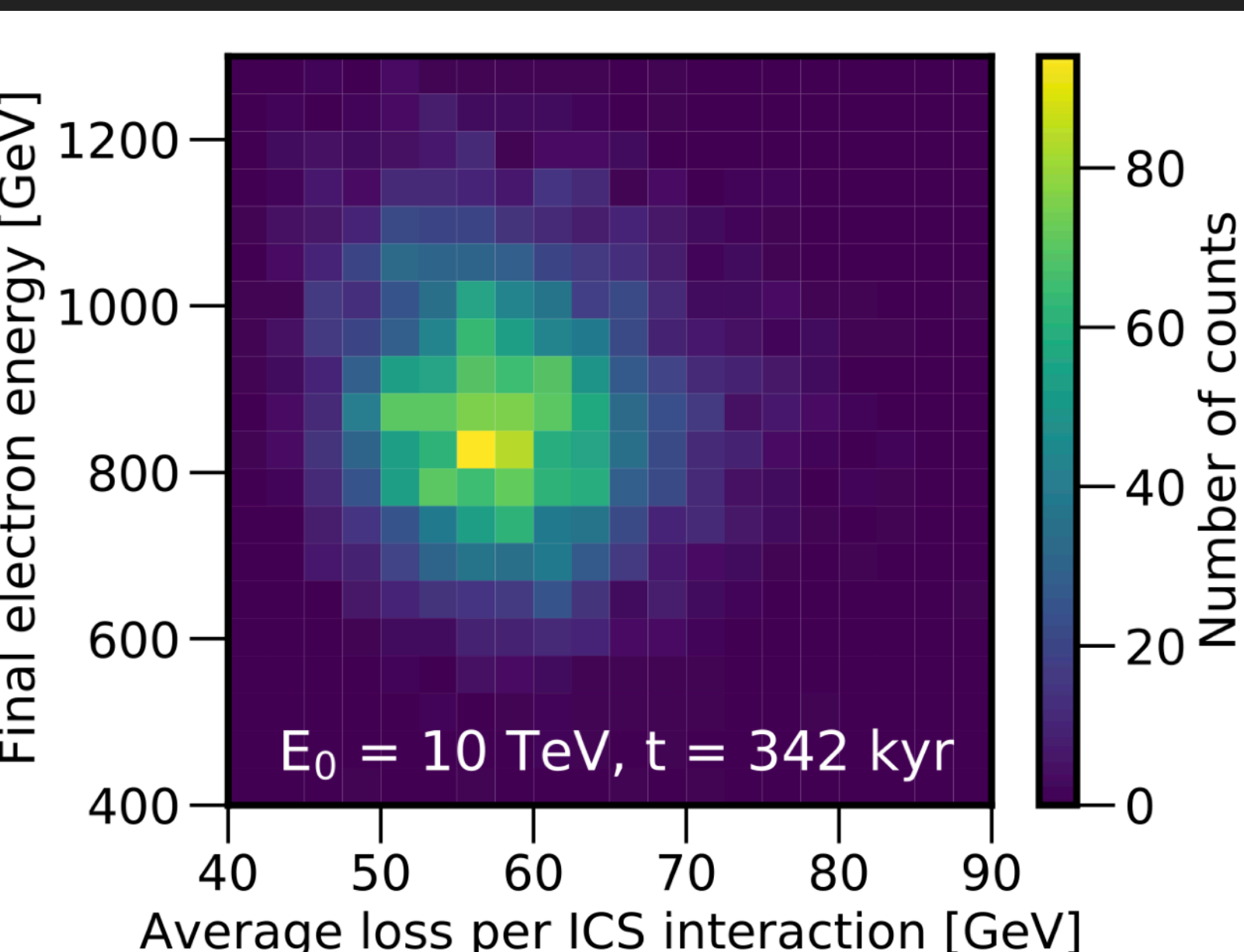
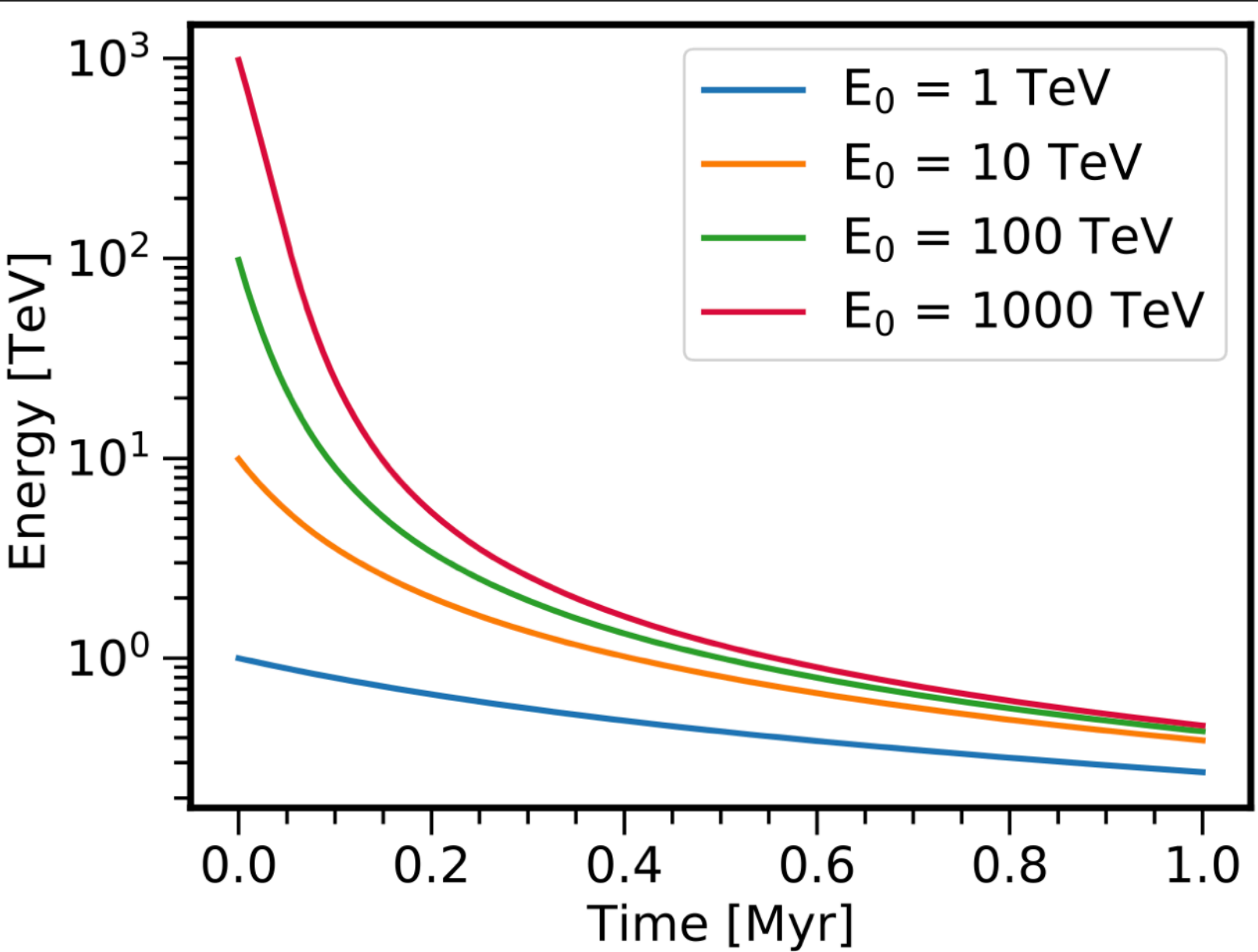
- Debates on the Number of Pulsars

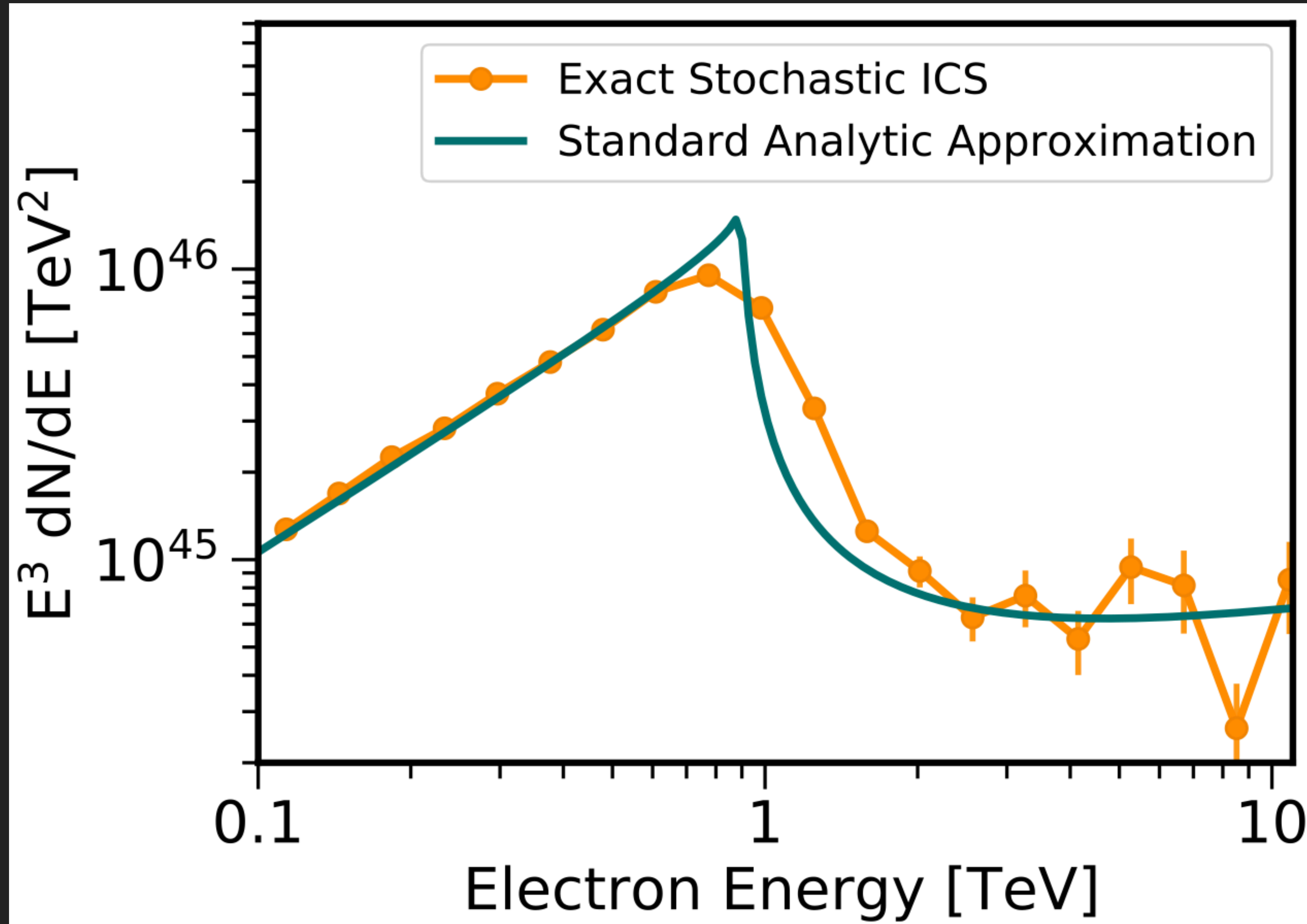


# IMPLICATION 1: THE POSITRON EXCESS

- ▶ For pulsars, there is a key error: Studies generally use a continuous approximation for electron energy losses:

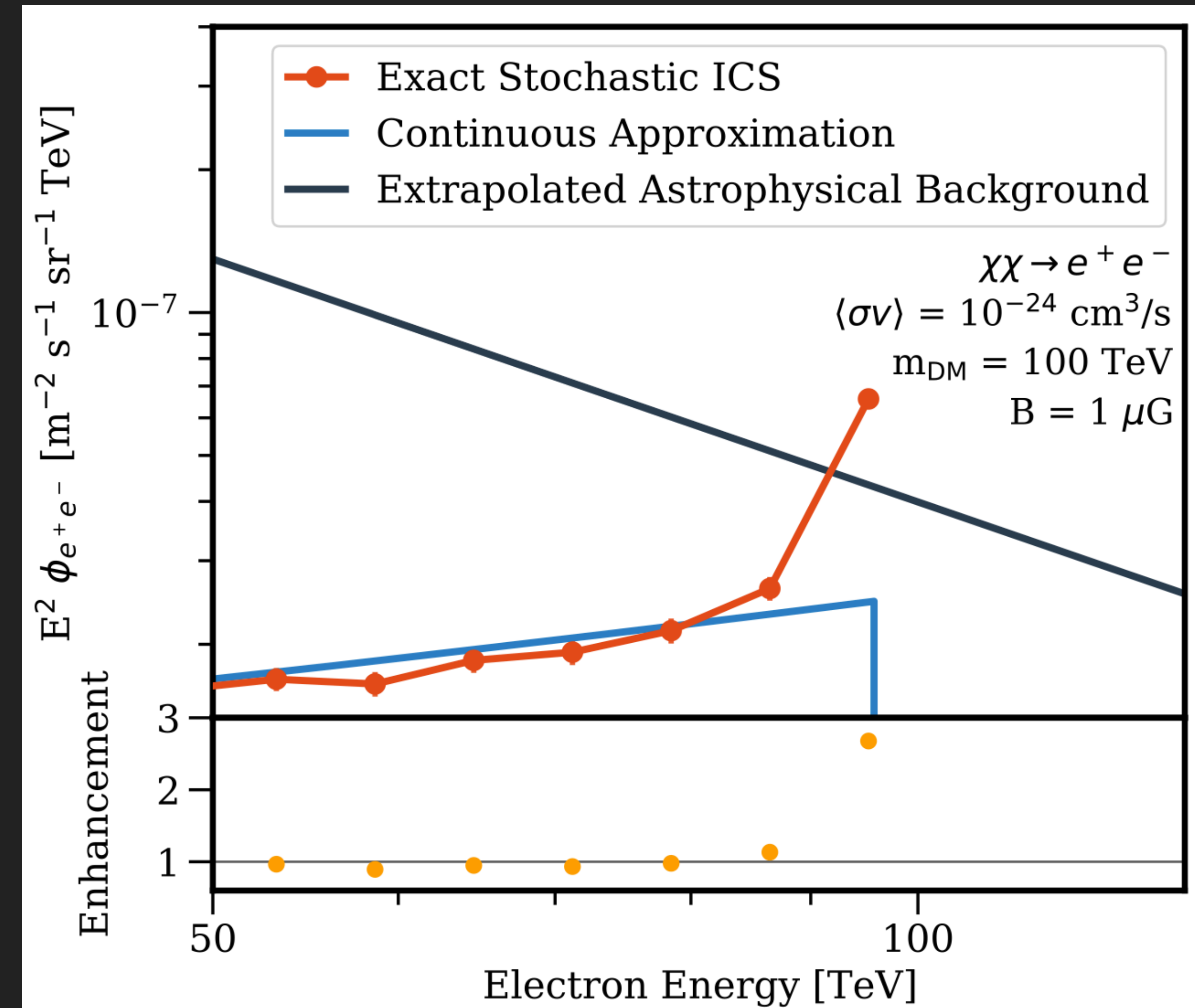
$$\frac{dE}{dt} = -\frac{4}{3}\sigma_T c \left(\frac{E}{m_e}\right)^2 \left[ \rho_B + \sum_i \rho_i(\nu_i) S(E, \nu_i) \right]$$



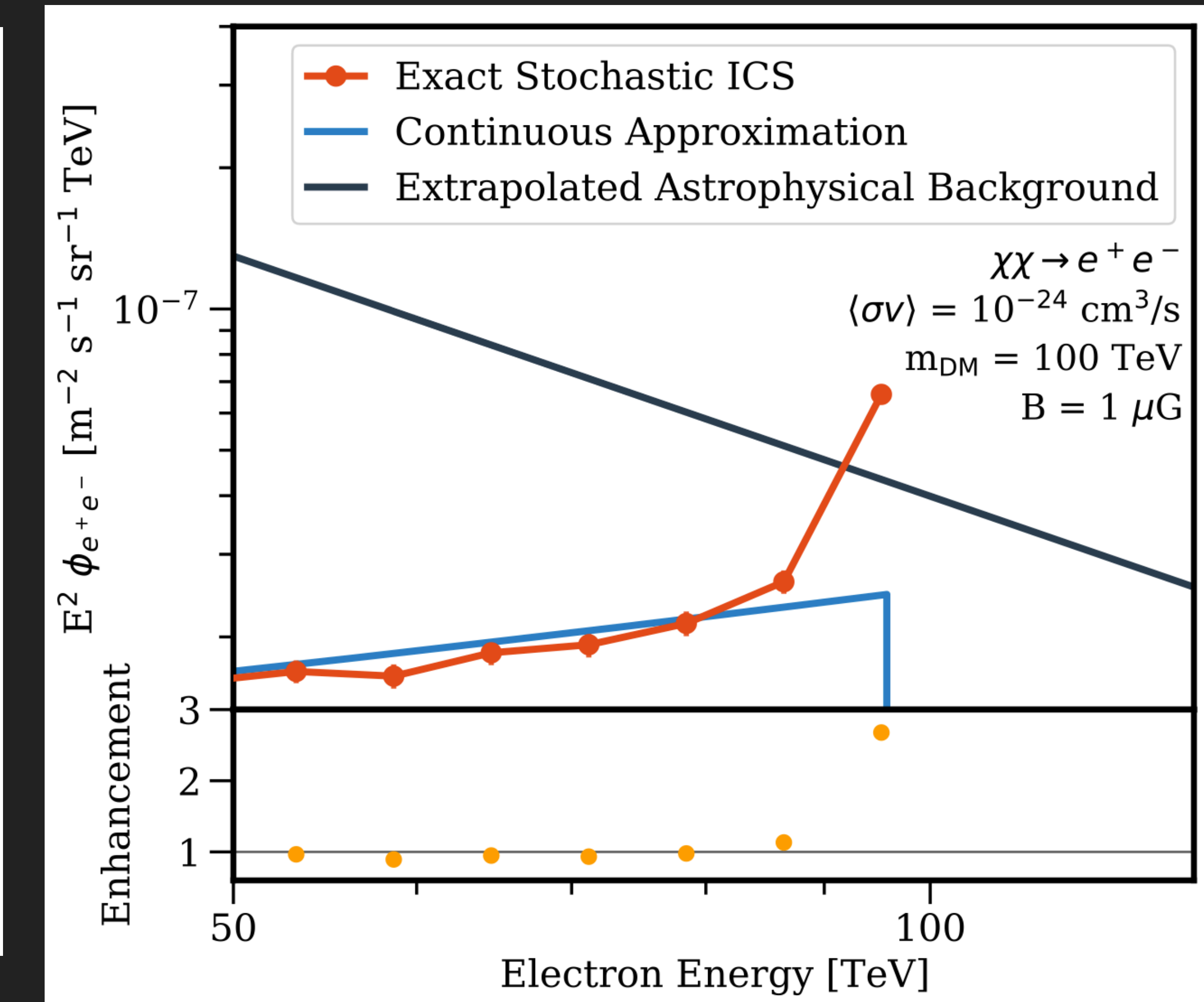
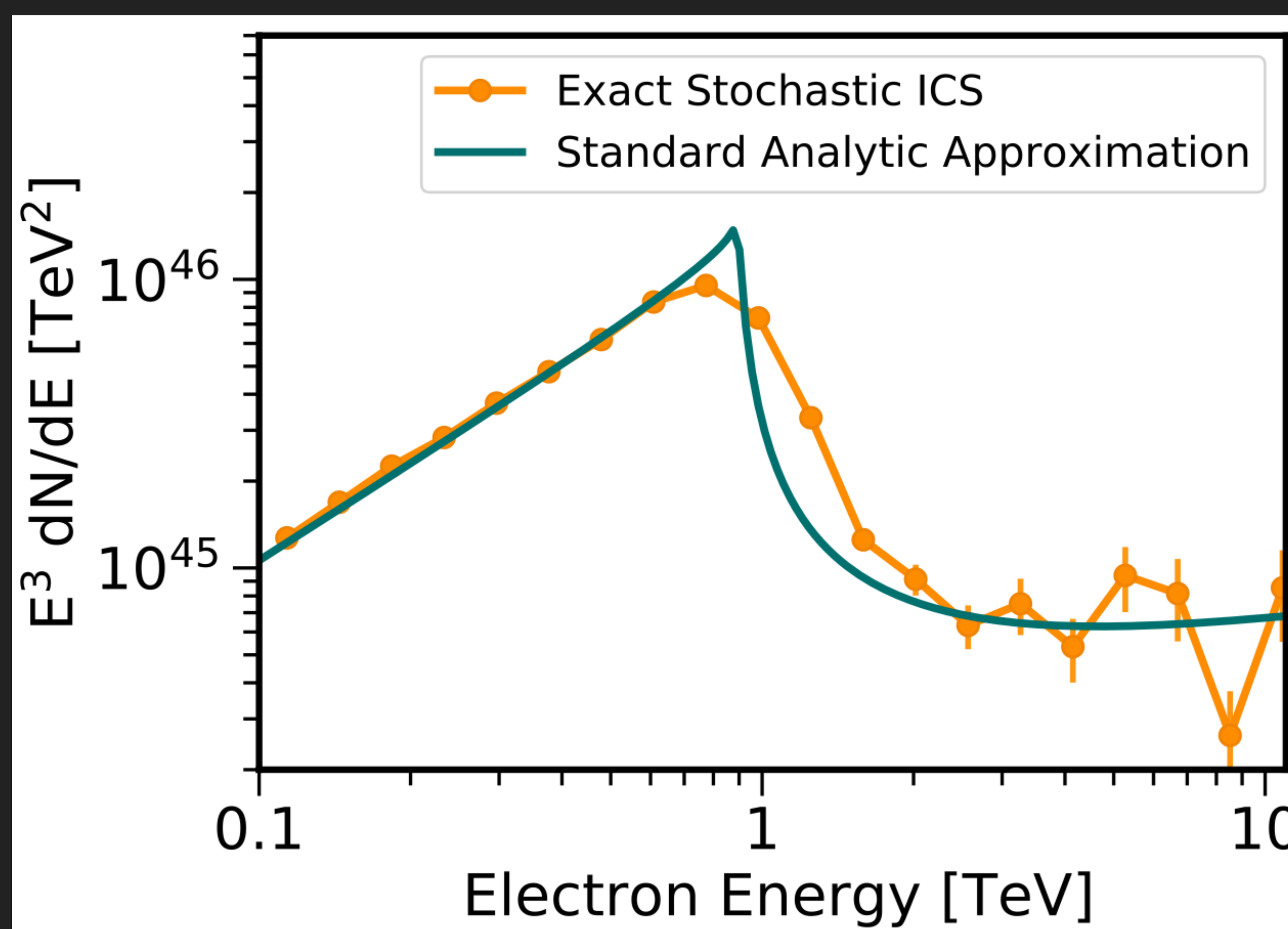


# IMPLICATION 1: THE POSITRON EXCESS

- For dark matter, the spectral cutoff is not produced by ICS cooling, but from the dark matter mass.
- The stochasticity of cooling instead means that some particles don't cool at all, enhancing the peak.
- Correctly accounting for ICS energy losses makes it possible to differentiate dark matter and pulsars via their positron spectrum.

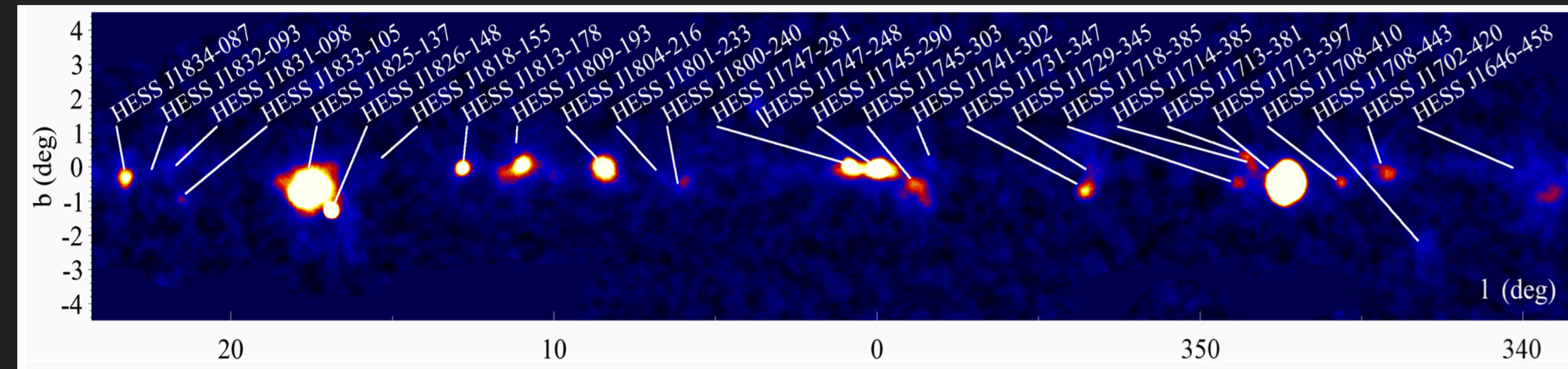


# EXCITING RESULT! ONLY DARK MATTER CAN PRODUCE LINES!



## IMPLICATION 2: MISSING TEV HALOS

- ▶ Radio pulsars are beamed!

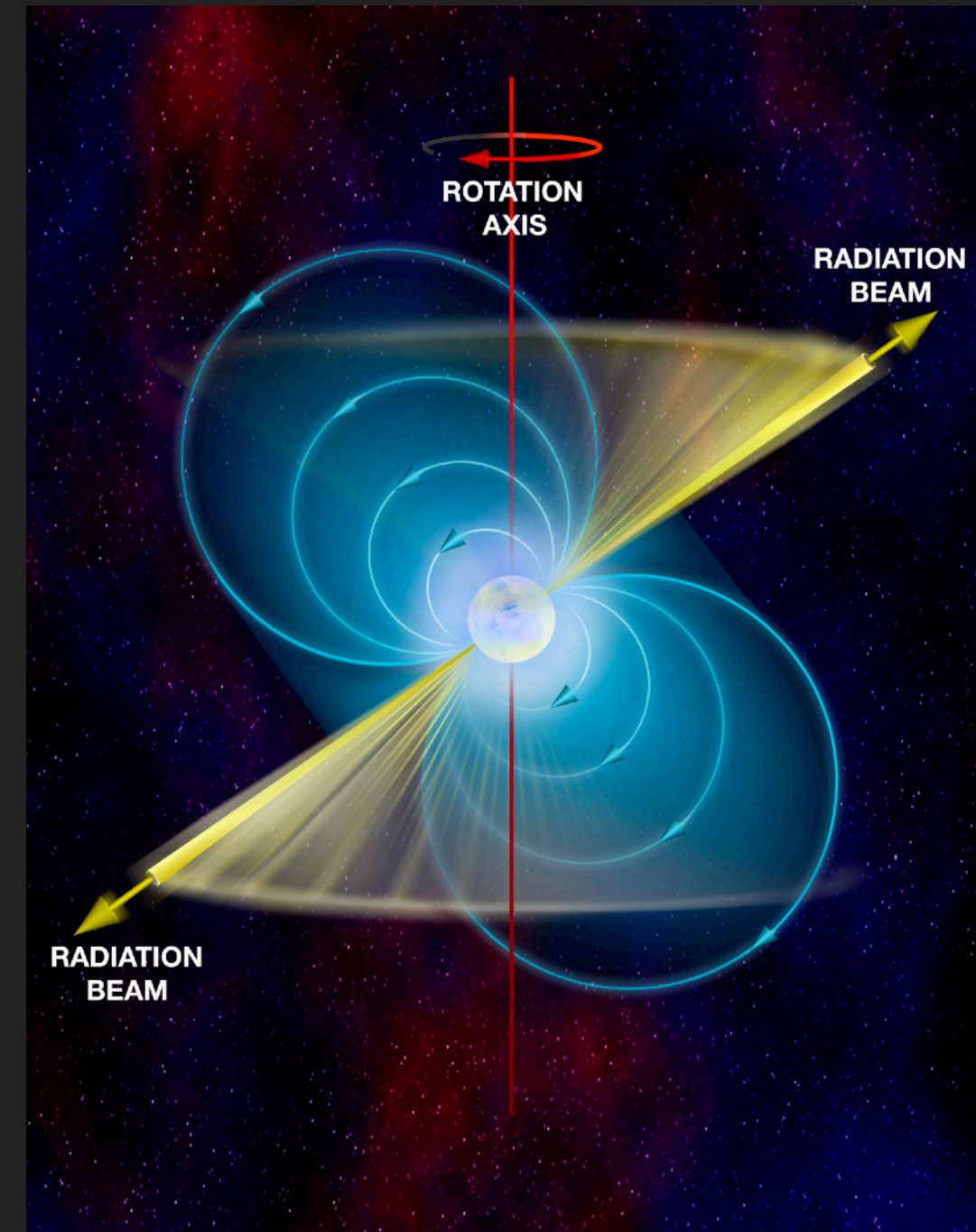


- ▶ Beaming fraction is small

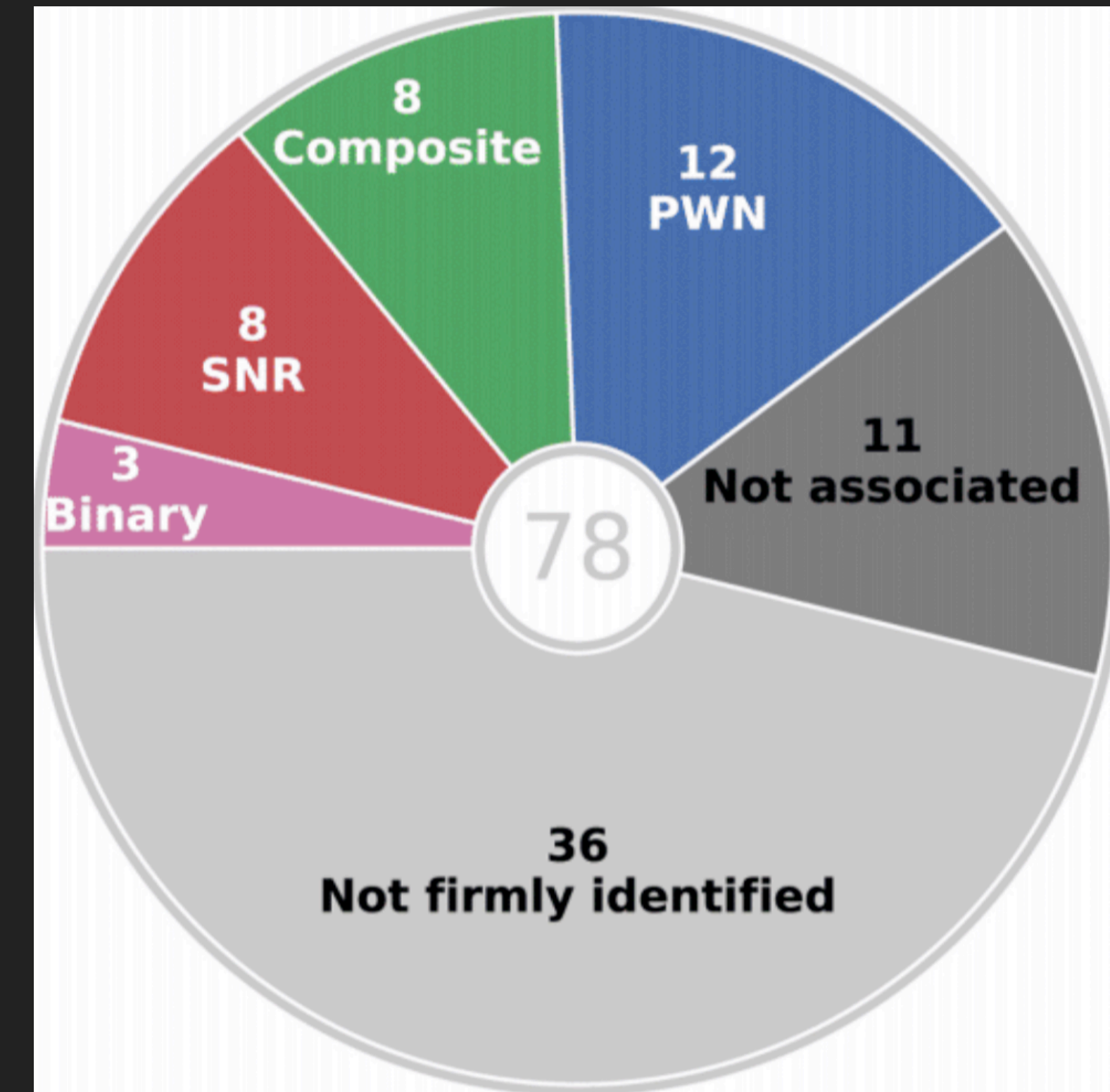
Tauris & Manchester (1998)

$$f = \left[ 1.1 \left( \log_{10} \left( \frac{\tau}{100 \text{ Myr}} \right) \right)^2 + 15 \right] \%$$

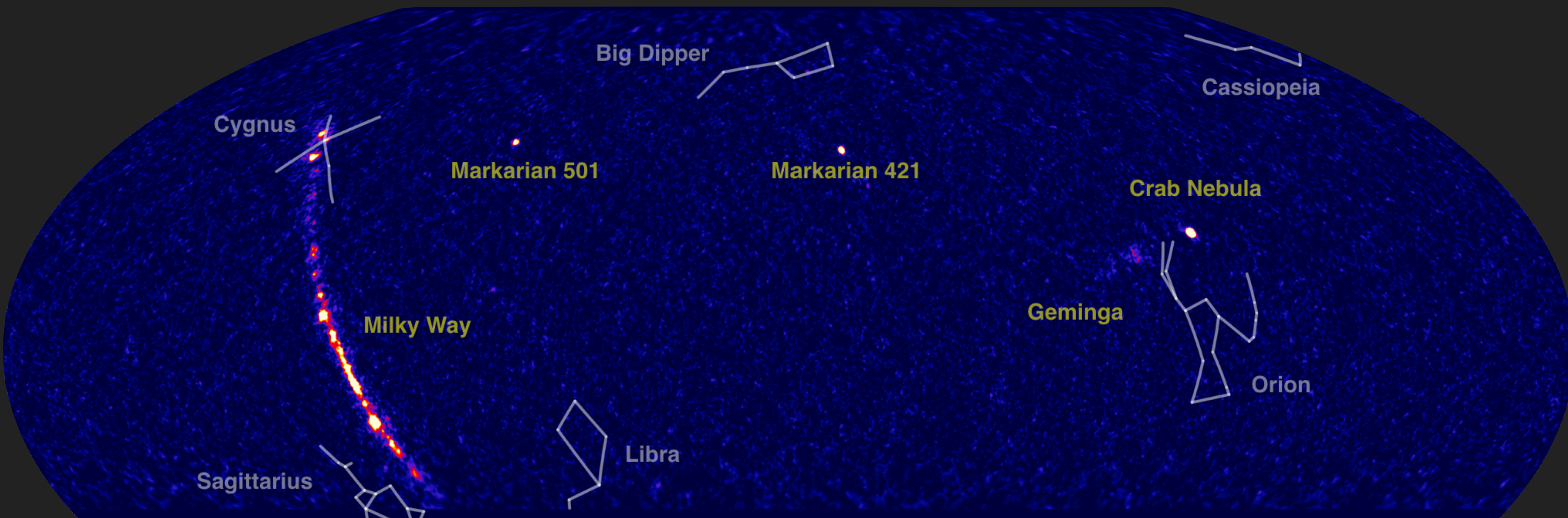
- ▶ This varies between 15-30%.



- ▶ Most pulsars are unseen in radio!

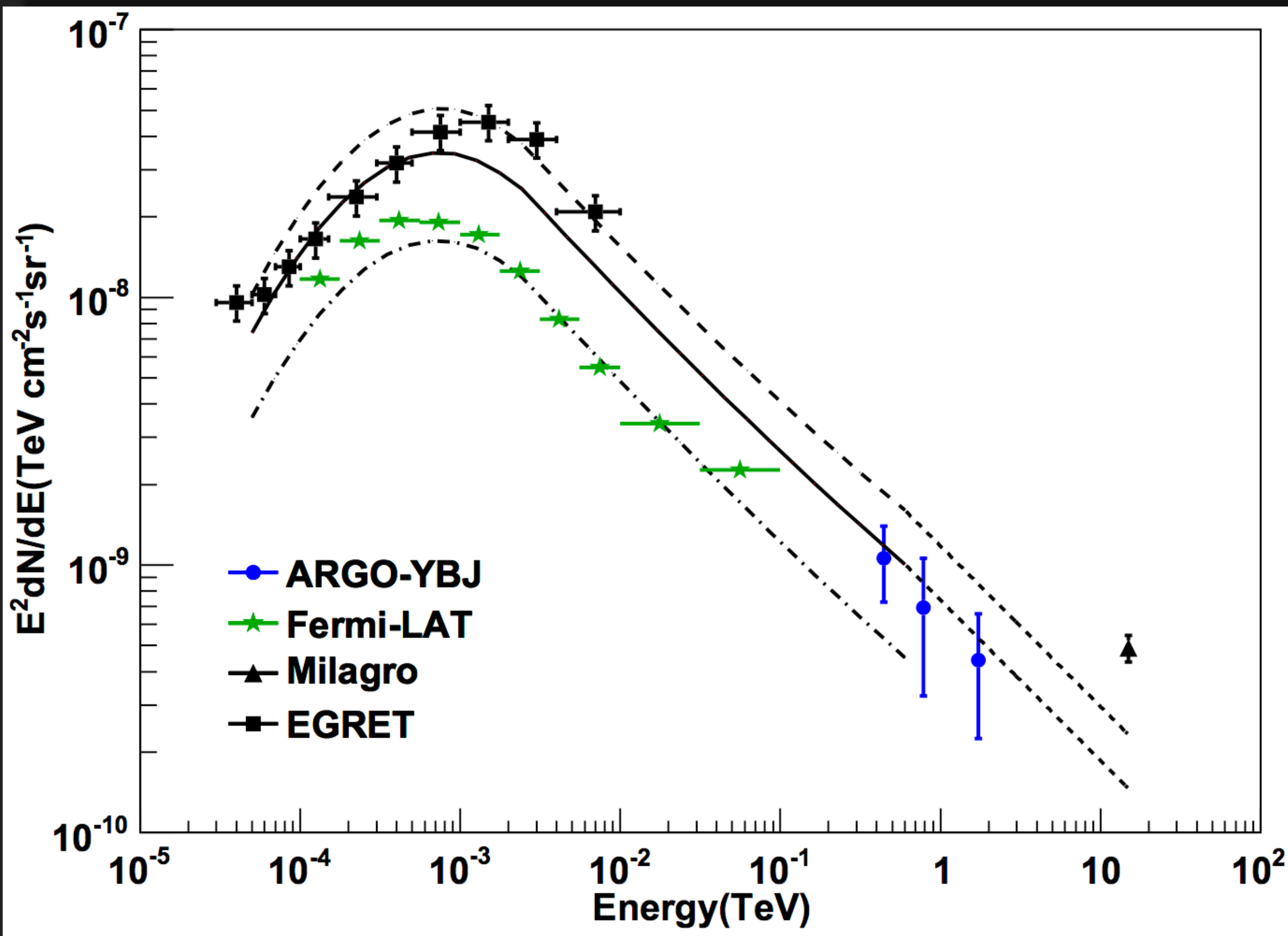


## IMPLICATION 3: DIFFUSE TEV GAMMA-RAYS



- There is bright diffuse gamma-ray emission across the galactic plane.
- Ratio of point source emission to diffuse emission is a powerful marker of emission mechanisms and local propagation.

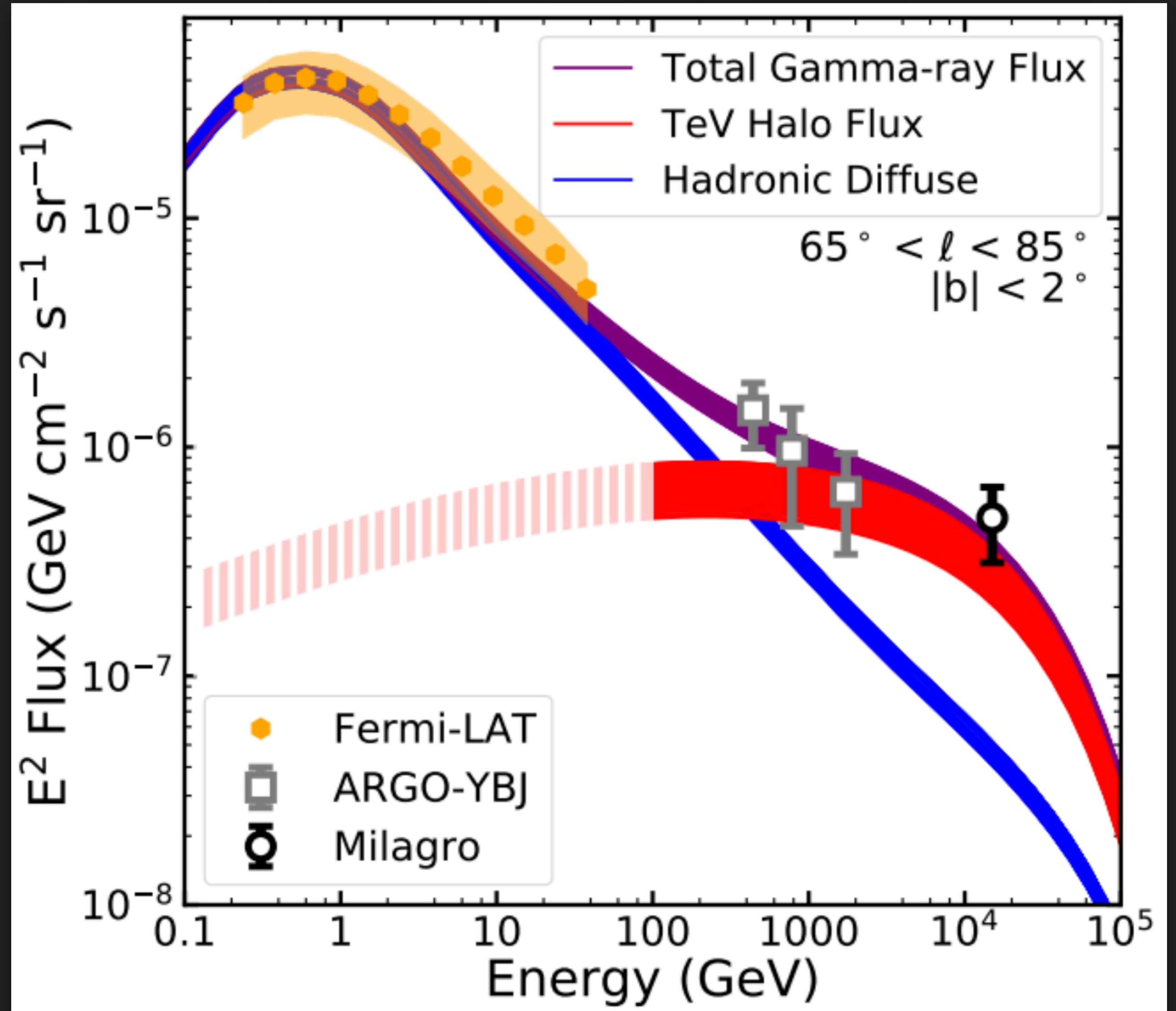
## IMPLICATION 3: DIFFUSE TEV GAMMA-RAYS



## IMPLICATION 3: DIFFUSE TEV GAMMA-RAYS

Linden & Buckman (2017; 1707.01905)

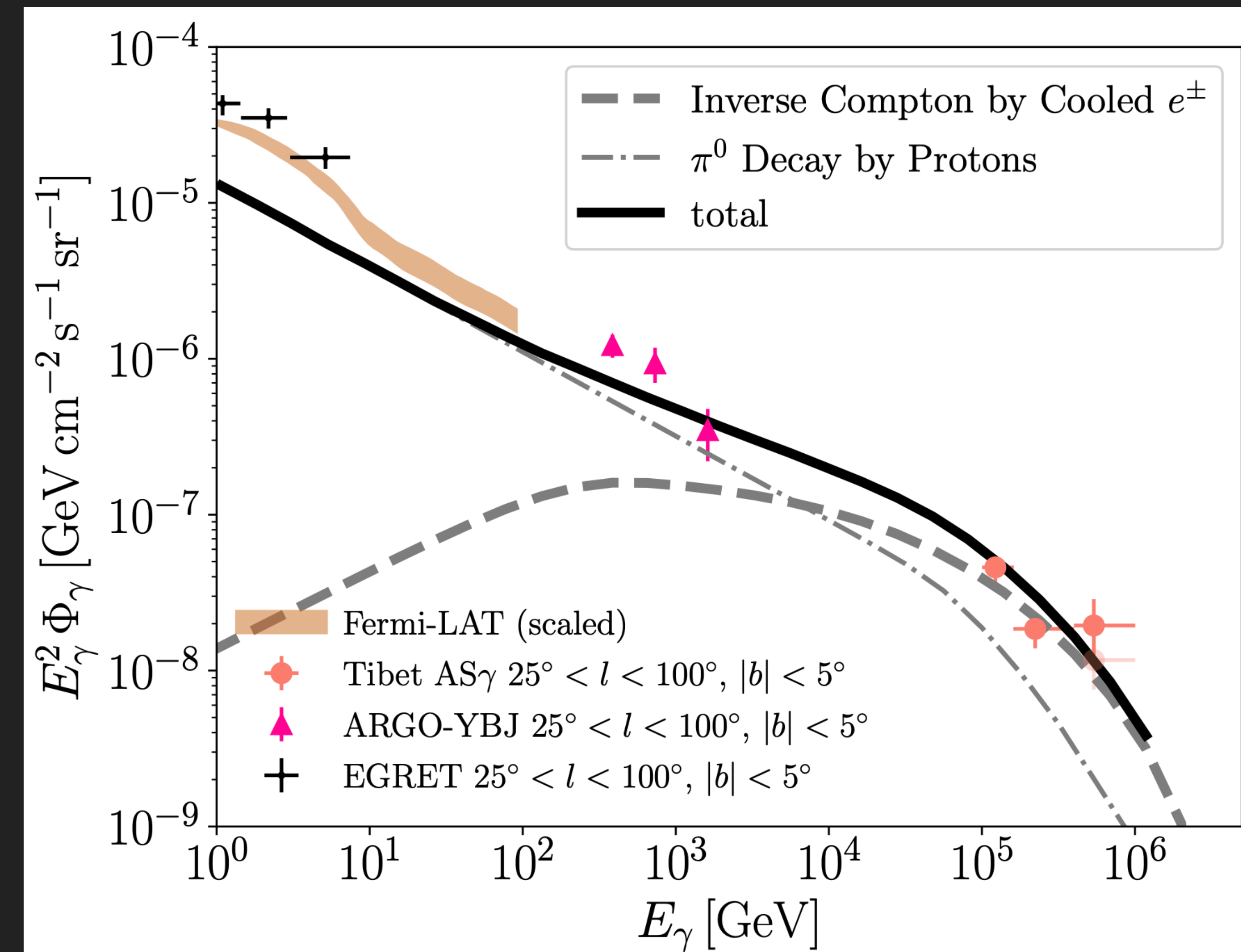
- TeV halos naturally explain the spectrum and intensity of this emission.
- Multiple halos observed with  $E^{-2.0}$  spectra.
- Note - "Halo" is not needed
  - Pulsar efficiency  $\sim 10\%$
  - Power must escape PWN



## IMPLICATION 3: DIFFUSE TEV GAMMA-RAYS

- TeV halos naturally explain the spectrum and intensity of this emission.
- Multiple halos observed with  $E^{-2.0}$  spectra.
- Note - "Halo" is not needed
  - Pulsar efficiency  $\sim 10\%$
  - Power must escape PWN

Fang & Murase (2021; 2104.09491)

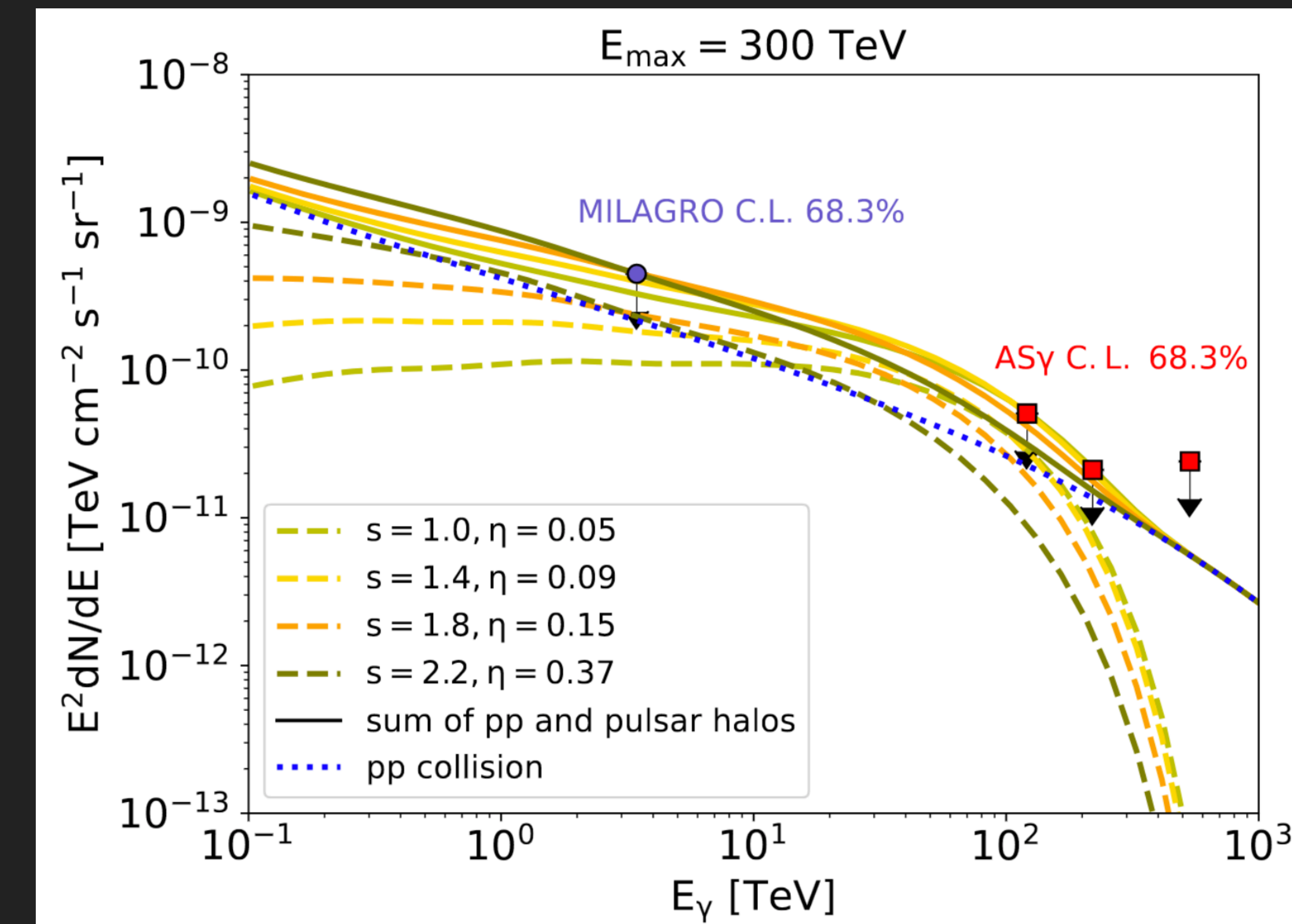


Tibet AS $\gamma$  data

## IMPLICATION 3: DIFFUSE TEV GAMMA-RAYS

- TeV halos naturally explain the spectrum and intensity of this emission.
- Multiple halos observed with  $E^{-2.0}$  spectra.
- Note - "Halo" is not needed
  - Pulsar efficiency  $\sim 10\%$
  - Power must escape PWN

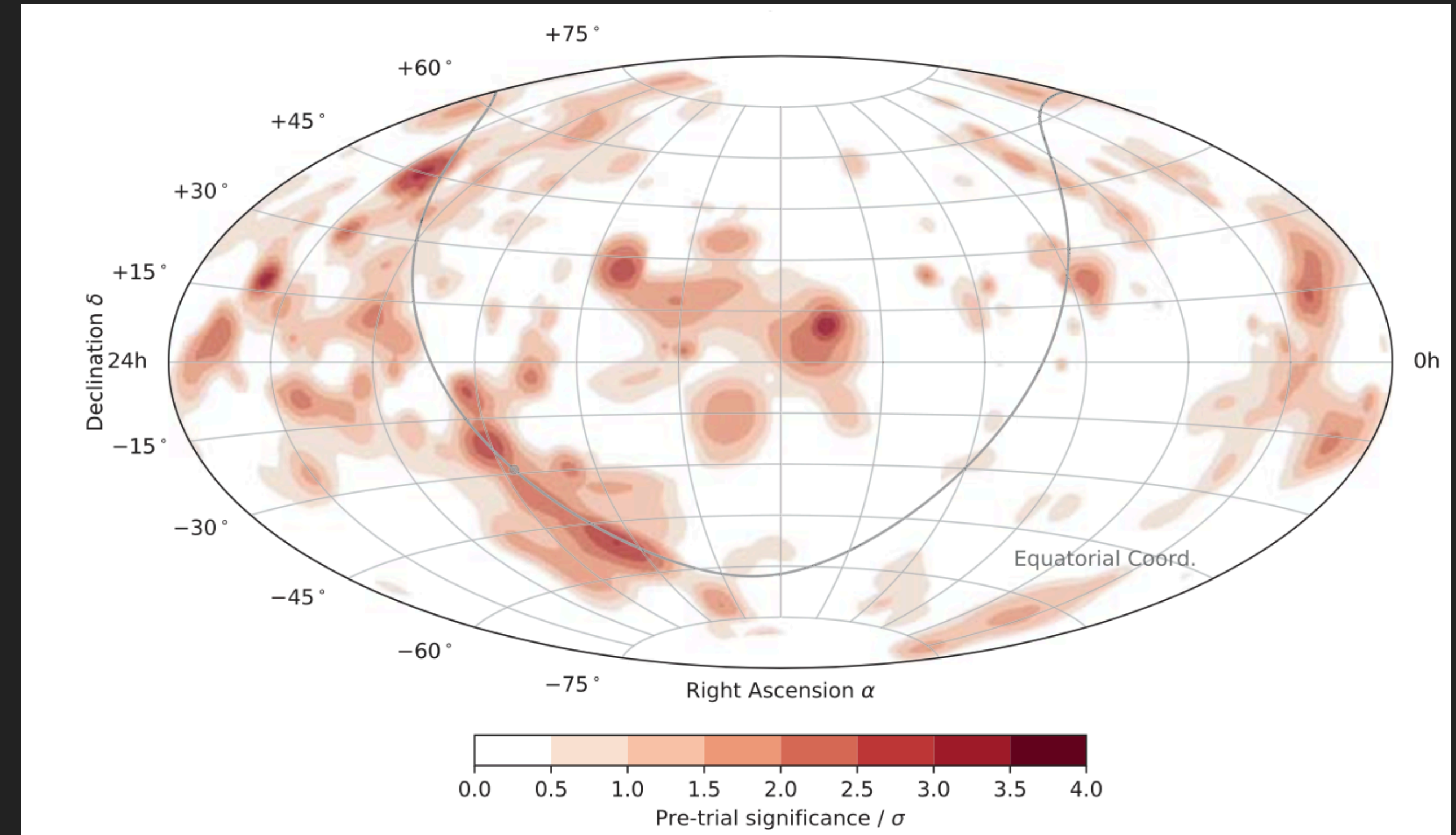
Yan & Liu (2023; 2304.12574)



LHAASO Data

# THE INVISIBLE ELEPHANT IN THE ROOM

IceCube Collaboration (2023)

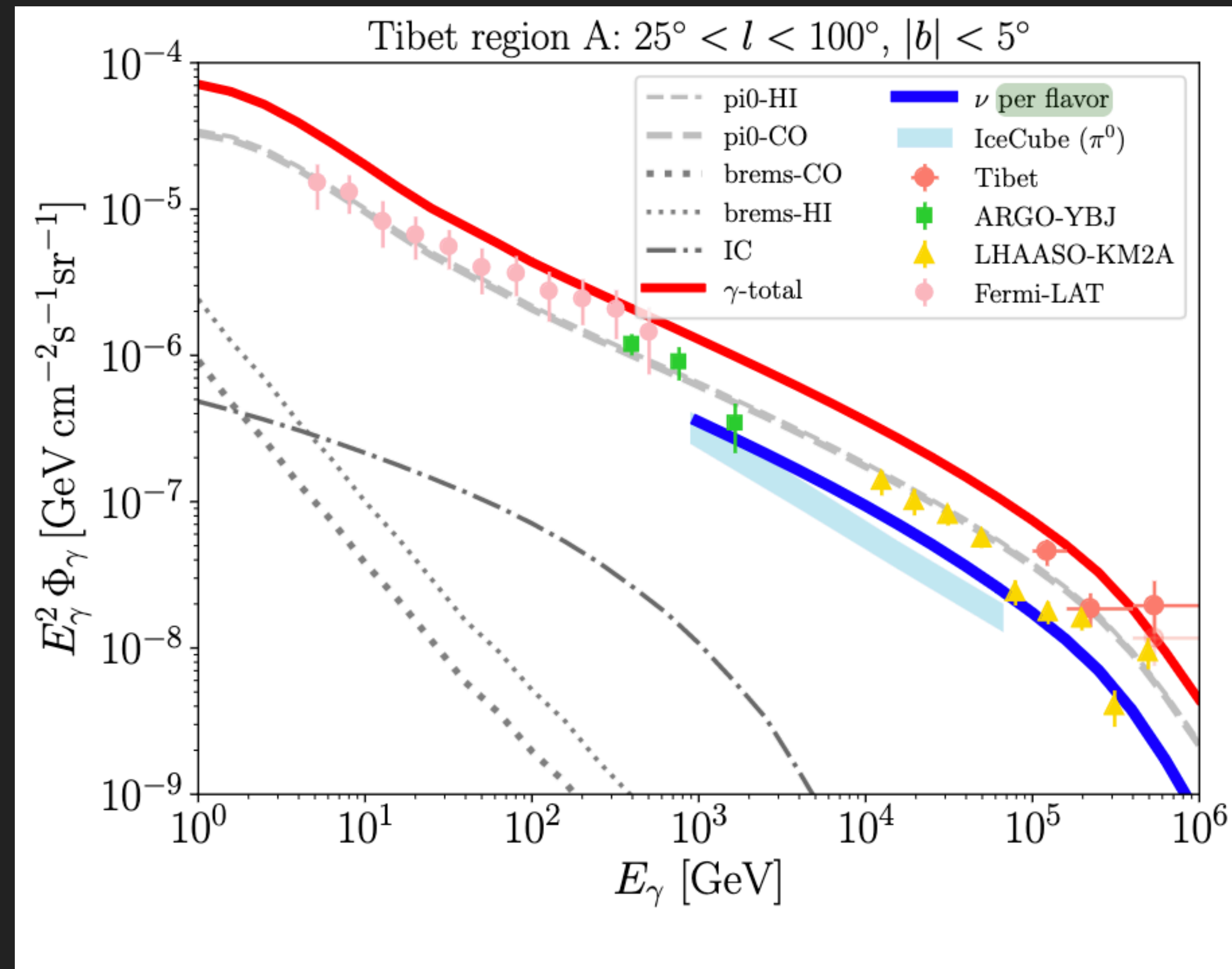


- ▶ IceCube detection of a galactic neutrino flux – with a normalization that is  $\sim 4\times$  brighter than expectations from the Fermi-LAT extrapolation.

# THE INVISIBLE ELEPHANT IN THE ROOM

Fang et al. (2023; 2306.17275)

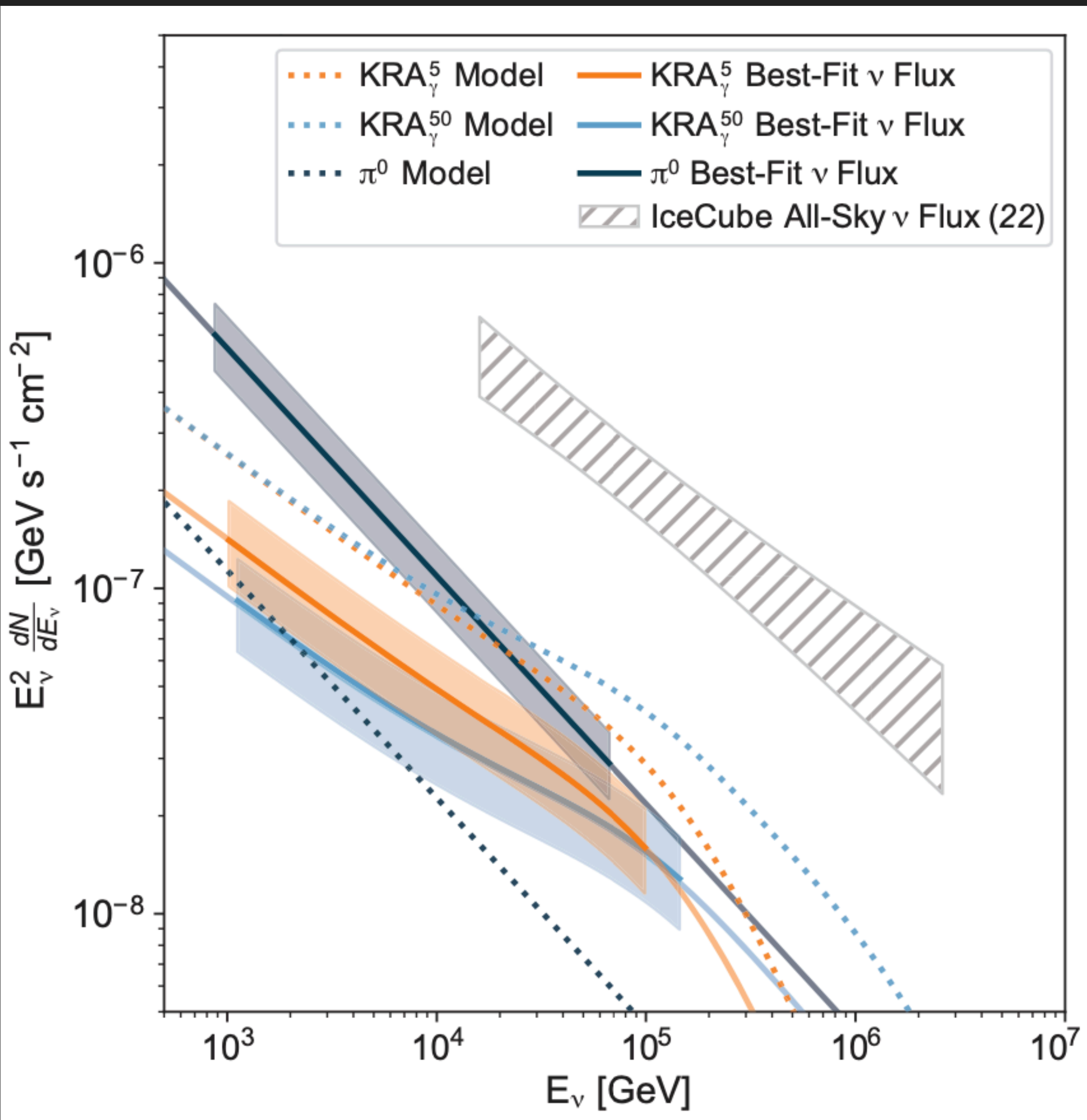
- ▶ If the IceCube neutrino flux from the galaxy is higher, then the gamma-ray flux from hadronic processes (i.e., not halos) could also be higher.
- ▶ In Fang et al. this is capable of producing the diffuse galactic gamma-ray emission



# MANY CAVEATS

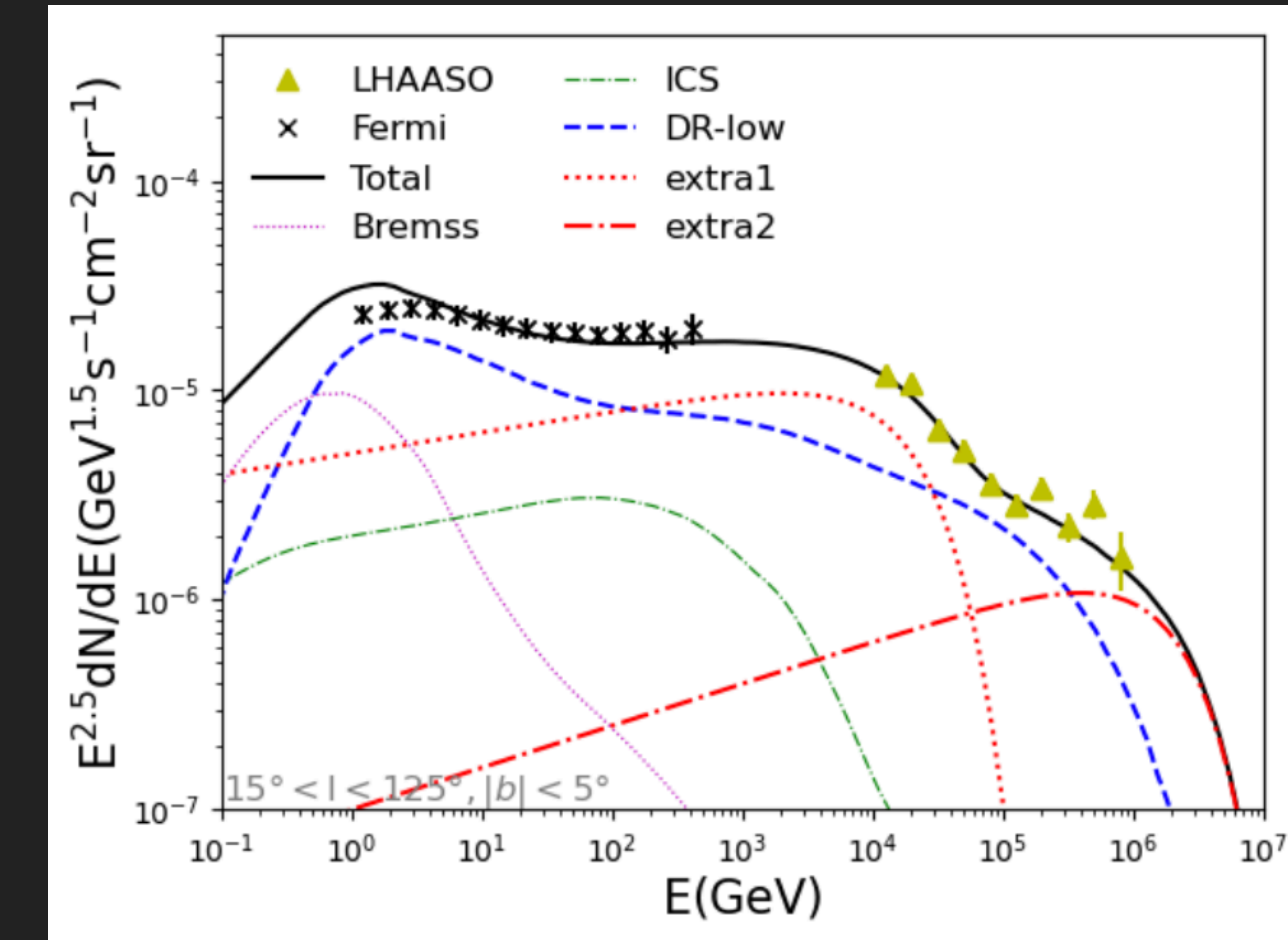
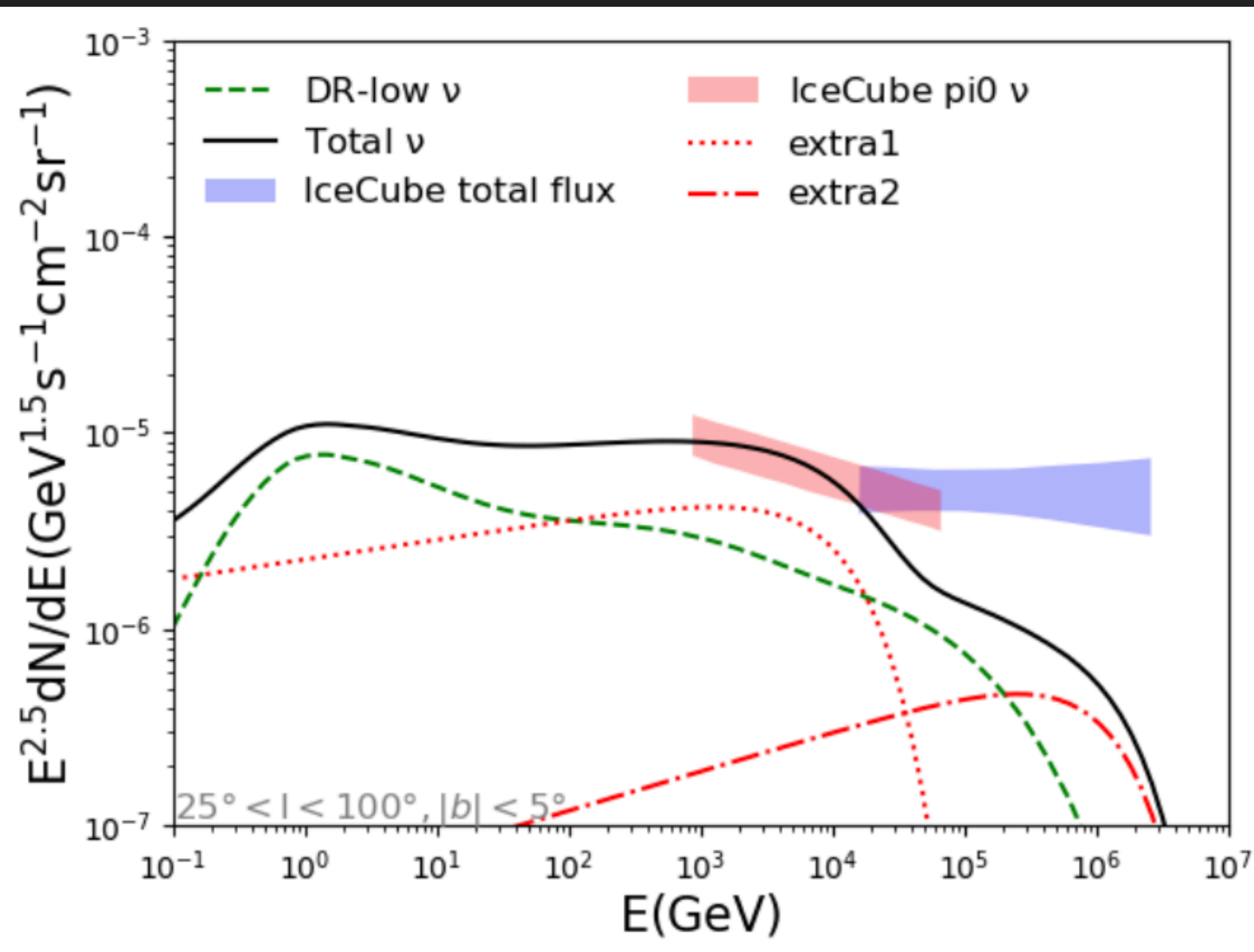
IceCube Collaboration (2023)

- ▶ IceCube neutrino flux is unknown at low energies (nearly order of magnitude uncertainties from models that fit the data to within  $1\sigma$ ).
- ▶ On top of this, there is an intrinsic factor of 2 uncertainty in even the IceCube flux measurement.
- ▶ There is also a factor of  $\sim 2$  uncertainty in the TeV halo flux owing to the “Geminga-like” assumption



# TEV HALO AND ICECUBE COMBINED MODEL

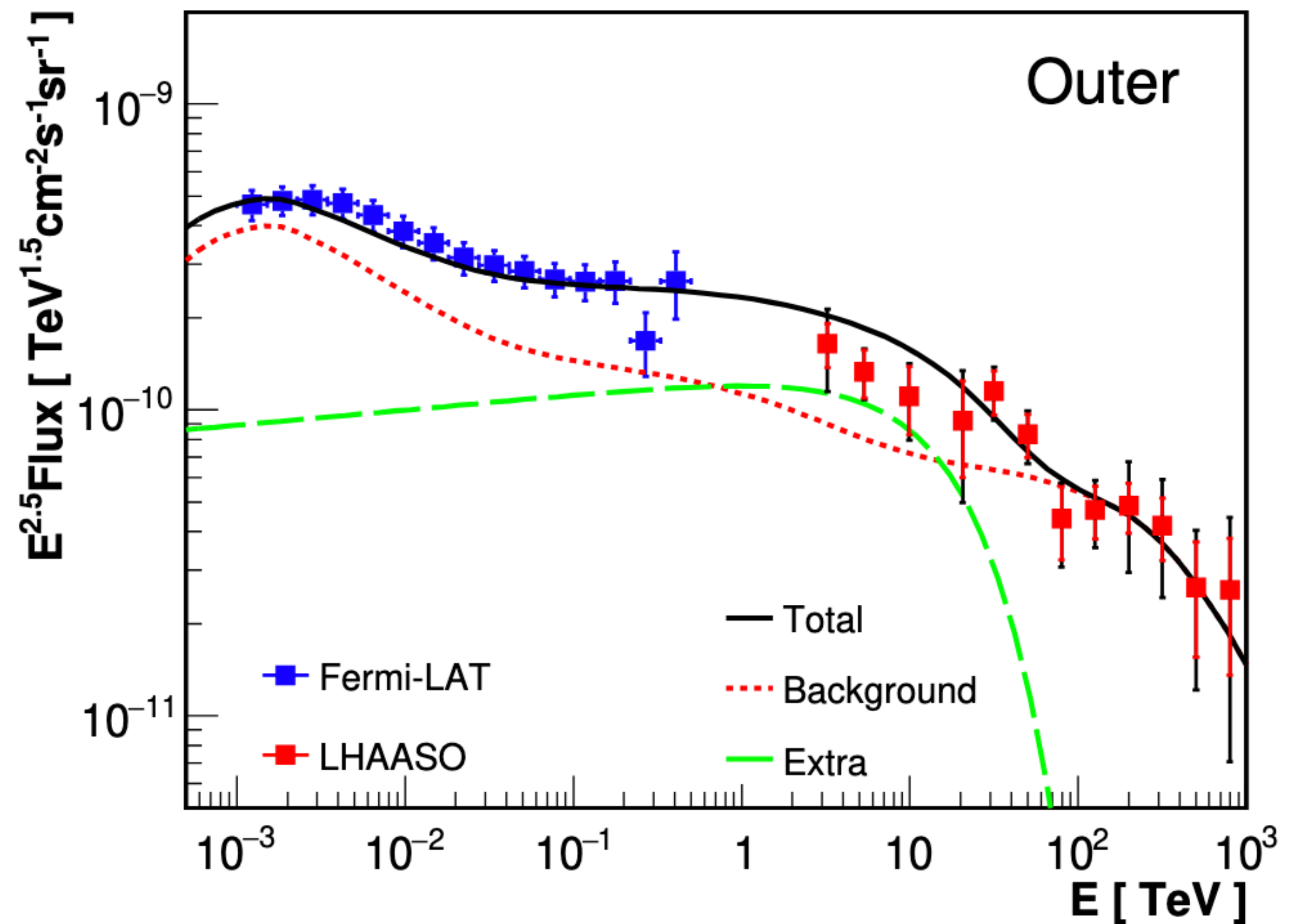
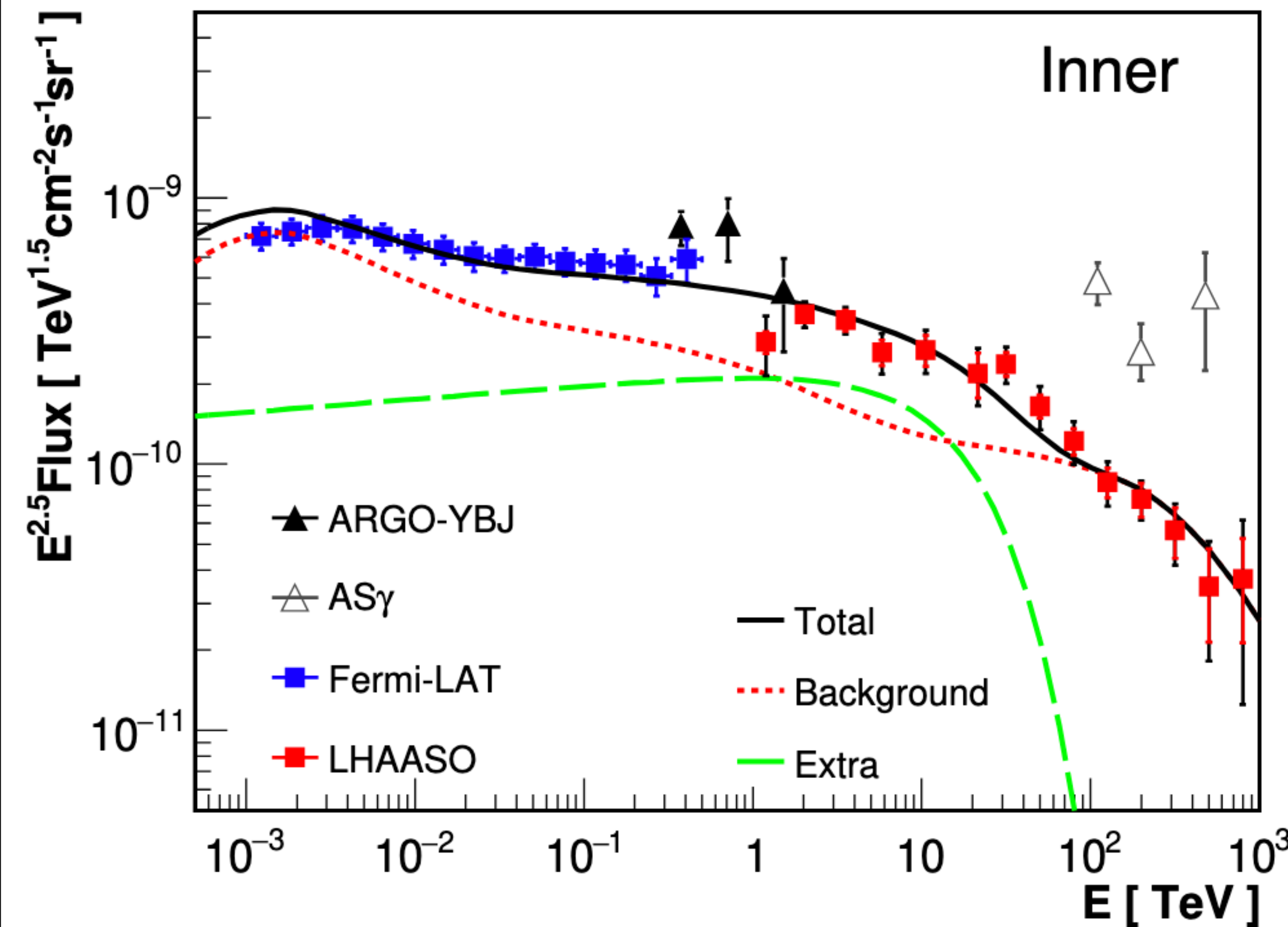
Shao et al. (2023; 2307.01038)



- Models that explain the IceCube neutrino flux still require an additional gamma-ray component (here: "Extra1 and Extra2") to produce the gamma-ray data from LHAASO.

# TEV HALO AND ICECUBE COMBINED MODEL

LHAASO Collaboration (2411.16021)



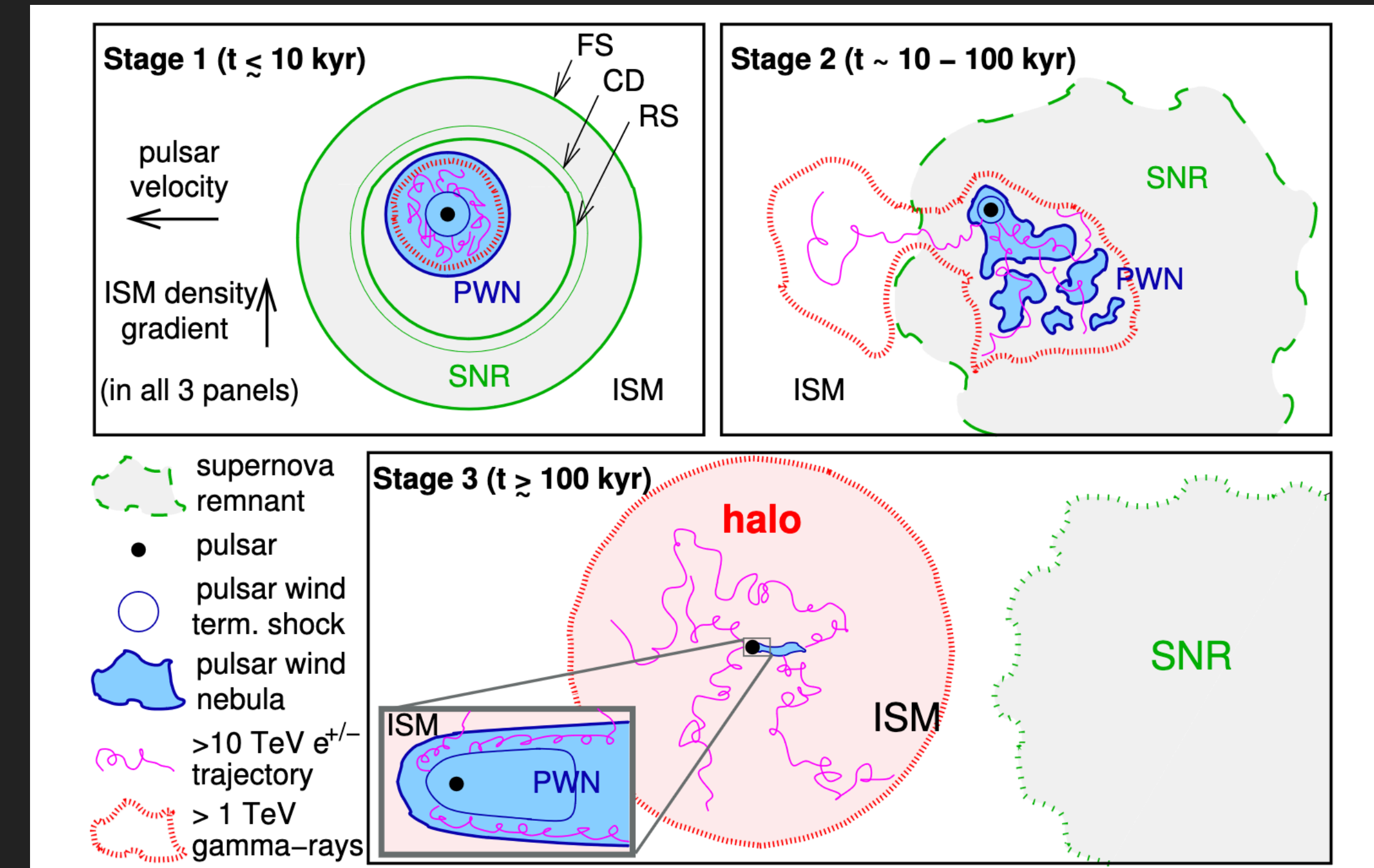
- Recently repeated in the LHAASO Diffuse Analysis

We're at now, now.



# DIFFERENCES IN DEFINITION - GOING BEYOND THE GEMINGA-MODEL

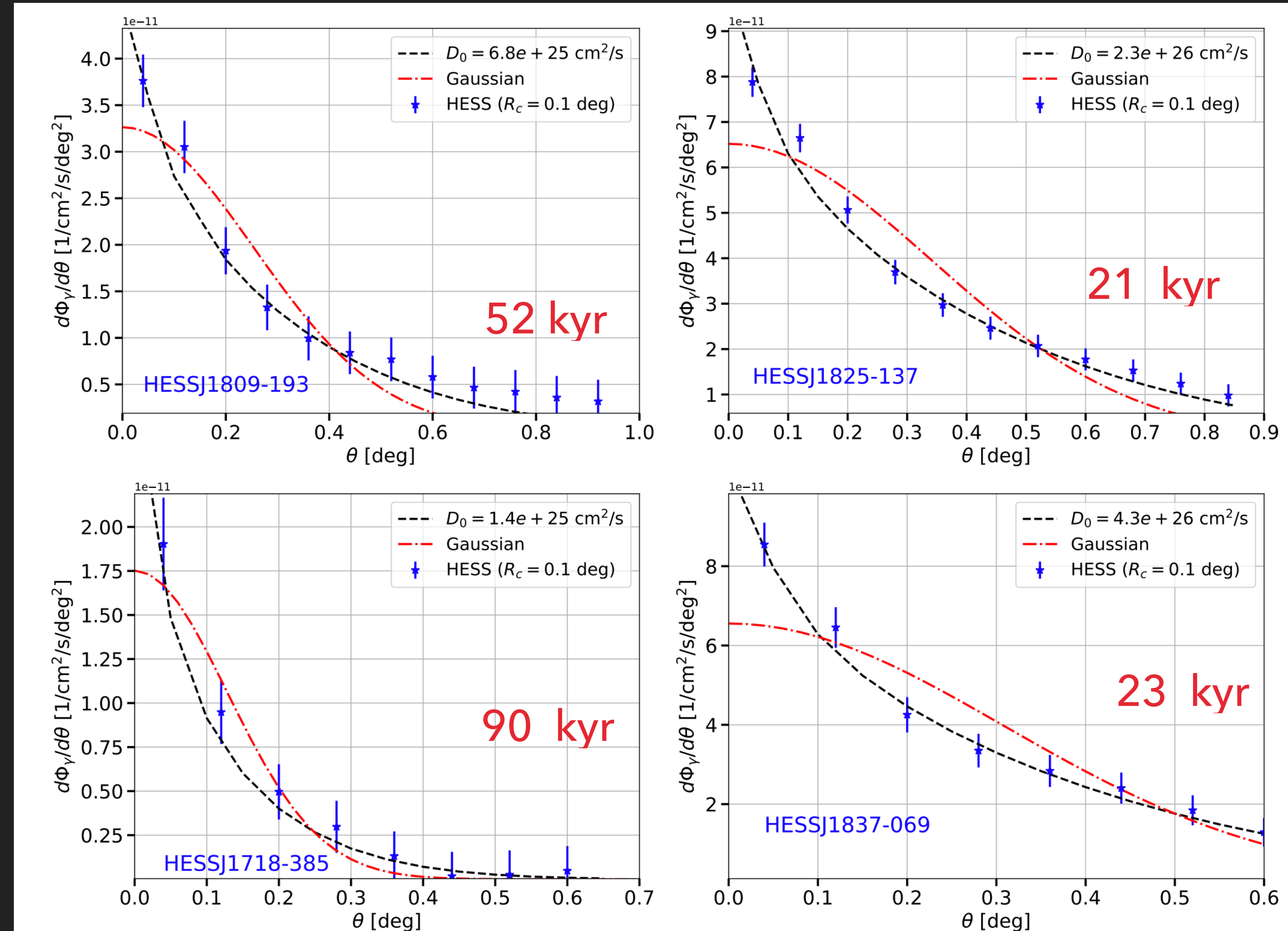
- An alternative definition of a “TeV halo” is used by Giacinti et al. 2019 (1907.12121)
- Linden et al. (2017) - A TeV halo is a leptonic gamma-ray source surrounding a pulsar, where the electrons are diffusing through the medium (rather than being driven by convective pulsar winds).
- Giacinti et al. (2019) - A TeV halo is a leptonic gamma-ray source surrounding a pulsar, where the emission stems from a region where the electron density falls below the ambient ISM electron density.



# ADOPTING A MAXIMALIST VERSION OF TEV HALOS - OBSERVATIONS

Di Mauro, Manconi, Donato (2019; 1908.03216)

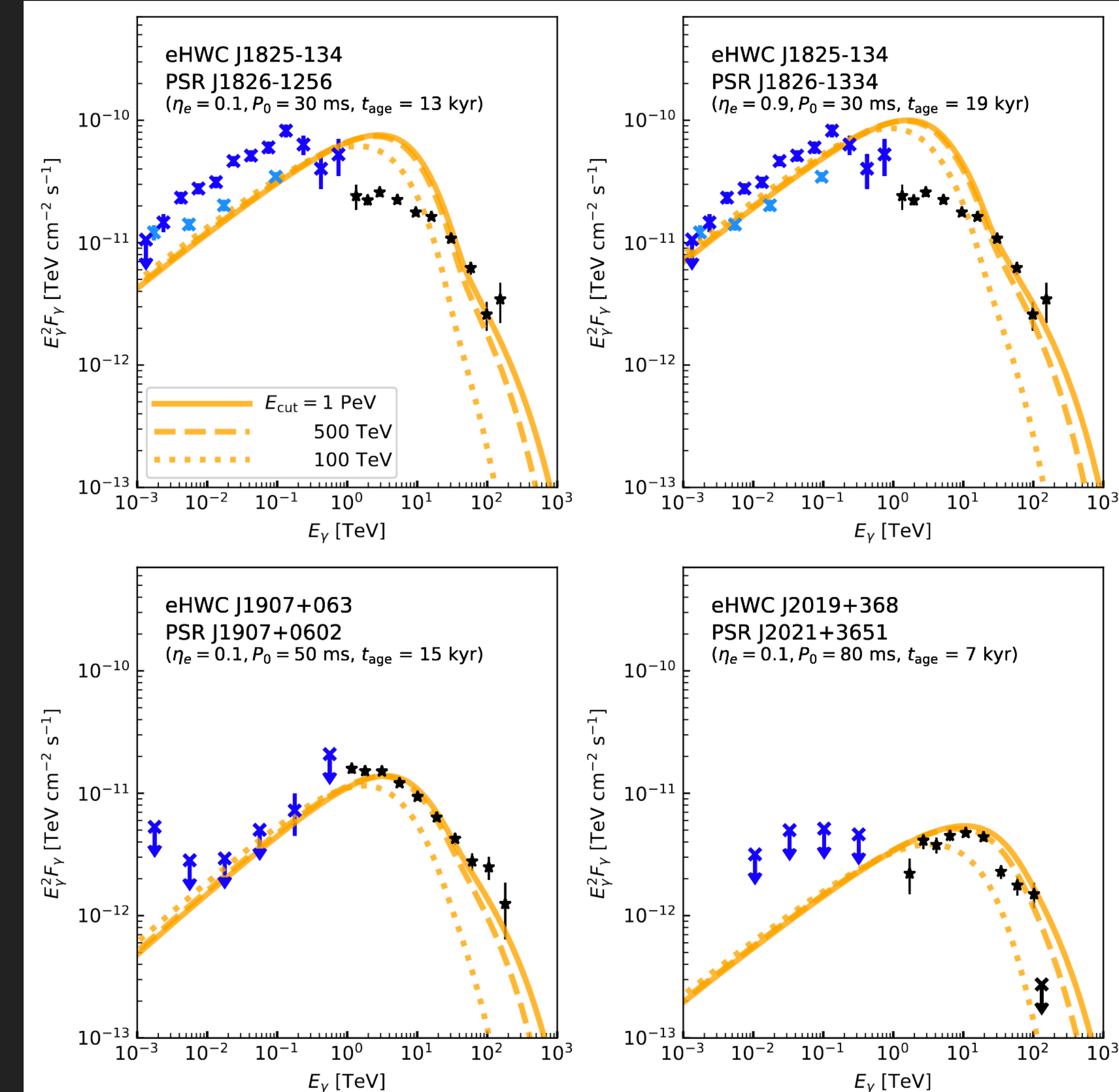
- ▶ In particular, this extended diffusive halos have been found in a number of young systems.
- ▶ Inhibited diffusion appears to occur very soon after system formation, and persist for a long time.



# ADOPTING A MAXIMALIST VERSION OF TEV HALOS - OBSERVATIONS

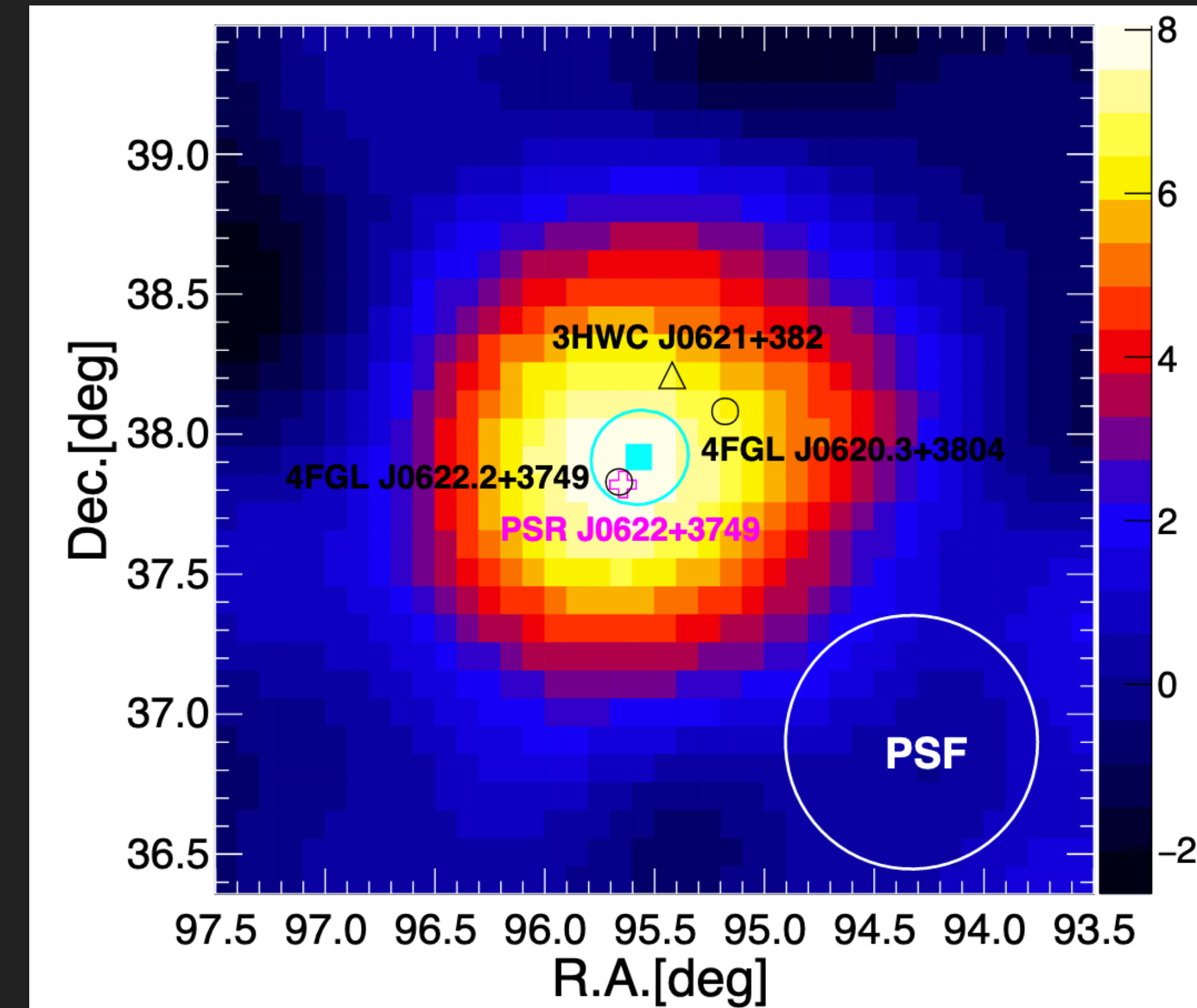
Sudoh, Linden, Hooper (2101.11026)

- ▶ 8 out of the 9 HAWC sources observed above 56 TeV are consistent with the location of young pulsars.
- ▶ Likely PWN or composite objects – but TeV halo contributions must be carefully examined.



# ADOPTING A MAXIMALIST VERSION OF TEV HALOS - OBSERVATIONS

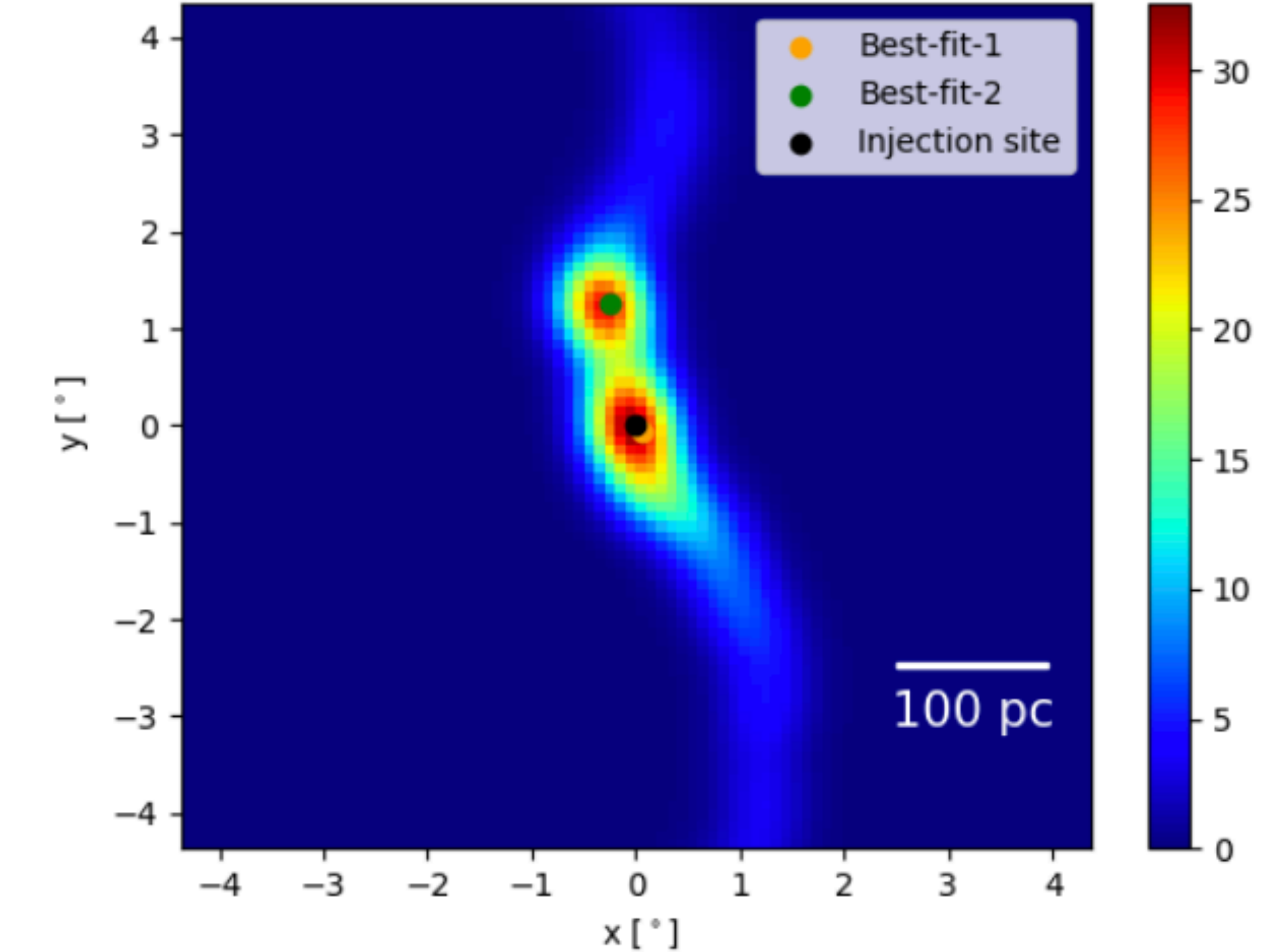
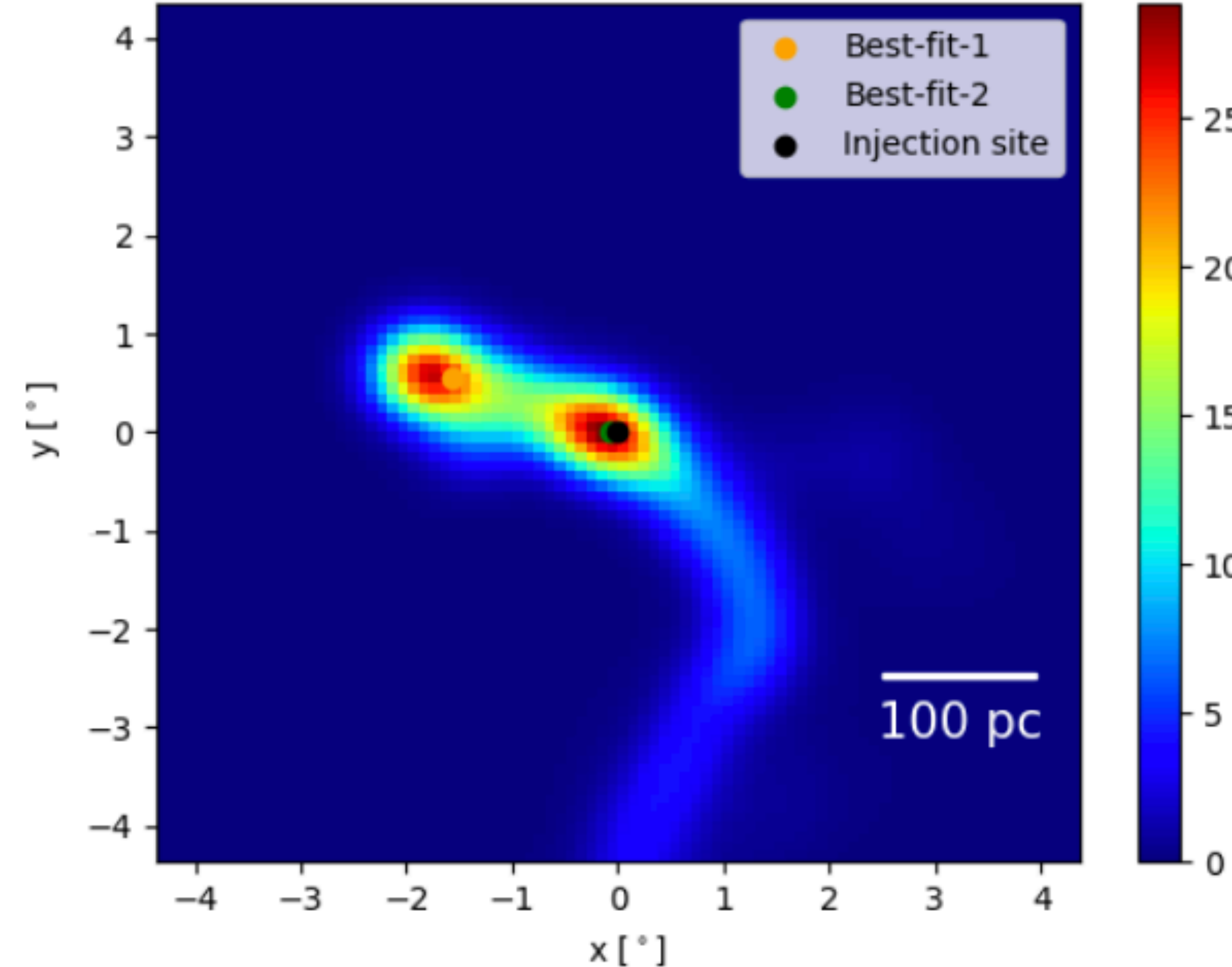
- ▶ TeV Halos (Observationally):
- ▶ Detected by all instruments (HAWC, LHAASO, HESS, VERITAS)
- ▶ Currently just the tip of the iceberg: Detected systems are nearby, or have high spin down power.



ATNF Name	Dec. ( $^{\circ}$ )	Distance (kpc)	Age (kyr)	Spindown Lum. ( $\text{erg s}^{-1}$ )	Spindown Flux ( $\text{erg s}^{-1} \text{kpc}^{-2}$ )	2HWC
J0633+1746	17.77	0.25	342	3.2e34	4.1e34	2HWC J0631+169
B0656+14	14.23	0.29	111	3.8e34	3.6e34	2HWC J0700+143
B1951+32	32.87	3.00	107	3.7e36	3.3e34	—
J1740+1000	10.00	1.23	114	2.3e35	1.2e34	—
J1913+1011	10.18	4.61	169	2.9e36	1.1e34	2HWC J1912+099
J1831-0952	-9.86	3.68	128	1.1e36	6.4e33	2HWC J1831-098
J2032+4127	41.45	1.70	181	1.7e35	4.7e33	2HWC J2031+415
B1822-09	-9.58	0.30	232	4.6e33	4.1e33	—
B1830-08	-8.45	4.50	147	5.8e35	2.3e33	—
J1913+0904	9.07	3.00	147	1.6e35	1.4e33	—
B0540+23	23.48	1.56	253	4.1e34	1.4e33	—

# ADOPTING A MAXIMALIST VERSION OF TEV HALOS - OBSERVATIONS

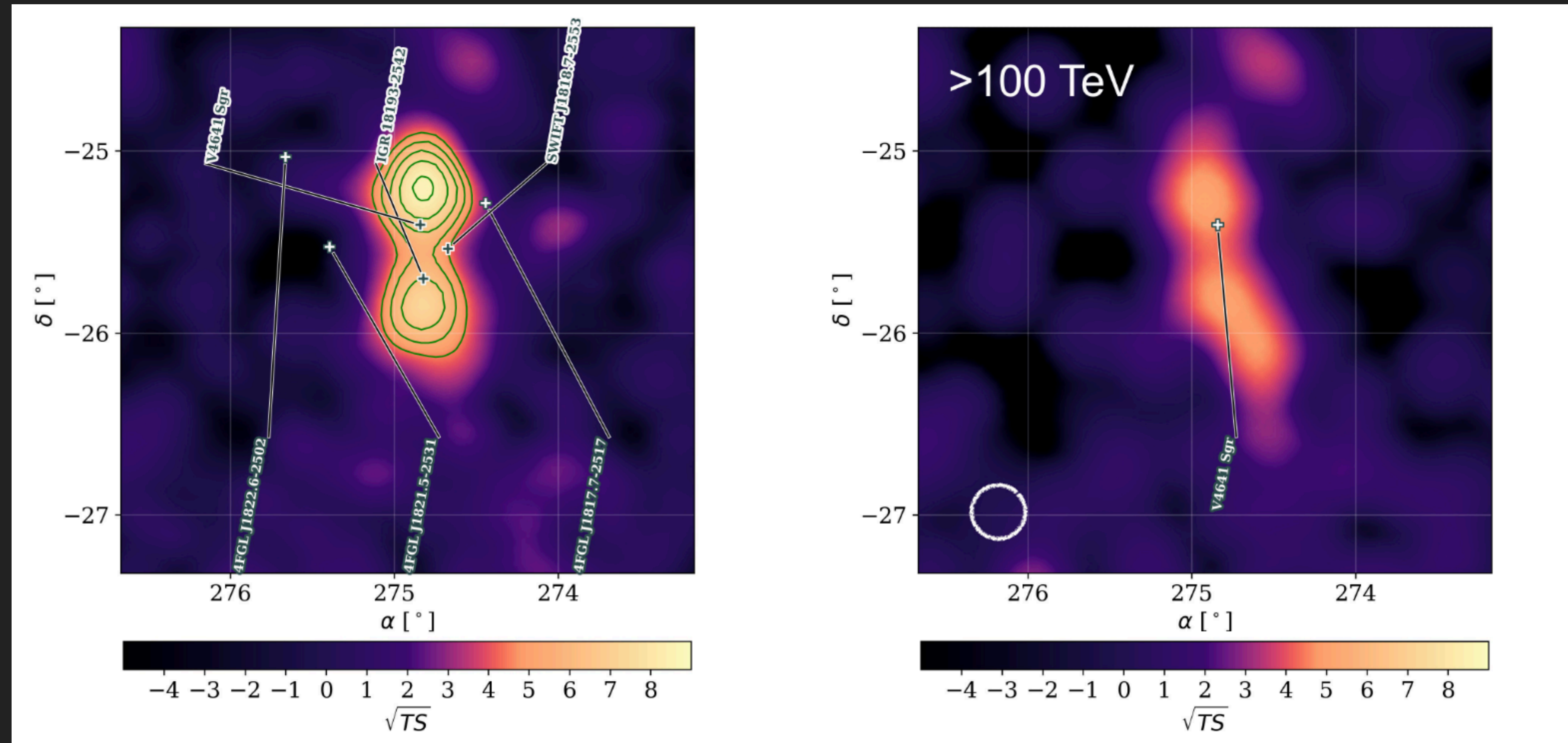
Bao et al. (2407.02478)



- ▶ “Mirage” TeV halos - Many more systems may be difficult to detect or analyze, because they break the modeling assumption of spherical symmetry.

# ADOPTING A MAXIMALIST VERSION OF TEV HALOS - OBSERVATIONS

HAWC Collaboration (2410.16117)



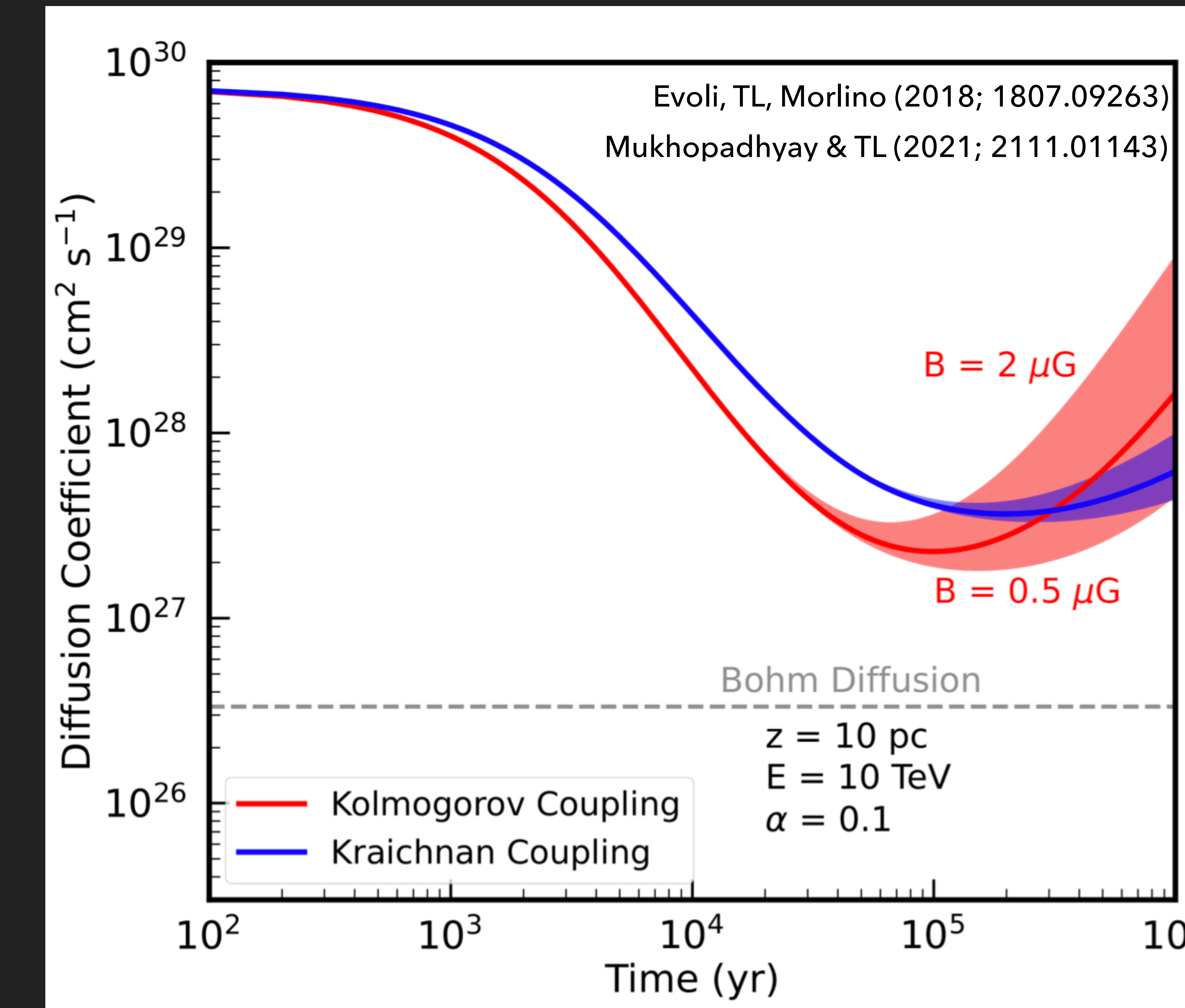
- May be particularly interesting in light of the V4641 Sgr Microquasar, which - while a different acceleration mechanism, also shows evidence of asymmetric diffusion.

# ADOPTING A MAXIMALIST VERSION OF TEV HALOS - THEORY

- ▶ Self-confinement models (and most other models for inhibited diffusion) - require the high energy of a very young pulsar.
- ▶ Probing the diffusion around the youngest systems is critical for understanding TeV halo dynamics.

$$\frac{\partial \mathcal{W}}{\partial t} + v_A \frac{\partial \mathcal{W}}{\partial z} = (\Gamma_{\text{CR}} - \Gamma_D) \mathcal{W}(k, z, t)$$

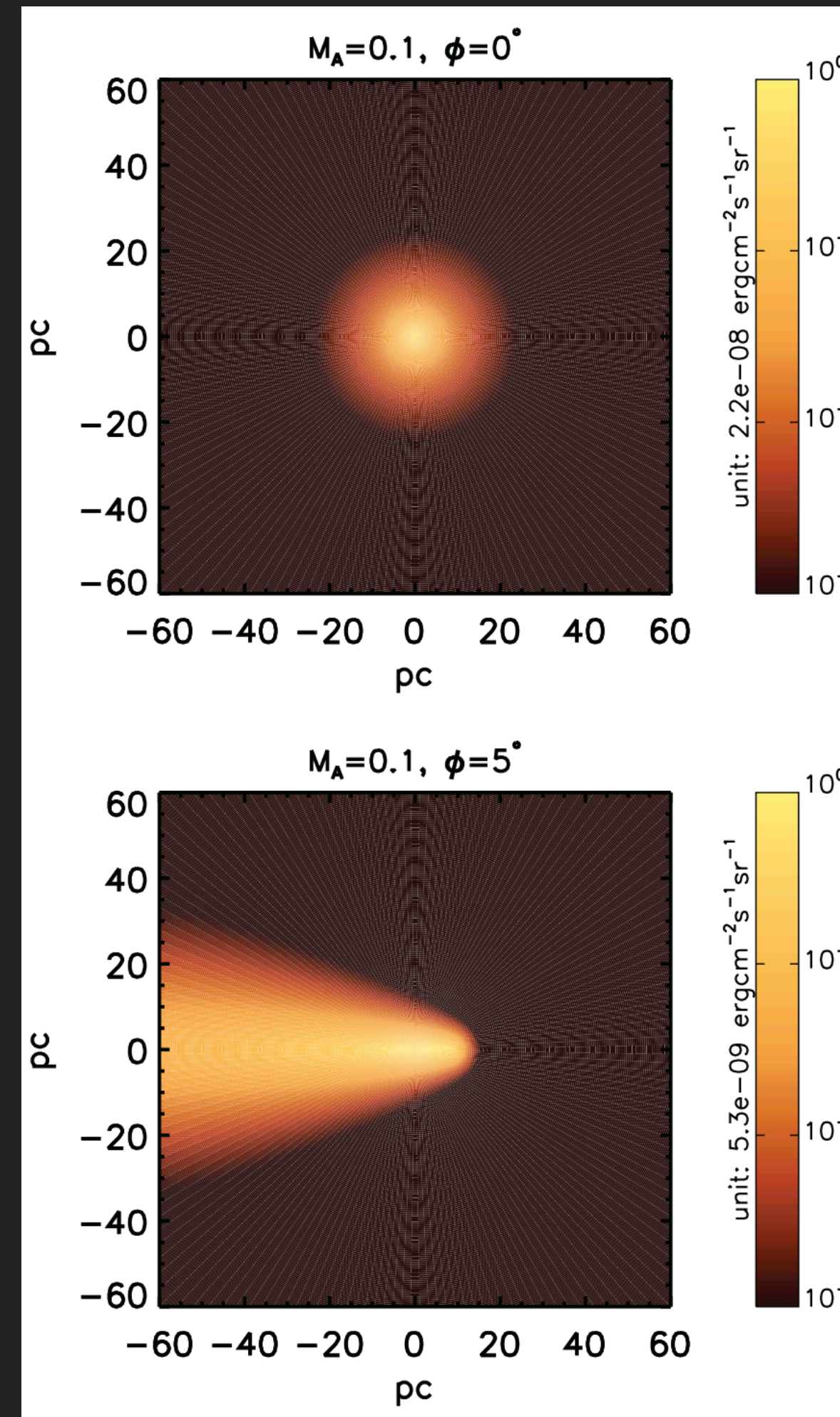
$$\Gamma_{\text{CR}}(k) = \frac{2\pi}{3} \frac{c|v_A|}{k\mathcal{W}(k) U_0} \left[ p^4 \frac{\partial f}{\partial z} \right]_{p_{\text{res}}}$$



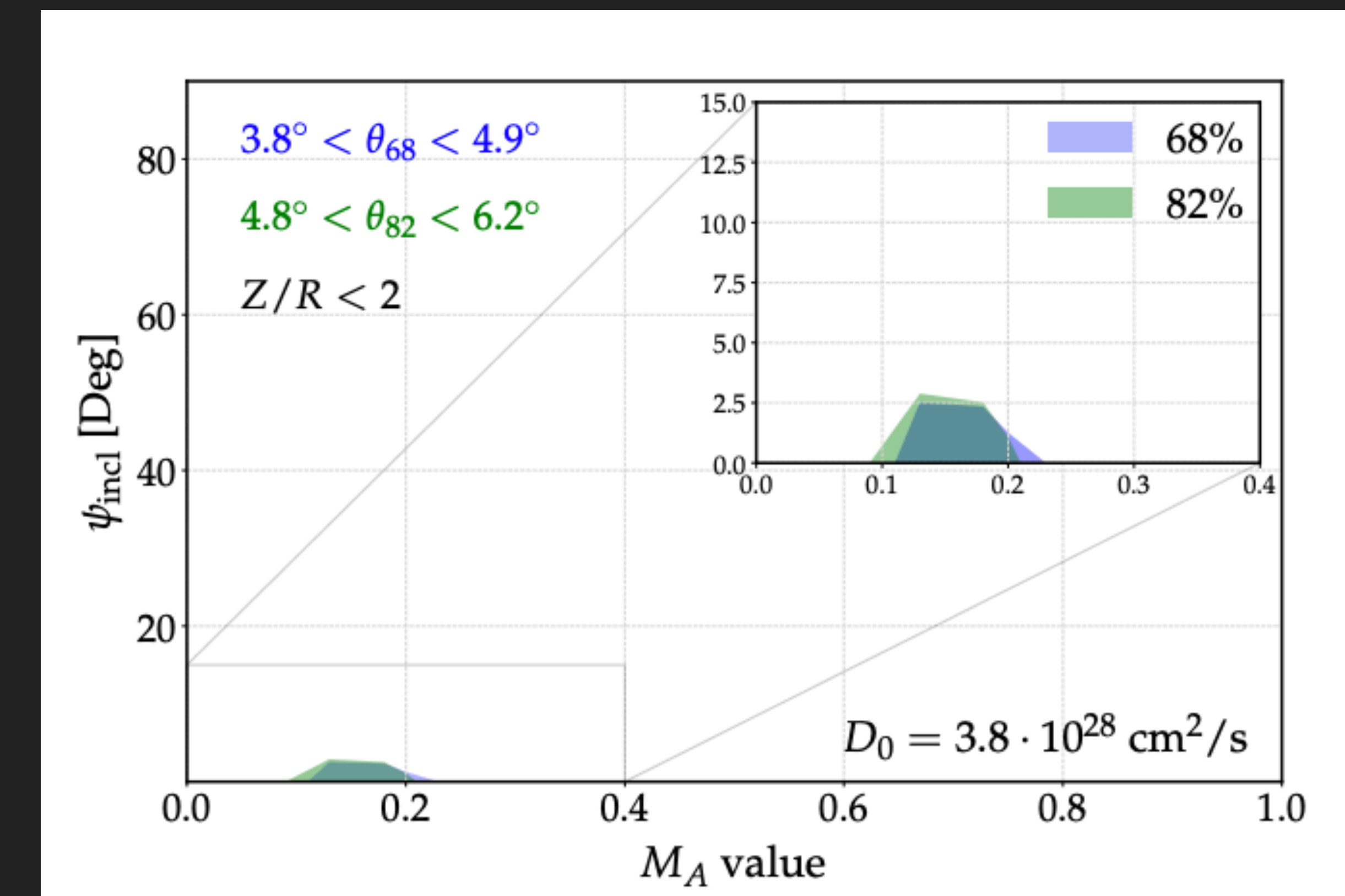
# THE PRESENT: UNDERSTANDING DIFFUSION IN TEV HALOS

- By combining the large number of TeV halo observations along with energetic considerations – we know that local diffusion must be inhibited.

Liu, Yan, Zhang (2019; 1904.11536)



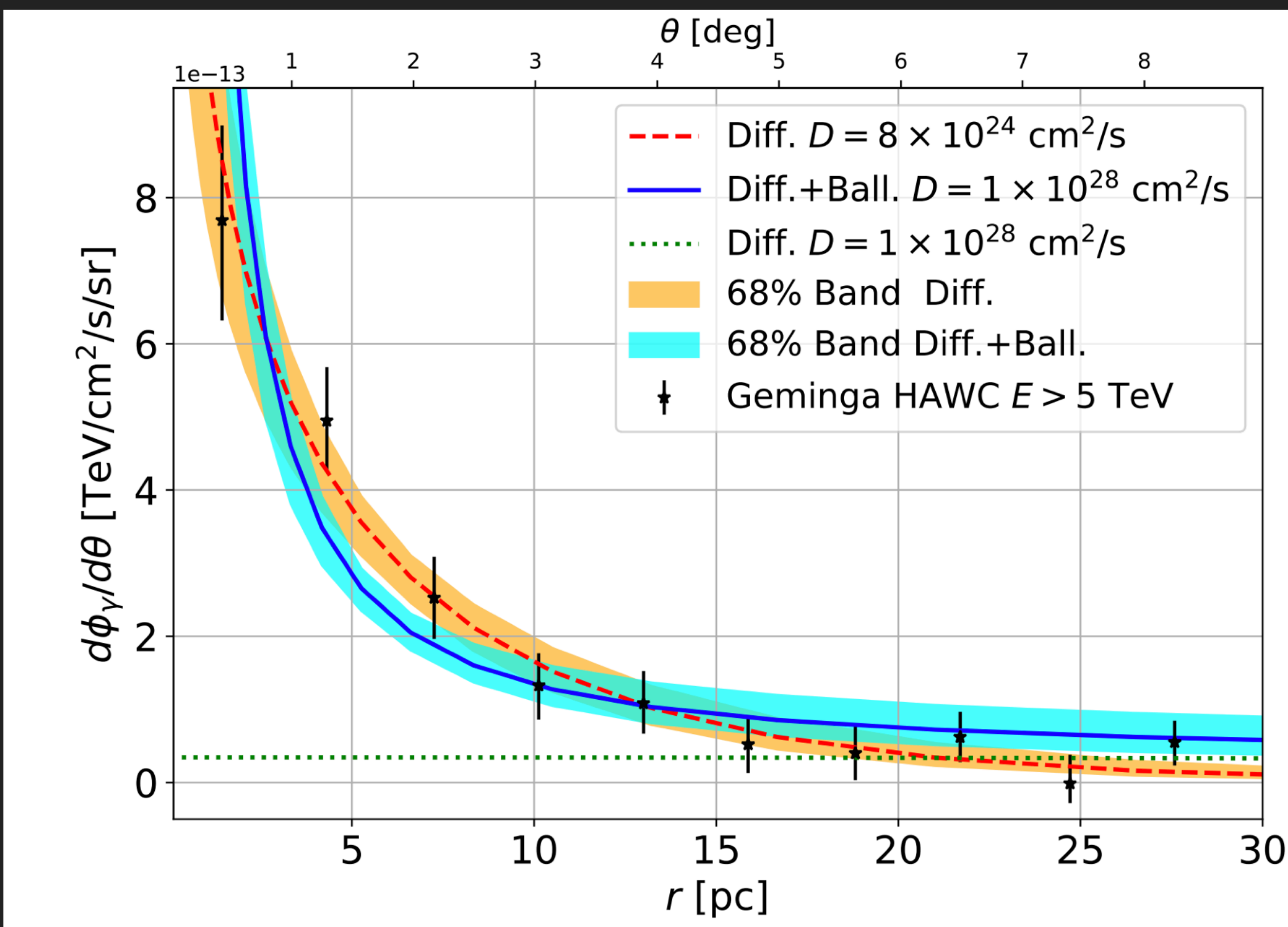
De la Torre Luque et al. (2022; 2205.08544)



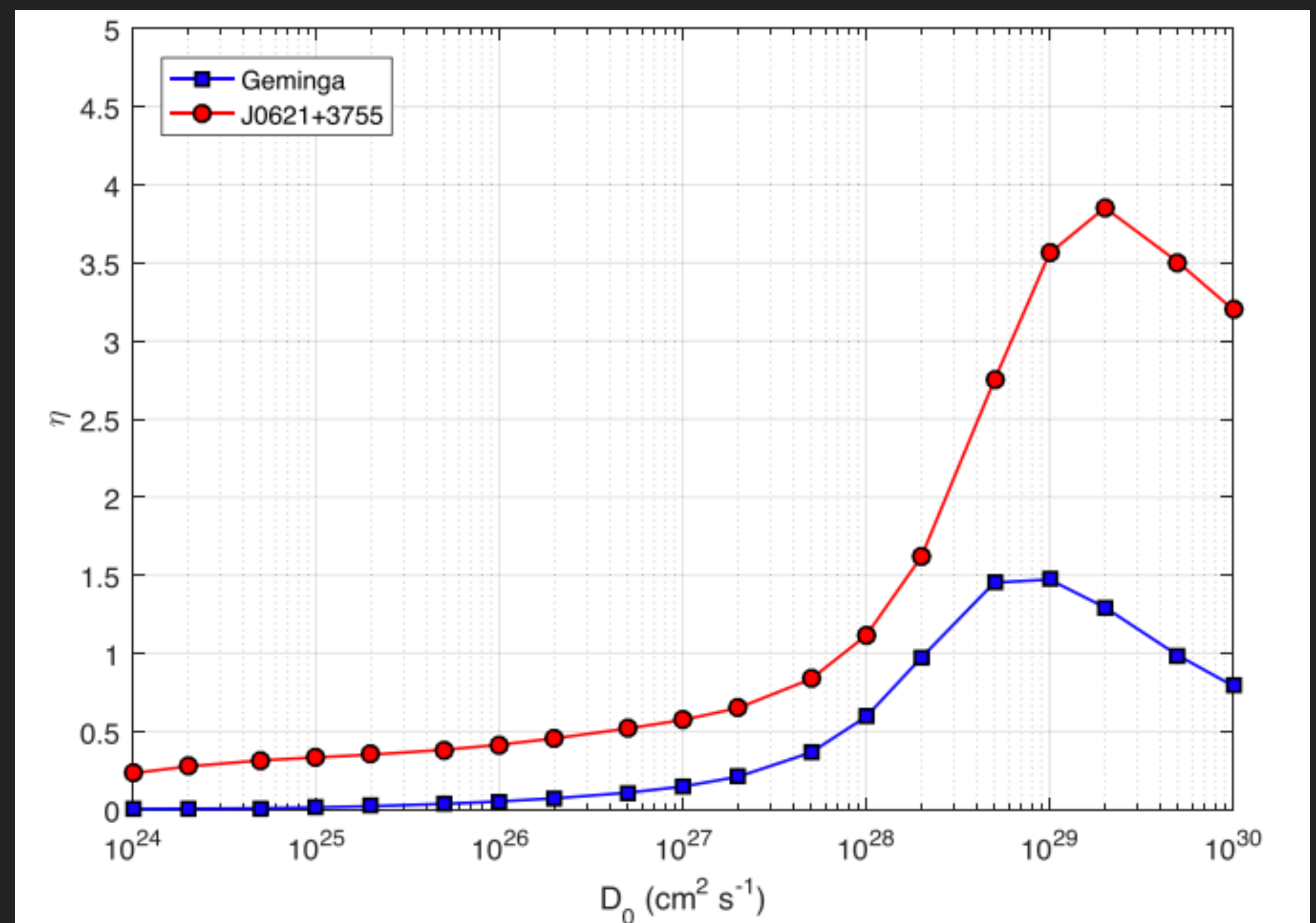
# TAKING A DEEPER DIVE INTO INHIBITED DIFFUSION

- By combining the large number of TeV halo observations along with energetic considerations – we know that local diffusion must be inhibited.

Recchia et al. (2021; 2106.02275)



Bao et al. (2021; 2107.07395)



# TEV HALOS SOLVE COSMIC-RAY DIFFUSION

Evoli, TL, Morlino (2018; 1807.09263)

Mukhopadhyay & TL (2021; 2111.01143)

$$\frac{\partial W}{\partial t} + v_A \frac{\partial W}{\partial z} = (\Gamma_{CR} + \Gamma_{NLD}) W(k, z, t)$$

$$\Gamma_{CR}(k) = \frac{2\pi}{3} \frac{c |v_\alpha|}{k W(k)} \left( \frac{B_0^2}{8\pi} \right)^{-1} \left[ p^4 \frac{\partial f}{\partial z} \right]_{p_{\text{res}}}$$

$$\Gamma_{NLD}(k) = c_k v_\alpha \begin{cases} k^{3/2} W^{1/2} & \text{Kolmogorov} \\ k^2 W & \text{Kraichnan} \end{cases}$$

$$D(p, t) = \frac{4}{3\pi} \frac{cr_L(p))}{k_{\text{res}} W(z, k_{\text{res}}))}$$

# TEV HALOS SOLVE COSMIC-RAY DIFFUSION

---

- ▶ Many uncertainties in these models:

- ▶ Role of Supernova Remnant

- ▶ Disruption by molecular gas or magnetic fields

- ▶ Pulsar Proper Motion

- ▶ 1D vs. 3D diffusion

- ▶ non-Resonant Terms

- ▶ Halos in close proximity

## Possible origin of the slow-diffusion region around Geminga

Kun Fang<sup>1\*</sup> Xiao-Jun Bi<sup>1,2†</sup> Peng-Fei Yin<sup>1‡</sup>

<sup>1</sup> Key Laboratory of Particle Astrophysics, Institute of High Energy Physics, Chinese Academy of Sciences, Beijing 100049, China

<sup>2</sup> School of Physical Sciences, University of Chinese Academy of Sciences, Beijing 100049, China

23 July 2019

### ABSTRACT

Geminga pulsar is surrounded by a multi-TeV  $\gamma$ -ray halo radiated by the high energy electrons and positrons accelerated by the central pulsar wind nebula (PWN). The angular profile of the  $\gamma$ -ray emission reported by HAWC indicates an anomalously slow diffusion for the cosmic-ray electrons and positrons in the halo region around Geminga. In the paper we study the possible mechanism for the origin of the slow diffusion. At first, we consider the self-generated Alfvén waves due to the streaming instability of the electrons and positrons released by Geminga. However, even considering a very optimistic scenario for the wave growth, we find this mechanism DOES NOT work to account for the extremely slow diffusion at the present day if taking the proper motion of Geminga pulsar into account. The reason is straightforward as the PWN is too weak to generate enough high energy electrons and positrons to stimulate strong turbulence at the late time. We then propose an assumption that the strong turbulence is generated by the shock wave of the parent supernova remnant (SNR) of Geminga. Geminga may still be inside the SNR, and we find that the SNR can provide enough energy to generate the slow-diffusion circumstance. The TeV halos around PSR B0656+14, Vela X, and PSR J1826-1334 may also be explained under this assumption.

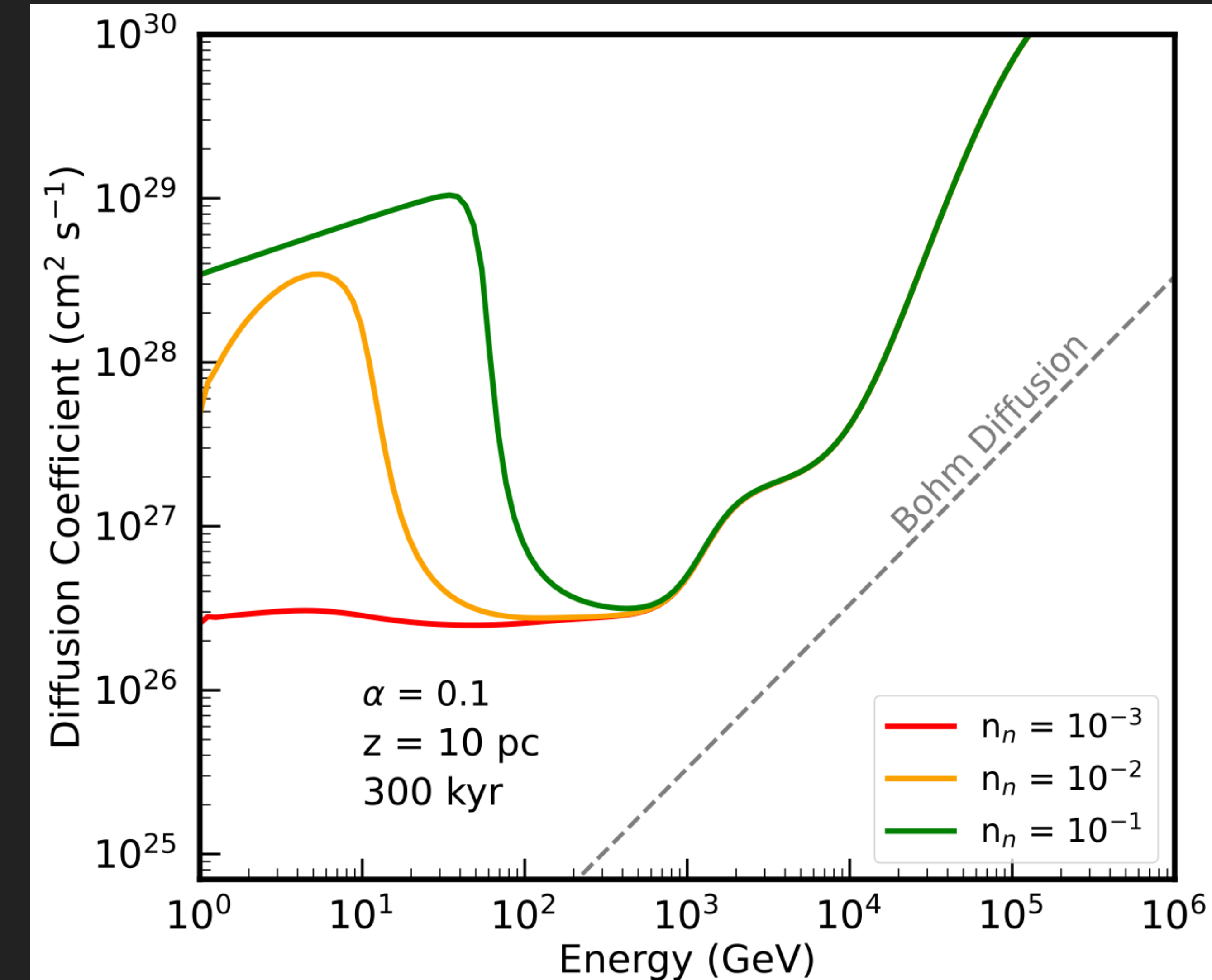
**Key words:** cosmic rays – ISM: individual objects: Geminga nebula – ISM: supernova remnants – turbulence

# TEV HALOS SOLVE COSMIC-RAY DIFFUSION

Evoli, TL, Morlino (2018; 1807.09263)

Mukhopadhyay & TL (2021; 2111.01143)

- ▶ Many uncertainties in these models:
  - ▶ Role of Supernova Remnant
  - ▶ Disruption by molecular gas or magnetic fields
  - ▶ Pulsar Proper Motion
  - ▶ 1D vs. 3D diffusion
  - ▶ non-Resonant Terms
  - ▶ Halos in close proximity



- ▶ Many uncertainties in these models:

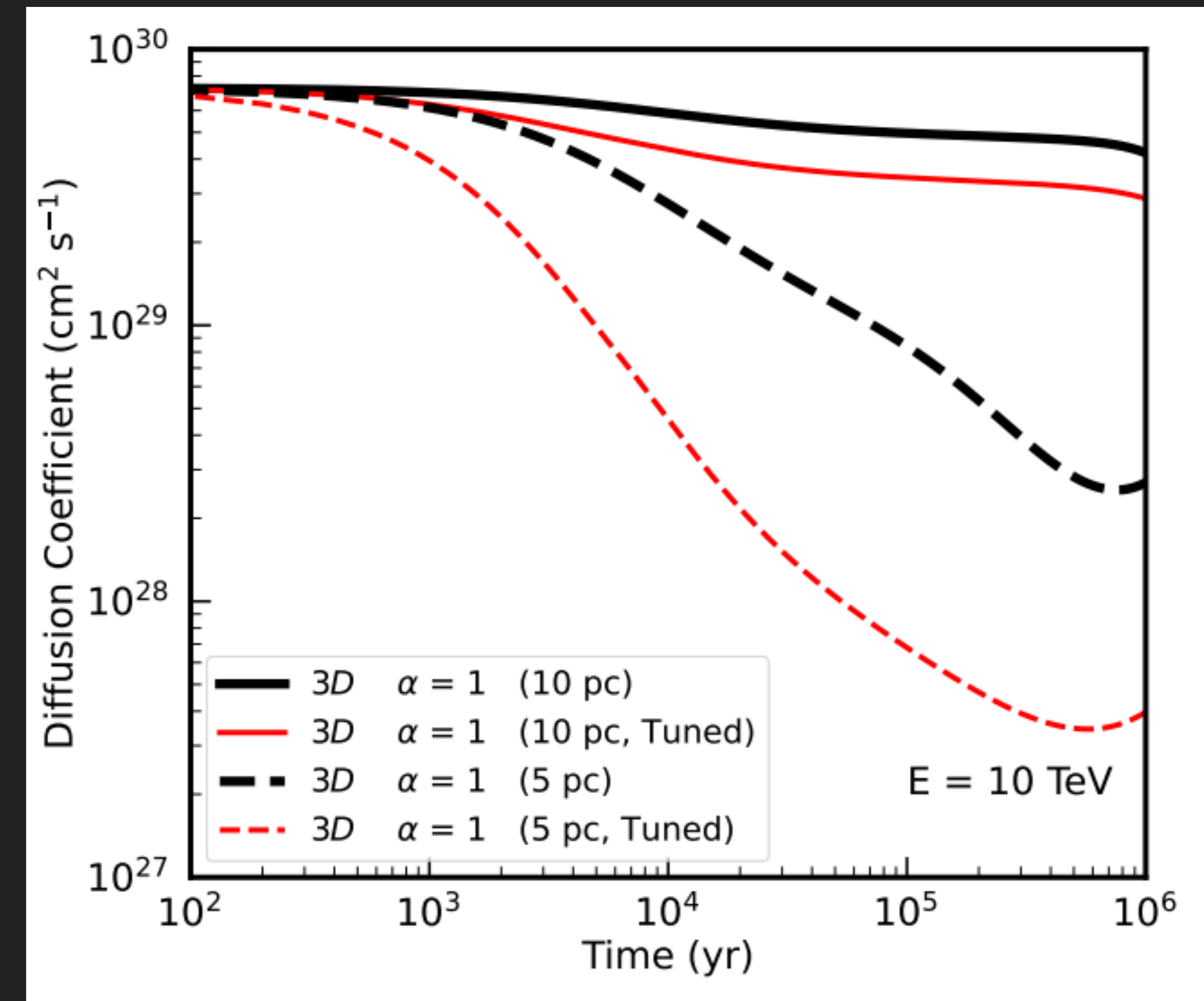
- ▶ Role of Supernova Remnant
- ▶ Disruption by molecular gas or magnetic fields
- ▶ Pulsar Proper Motion
- ▶ 1D vs. 3D diffusion
- ▶ non-Resonant Terms
- ▶ Halos in close proximity



# TEV HALOS SOLVE COSMIC-RAY DIFFUSION

Mukhopadhyay & TL (2021; 2111.01143)

- ▶ Many uncertainties in these models:
  - ▶ Role of Supernova Remnant
  - ▶ Disruption by molecular gas or magnetic fields
  - ▶ Pulsar Proper Motion
  - ▶ 1D vs. 3D diffusion
  - ▶ non-Resonant Terms
  - ▶ Halos in close proximity



- ▶ Many uncertainties in these models:

- ▶ Role of Supernova Remnant
- ▶ Disruption by molecular gas or magnetic fields
- ▶ Pulsar Proper Motion
- ▶ 1D vs. 3D diffusion
- ▶ non-Resonant Terms
- ▶ Halos in close proximity



- ▶ Many uncertainties in these models:

- ▶ Role of Supernova Remnant
- ▶ Disruption by molecular gas or magnetic fields
- ▶ Pulsar Proper Motion
- ▶ 1D vs. 3D diffusion
- ▶ non-Resonant Terms
- ▶ Halos in close proximity

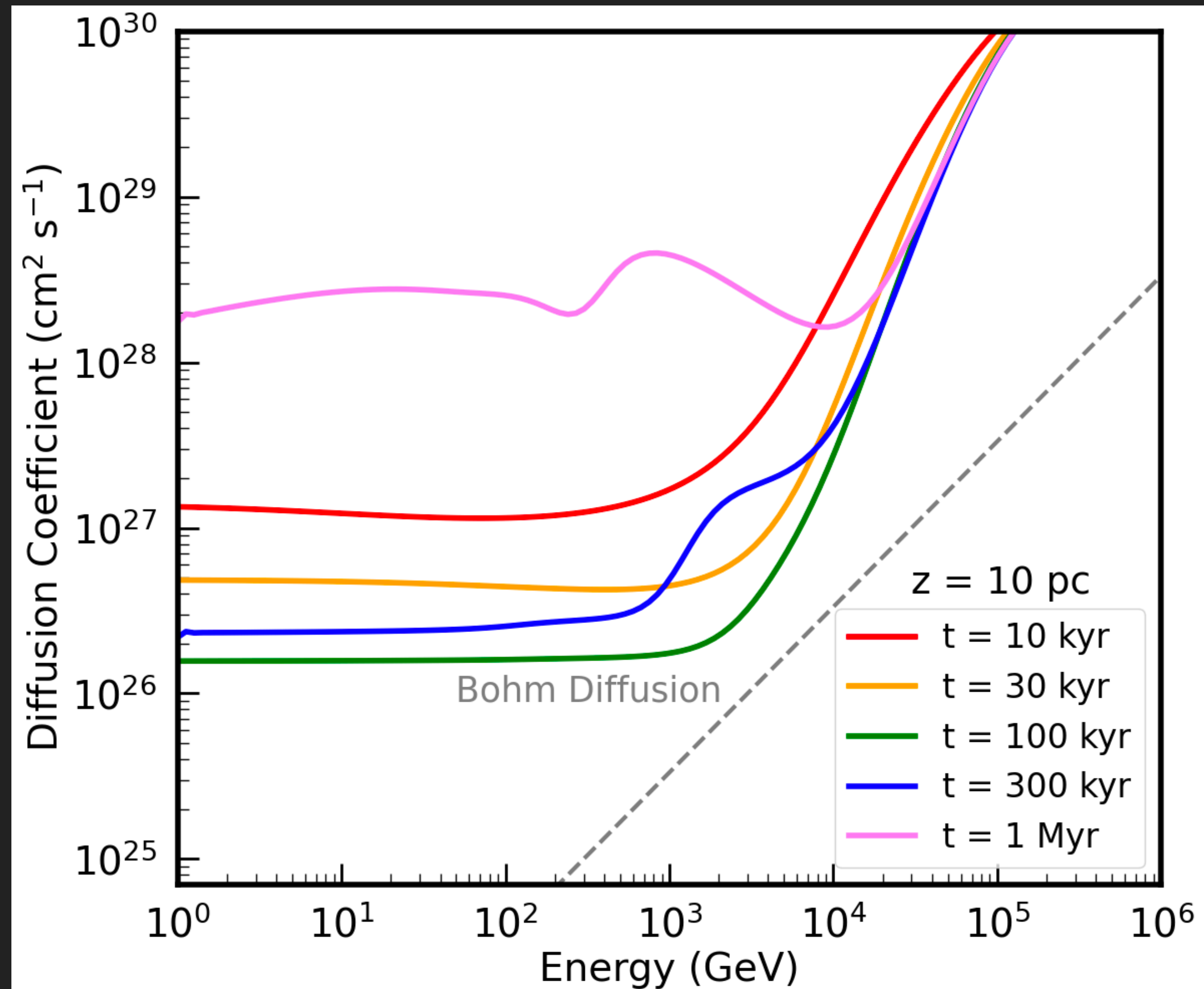


# TEV HALOS SOLVE COSMIC-RAY DIFFUSION

Evoli, TL, Morlino (2018; 1807.09263)

Mukhopadhyay & TL (2021; 2111.01143)

- ▶ Several Predictions of these Models:
  - ▶ Relatively flat low-energy diffusion coefficient.
  - ▶ Highly energy dependent diffusion coefficient at high energies.





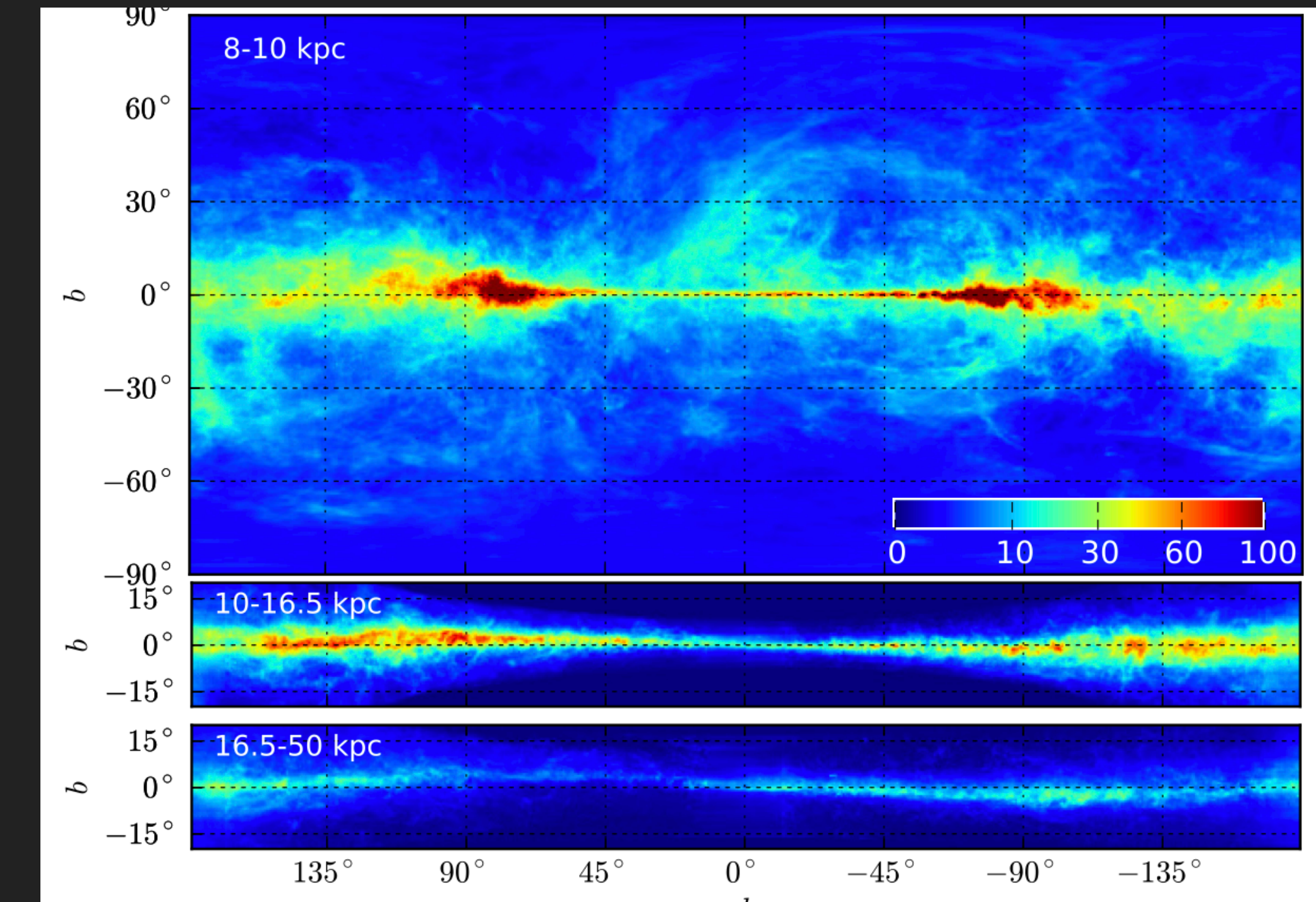
# THE FUTURE: THE PROMISE OF TEV HALOS FOR DIFFUSE EMISSION STUDIES

---

- ▶ High Angular Resolution
- ▶ Long energy-lever arm (20 GeV – 100 TeV)
- ▶ Bifurcation in electron/proton morphology
  - ▶  $D_{\text{proton}} \propto E^{\delta/2}$
  - ▶  $D_{\text{electron}} \propto E^{\delta/2-1}$

# NEED MODELS IN ORDER TO USE THESE OBSERVATIONS TO UNDERSTAND PHYSICS

$$\frac{\overbrace{\frac{\partial \psi(\vec{r}, p, t)}{\partial t}}^{\text{flux}}}{\text{source}} = \overbrace{Q(\vec{r}, p, t)} + \overbrace{\vec{\nabla} \times (\overbrace{D_{xx} \vec{\nabla} \psi}^{\text{diffusion}} - \overbrace{\vec{V} \psi}^{\text{convection}})} + \overbrace{\frac{\partial}{\partial p} p^2 D_{pp} \frac{\partial}{\partial p^2} \psi}^{\text{re-acceleration}}$$
$$-\underbrace{\frac{\partial}{\partial p} \left( \dot{p} \psi - \frac{p}{3} (\vec{\nabla} \times \vec{V}) \psi \right)}_{\text{energy loss}} - \underbrace{\frac{\psi}{\tau_f}}_{\text{fragmentation}} - \underbrace{\frac{\psi}{\tau_r}}_{\text{radioactive decay}}$$



# OVERVIEW OF DIFFUSE EMISSION MODELS AT GEV SCALES

---

## The GALPROP Cosmic-ray Propagation and Nonthermal Emissions Framework: Release v57

T. A. Porter<sup>1</sup> , G. Jóhannesson<sup>2</sup> , and I. V. Moskalenko<sup>1</sup> 

<sup>1</sup> W.W. Hansen Experimental Physics Laboratory and Kavli Institute for Particle Astrophysics and Cosmology, Stanford University, Stanford, CA 94305, USA  
[tporter@stanford.edu](mailto:tporter@stanford.edu)

<sup>2</sup> Science Institute, University of Iceland, IS-107 Reykjavik, Iceland

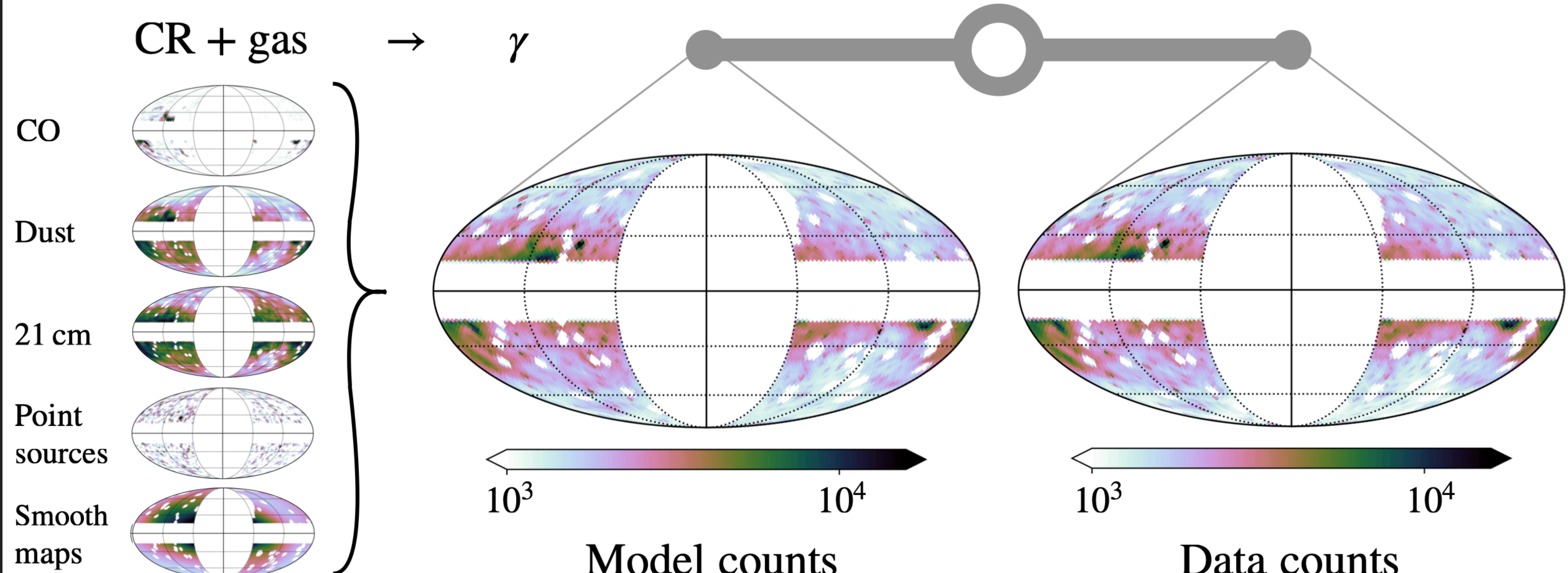
*Received 2021 December 22; revised 2022 July 10; accepted 2022 July 12; published 2022 September 9*

### Abstract

The past decade has brought impressive advances in the astrophysics of cosmic rays (CRs) and multiwavelength astronomy, thanks to the new instrumentation launched into space and built on the ground. Modern technologies employed by those instruments provide measurements with unmatched precision, enabling searches for subtle signatures of dark matter and new physics. Understanding the astrophysical backgrounds to better precision than the observed data is vital in moving to this new territory. A state-of-the-art CR propagation code, called GALPROP, is designed to address exactly this challenge. Having 25 yr of development behind it, the GALPROP framework has become a de facto standard in the astrophysics of CRs, diffuse photon emissions (radio to  $\gamma$ -rays), and searches for new physics. GALPROP uses information from astronomy, particle physics, and nuclear physics to predict CRs and their associated emissions self-consistently, providing a unifying modeling framework. The range of its physical validity covers 18 orders of magnitude in energy, from sub-keV to PeV energies for particles and from  $\mu$ eV to PeV energies for photons. The framework and the data sets are public and are extensively used by many experimental collaborations and by thousands of individual researchers worldwide for interpretation of their data and for making predictions. This paper details the latest release of the GALPROP framework and updated cross sections, further developments of its initially auxiliary data sets for models of the interstellar medium that grew into independent studies of the Galactic structure—distributions of gas, dust, radiation, and magnetic fields—as well as the extension of its modeling capabilities. Example applications included with the distribution illustrating usage of the new

# TEV HALOS BREAK GEV GAMMA-RAY DIFFUSE EMISSION MODELS

Widmark et al. (2022; 2208.11704)

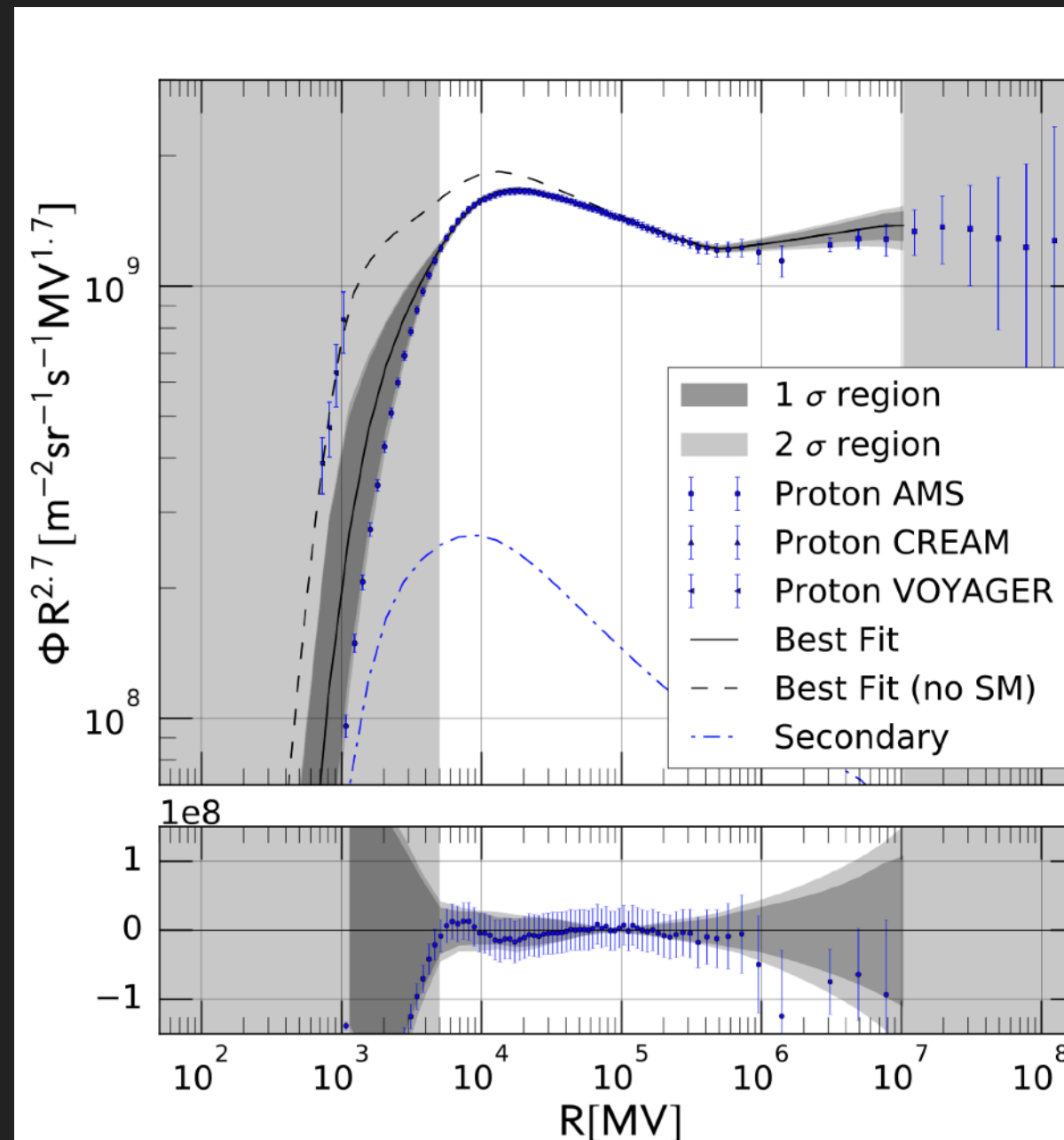


- Target models come from gas and dust tracers.
- CR density comes from Galprop simulations.

# TEV HALOS BREAK GEV GAMMA-RAY DIFFUSE EMISSION MODELS

Korsmeier & Cuoco (2016; 1607.06093)

Fit parameters	(uni-PHe)	(uni-PHePbar)	(P)	(PHe)	(main)	(diMauro)	(1GV)	(noVc-1GV)	(noVc-5GV)
$\gamma_{1,p}$	-	-	-	$1.52^{+0.21}_{-0.32}$	$1.27^{+0.11}_{-0.07}$	$1.36^{+0.07}_{-0.10}$	$1.38^{+0.07}_{-0.10}$	$1.32^{+0.05}_{-0.12}$	$1.61^{+0.06}_{-0.10}$
$\gamma_{2,p}$	-	-	-	$2.52^{+0.12}_{-0.45}$	$2.069^{+0.098}_{-0.069}$	$2.493^{+0.010}_{-0.026}$	$2.499^{+0.026}_{-0.014}$	$2.455^{+0.014}_{-0.007}$	$2.421^{+0.010}_{-0.014}$
$\gamma_1$	$1.92^{+0.08}_{-0.14}$	$1.50^{+0.07}_{-0.12}$	-	$1.53^{+0.24}_{-0.11}$	$1.29^{+0.04}_{-0.09}$	$1.26^{+0.10}_{-0.06}$	$1.32^{+0.06}_{-0.12}$	$1.65^{+0.07}_{-0.11}$	$1.70^{+0.06}_{-0.07}$
$\gamma_2$	$2.582^{+0.010}_{-0.034}$	$2.404^{+0.006}_{-0.022}$	-	$2.003^{+0.094}_{-0.003}$	$2.440^{+0.006}_{-0.018}$	$2.451^{+0.018}_{-0.010}$	$2.412^{+0.012}_{-0.006}$	$2.381^{+0.010}_{-0.010}$	$2.407^{+0.022}_{-0.014}$
$R_0$ [GV]	$8.16^{+1.22}_{-1.54}$	$8.79^{+1.17}_{-1.55}$	$4.38^{+3.23}_{-1.54}$	$10.5^{+1.40}_{-1.59}$	$5.54^{+0.76}_{-0.54}$	$5.44^{+0.54}_{-0.54}$	$5.52^{+0.33}_{-0.83}$	$7.01^{+0.98}_{-0.54}$	$8.63^{+0.98}_{-0.76}$
$s$	$0.32^{+0.08}_{-0.02}$	$0.41^{+0.09}_{-0.07}$	$0.48^{+0.16}_{-0.31}$	$0.59^{+0.16}_{-0.04}$	$0.50^{+0.02}_{-0.04}$	$0.50^{+0.05}_{-0.03}$	$0.43^{+0.04}_{-0.03}$	$0.31^{+0.03}_{-0.03}$	$0.32^{+0.04}_{-0.05}$
$\delta$	$0.16^{+0.03}_{-0.02}$	$0.36^{+0.04}_{-0.03}$	$0.29^{+0.46}_{-0.18}$	$0.72^{+0.01}_{-0.11}$	$0.28^{+0.03}_{-0.01}$	$0.27^{+0.02}_{-0.04}$	$0.32^{+0.03}_{-0.02}$	$0.40^{+0.01}_{-0.01}$	$0.36^{+0.02}_{-0.02}$
$D_0$ [ $10^{28} \text{ cm}^2/\text{s}$ ]	$2.77^{+2.95}_{-0.53}$	$2.83^{+0.90}_{-0.50}$	$4.78^{+5.22}_{-3.49}$	$5.95^{+0.83}_{-1.37}$	$9.30^{+0.70}_{-5.48}$	$9.04^{+0.96}_{-3.95}$	$8.19^{+1.81}_{-4.68}$	$4.92^{+1.12}_{-2.36}$	$4.60^{+2.71}_{-2.04}$
$v_A$ [km/s]	$6.80^{+1.18}_{-2.73}$	$29.2^{+2.80}_{-1.47}$	$21.2^{+38.8}_{-21.2}$	$1.84^{+2.36}_{-1.08}$	$20.2^{+3.26}_{-6.33}$	$18.2^{+3.15}_{-5.91}$	$25.0^{+0.92}_{-2.30}$	$22.8^{+1.46}_{-1.05}$	$20.7^{+1.14}_{-3.43}$
$v_{0,c}$ [km/s]	$40.9^{+59.1}_{-5.89}$	$40.2^{+38.1}_{-25.2}$	$5.82^{+94.2}_{-5.82}$	$87.8^{+12.2}_{-7.57}$	$69.7^{+22.0}_{-24.7}$	$57.3^{+41.1}_{-12.3}$	$44.0^{+8.4}_{-16.5}$	-	-
$z_h$ [kpc]	$3.77^{+3.23}_{-1.77}$	$2.04^{+0.40}_{-0.04}$	$4.22^{+2.78}_{-2.22}$	$6.55^{+0.45}_{-1.63}$	$5.43^{+1.57}_{-3.43}$	$5.84^{+1.16}_{-3.84}$	$6.00^{+1.00}_{-4.00}$	$5.05^{+1.95}_{-3.05}$	$4.12^{+2.88}_{-2.12}$
$\phi_{\text{AMS}}$	$300^{+60}_{-80}$	$780^{+80}_{-40}$	$620^{+180}_{-195}$	$580^{+45}_{-115}$	$400^{+90}_{-40}$	$360^{+115}_{-45}$	$700^{+20}_{-50}$	$640^{+20}_{-20}$	$340^{+45}_{-125}$



- Assume CR propagation is homogeneous.
- Fit data to local AMS-02 observables.



Moon (To Scale)

Geminga



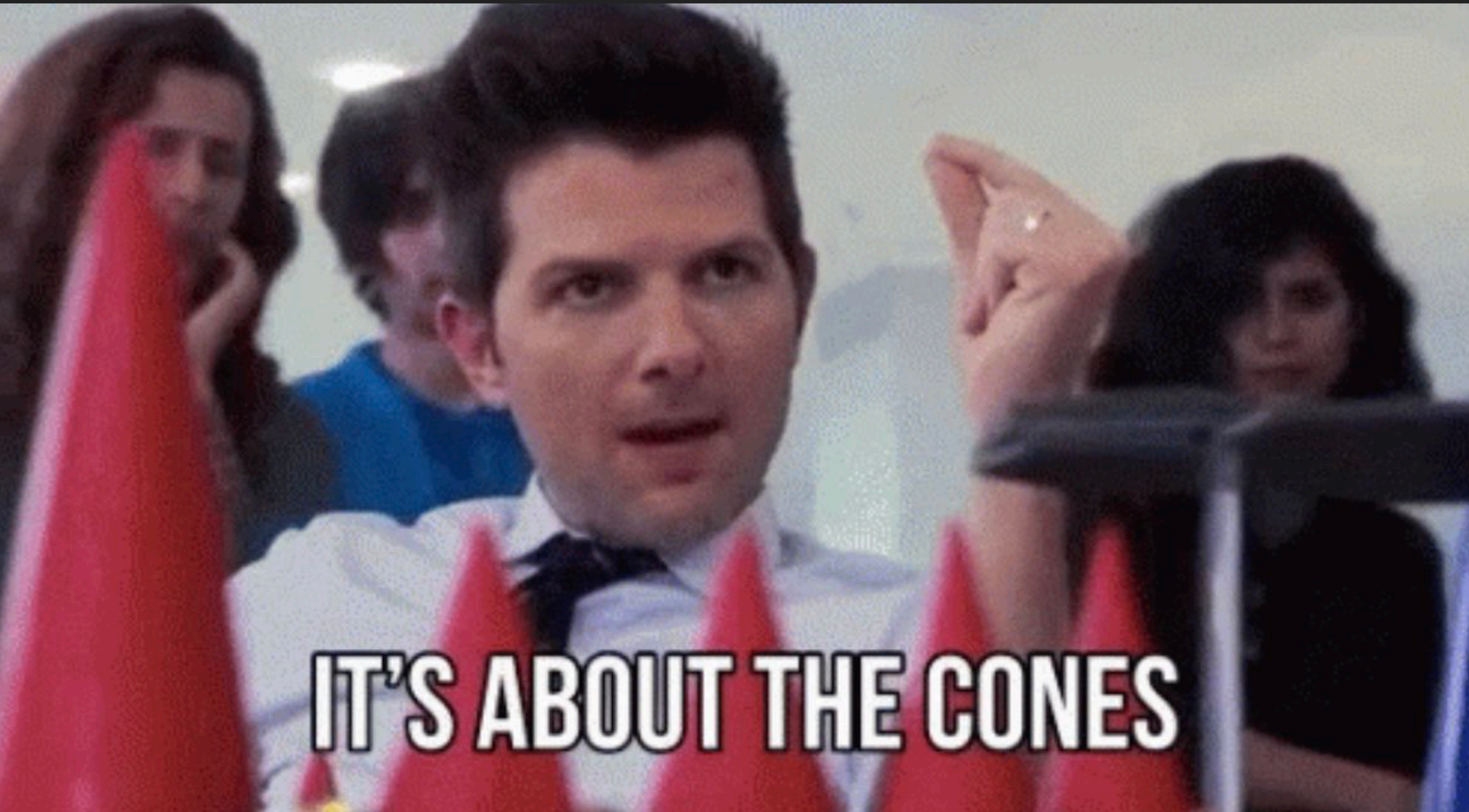
- But propagation is not homogeneous.
- Local TeV observations might not tell you anything!

PSR B0656+14

# USING TEV HALOS TO FIX COSMIC-RAY DIFFUSION MODELS

---

- ▶ It's about the sources.



# TEV HALOS SOLVE COSMIC-RAY DIFFUSION

► Pulsar catalogs provide an answer:

► >3000 pulsars

► Specific locations, ages, and spin down powers

► Translates directly into local diffusion model in streaming instability models.

#	PSRJ	P0 (s)	P1	DIST (kpc)	AGE (Yr)	BSURF (G)	EDOT (ergs/s)
1	J0537-6910	0.016122	5.18e-14	49.700	4.93e+03	9.25e+11	4.88e+38
2	J0534+2200	0.033392	4.21e-13	2.000	1.26e+03	3.79e+12	4.46e+38
3	J0540-6919	0.050570	4.79e-13	49.700	1.67e+03	4.98e+12	1.46e+38
4	J1813-1749	0.044741	1.27e-13	4.700	5.58e+03	2.41e+12	5.60e+37
5	J1400-6325	0.031182	3.89e-14	7.000	1.27e+04	1.11e+12	5.07e+37
6	J1747-2809	0.052153	1.56e-13	8.141	5.31e+03	2.88e+12	4.33e+37
7	J1833-1034	0.061884	2.02e-13	4.100	4.85e+03	3.58e+12	3.37e+37
8	J2022+3842	0.048579	8.61e-14	10.000	8.94e+03	2.07e+12	2.96e+37
9	J0205+6449	0.065716	1.94e-13	3.200	5.37e+03	3.61e+12	2.70e+37
10	J2229+6114	0.051624	7.83e-14	3.000	1.05e+04	2.03e+12	2.25e+37
11	J1513-5908	0.151582	1.53e-12	4.400	1.57e+03	1.54e+13	1.73e+37
12	J1617-5055	0.069357	1.35e-13	4.743	8.13e+03	3.10e+12	1.60e+37
13	J1124-5916	0.135477	7.53e-13	5.000	2.85e+03	1.02e+13	1.19e+37
14	J1930+1852	0.136855	7.51e-13	7.000	2.89e+03	1.03e+13	1.16e+37
15	J1023-5746	0.111472	3.84e-13	2.080	4.60e+03	6.62e+12	1.09e+37
16	J1420-6048	0.068180	8.32e-14	5.632	1.30e+04	2.41e+12	1.04e+37
17	J1410-6132	0.050052	3.20e-14	13.510	2.48e+04	1.28e+12	1.01e+37
18	J1849-0001	0.038523	1.42e-14	*	4.31e+04	7.47e+11	9.78e+36
19	J1402+13	0.005890	4.83e-17	*	1.93e+06	1.71e+10	9.34e+36
20	J1846-0258	0.326571	7.11e-12	5.800	7.28e+02	4.88e+13	8.06e+36
21	J0835-4510	0.089328	1.25e-13	0.280	1.13e+04	3.38e+12	6.92e+36
22	J1811-1925	0.064667	4.40e-14	5.000	2.33e+04	1.71e+12	6.42e+36
23	J1111-6039	0.106670	1.95e-13	*	8.66e+03	4.62e+12	6.35e+36
24	J1813-1246	0.048072	1.76e-14	2.635	4.34e+04	9.30e+11	6.24e+36
25	J1838-0537	0.145708	4.72e-13	*	4.89e+03	8.39e+12	6.02e+36
26	J1838-0655	0.070498	4.92e-14	6.600	2.27e+04	1.89e+12	5.55e+36
27	J1418-6058	0.110573	1.69e-13	1.885	1.03e+04	4.38e+12	4.95e+36
28	J1935+2025	0.080118	6.08e-14	4.598	2.09e+04	2.23e+12	4.66e+36
29	J1856+0245	0.080907	6.21e-14	6.318	2.06e+04	2.27e+12	4.63e+36
30	J1112-6103	0.064962	3.15e-14	4.500	3.27e+04	1.45e+12	4.53e+36
31	J1640-4631	0.206443	9.76e-13	12.750	3.35e+03	1.44e+13	4.38e+36
32	J1844-0346	0.112855	1.55e-13	*	1.16e+04	4.23e+12	4.25e+36
33	J1952+3252	0.039531	5.84e-15	3.000	1.07e+05	4.86e+11	3.74e+36
34	J1826-1256	0.110224	1.21e-13	1.550	1.44e+04	3.70e+12	3.58e+36
35	J1709-4429	0.102459	9.30e-14	2.600	1.75e+04	3.12e+12	3.41e+36
36	J2021+3651	0.103741	9.57e-14	1.800	1.72e+04	3.19e+12	3.38e+36
37	J1524-5625	0.078219	3.90e-14	3.378	3.18e+04	1.77e+12	3.21e+36
38	J1357-6429	0.166108	3.60e-13	3.100	7.31e+03	7.83e+12	3.10e+36
39	J1913+1011	0.035909	3.37e-15	4.613	1.69e+05	3.52e+11	2.87e+36
40	J1826-1334	0.101487	7.53e-14	3.606	2.14e+04	2.80e+12	2.84e+36

# Pulsar searches and timing with the square kilometre array

R. Smits<sup>1</sup>, M. Kramer<sup>1</sup>, B. Stappers<sup>1</sup>, D. R. Lorimer<sup>2,3</sup>, J. Cordes<sup>4</sup>, and A. Faulkner<sup>1</sup>

<sup>1</sup> Jodrell Bank Centre for Astrophysics, University of Manchester, UK

e-mail: Roy.Smits@manchester.ac.uk

<sup>2</sup> Department of Physics, 210 Hodges Hall, West Virginia University, Morgantown, WV 26506, USA

<sup>3</sup> National Radio Astronomy Observatory, Green Bank, USA

<sup>4</sup> Astronomy Department, Cornell University, Ithaca, NY, USA

Received 13 June 2008 / Accepted 31 October 2008

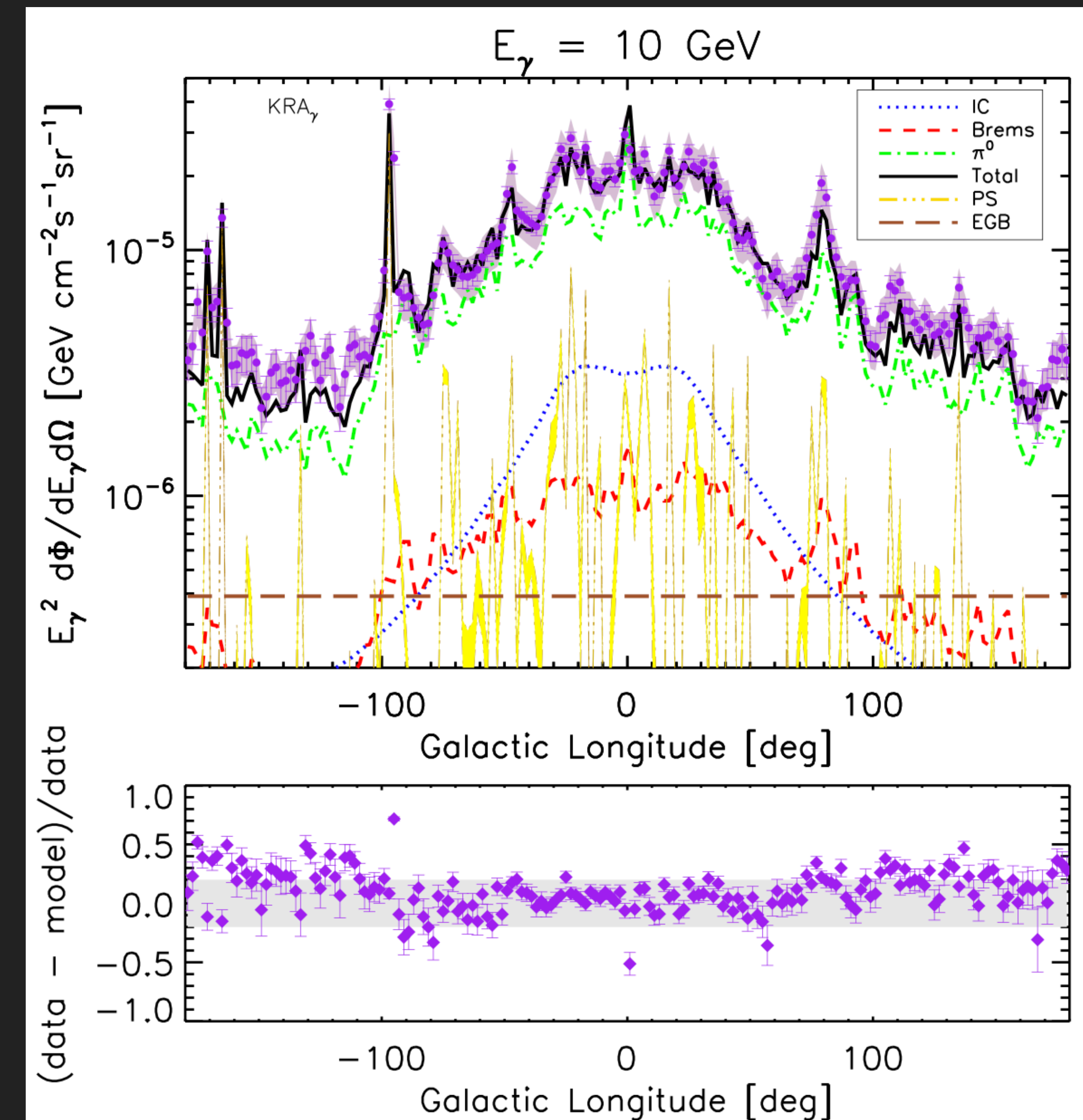
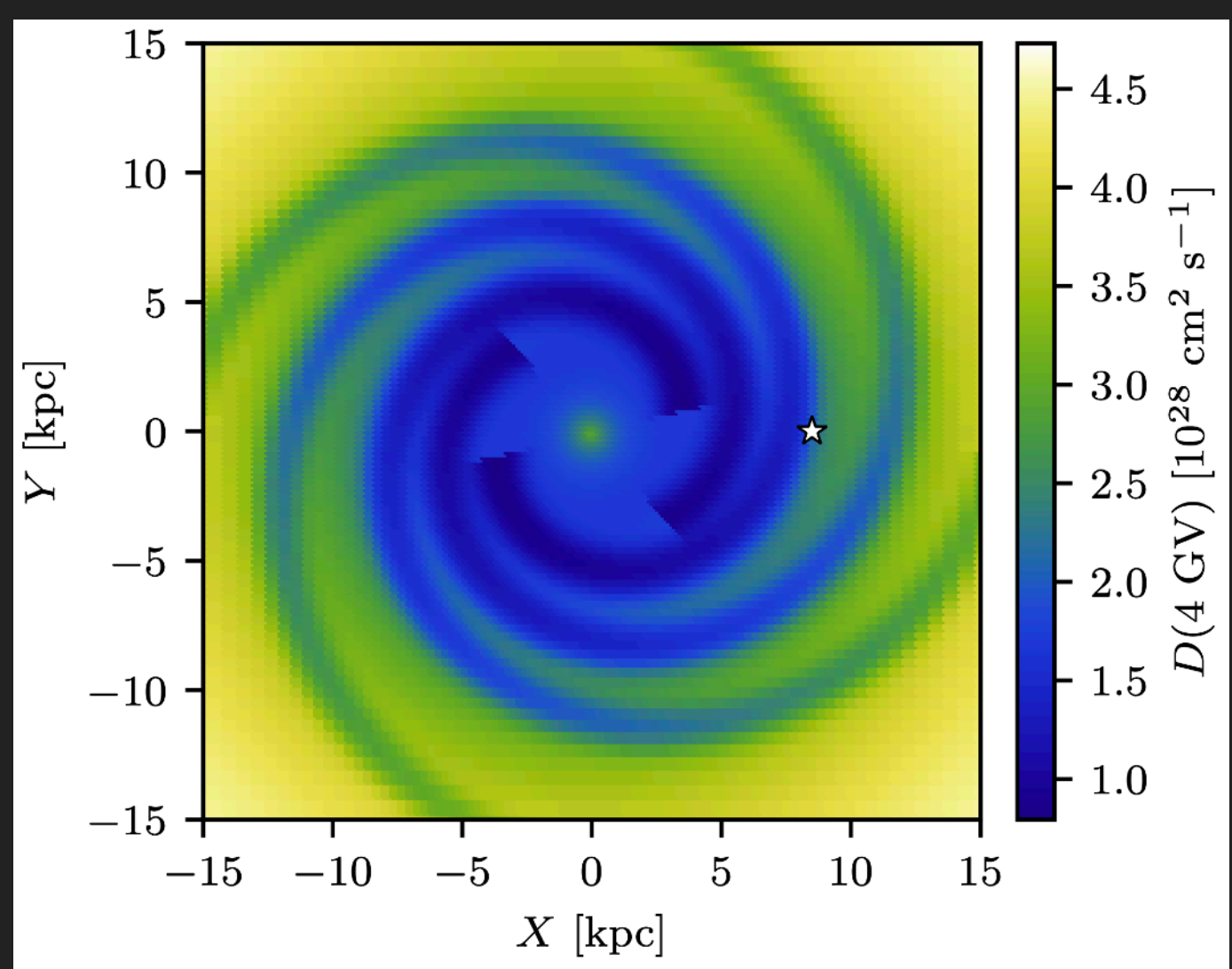
## ABSTRACT

The square kilometre array (SKA) is a planned multi purpose radio telescope with a collecting area approaching 1 million square metres. One of the key science objectives of the SKA is to provide exquisite strong-field tests of gravitational physics by finding and timing pulsars in extreme binary systems such as a pulsar-black hole binary. To find out how three preliminary SKA configurations will affect a pulsar survey, we have simulated SKA pulsar surveys for each configuration. We estimate that the total number of pulsars the SKA will detect, is around 14 000 normal pulsars and 6000 millisecond pulsars, using only the 1-km core and 30-mn integration time. We describe a simple strategy for follow-up timing observations and find that, depending on the configuration, it would take 1–6 days to obtain a single timing point for 14 000 pulsars. Obtaining one timing point for the high-precision timing projects of the SKA, will take less than 14 h, 2 days, or 3 days, depending on the configuration. The presence of aperture arrays will be of great benefit here. We also study the computational requirements for beam forming and data analysis for a pulsar survey. Beam forming of the full field of view of the single pixel feed 15 m dishes using the 1 km core of the SKA requires about  $2.2 \times 10^{15}$  operations.

# TEV HALOS SOLVE COSMIC-RAY DIFFUSION

Gaggero et al. (2014; 1411.7623)

- ▶ First attempts at this approach.
- ▶ Decreasing diffusion in the spiral arms produces better fits to GeV gamma-ray data



## CONCLUSIONS - TEV GAMMA-RAY MODELING

---

- ▶ TeV halos are a common feature around middle-aged (and possibly young and recycled pulsars).
- ▶ Understanding the earliest stages of TeV halo formation (or composite sources, if you prefer), is critical for understanding TeV halo evolution.
- ▶ TeV halos provide critical information that will be necessary to make detailed TeV emission models.
- ▶ The Rise of the Leptons: PWN and TeV halo activity may dominate the diffuse TeV emission, important interplay between CTA/HAWC/LHAASO and IceCube.